5. CAPÍTULO 1

3D structure determination of STARP peptides implicated in *P. falciparum* invasion of hepatic cells.

STARP proteína del esporozoito rica en treoninas y asparaginas, ha sido encontrada en diferentes especies de *plasmodium* (59, 137) y se ha demostrado que se expresa en la superficie de los esporozoitos (59) que invaden las células hepáticas. Los péptidos nativos 20546 y 20570 y sus modificados (variados en los aminoácidos de alta afinidad de unión a células blancos o en sus vecinos) provenientes de esta proteína, fueron obtenidos por síntesis química, evaluados a nivel de respuesta inmune en ensayos *in vivo* y analizados por RMN ^{1}H con el fin de encontrar correlaciones entre sus características inmunes y su estructura tridimensional. Los péptidos nativos presentaron una región α helical menos estructurada que los péptidos modificados y las cadenas laterales de los aminoácidos de estos últimos involucrados en los motivos y registros de unión a moléculas HLA-DRβ1* adquirieron orientaciones diferentes a los nativos, esta alteración en la orientación posiblemente influyó en el cambio de las propiedades inmunológicas, ya que los péptidos nativos fueron no inmunogénicos mientras algunos péptidos modificados fueron inductores de una respuesta humoral, contribuyendo posiblemente en el ajuste del complejo CMH II-Pep-TCR y generando nuevos candidatos a ser incluidos en el diseño de una vacuna contra malaria multiestadío, multiepitópica y químicamente sintetizada.

Vaccine xxx (2010) xxx–xxx

Contents lists available at ScienceDirect

Vaccine

journal homepage: www.elsevier.com/locate/vaccine

3D structure determination of STARP peptides implicated in *P. falciparum* invasion of hepatic cells

Adriana Bermúdez[a,b], Martha Patricia Alba[a,b], Magnolia Vanegas[a,b], Manuel Elkin Patarroyo[a,c,*]

[a] *Fundación Instituto de Inmunología de Colombia (FIDIC), Colombia*
[b] *Universidad del Rosario, Colombia*
[c] *Universidad Nacional de Colombia, Colombia*

ARTICLE INFO

Article history:
Received 11 March 2010
Received in revised form 17 April 2010
Accepted 7 May 2010
Available online xxx

Keywords:
Structure
1H NMR
Malaria vaccine
Sporozoite

ABSTRACT

To block the different stages of *Plasmodium falciparum* invasion into human hepatocytes and red blood cells, we have focused on those proteins belonging to the pre-erythrocytic stage. One of these proteins is Sporozoite Threonine and Asparagine Rich Protein (STARP), which is a ligand used by *P. falciparum* parasites to bind Hepatic cells (HepG2). Previous studies on this protein identified two conserved peptides binding with high activity to HepG2 cells (namely 20546 and 20570) with corresponding critical hepatic-cell binding residues and determined an important role for these two peptides in the invasion process. This study shows the results of immunization trials in *Aotus* monkeys with native STARP peptides and analogues modified in critical hepatic-cell binding residues. The results show that native peptides are not immunogenic but can induce high-antibody titers when their critical residues are replaced by other with similar volume and mass but different polarity. Nuclear Magnetic Resonance (^{1}H NMR) studies revealed that native peptides (non-immunogenic) displayed shorter α-helical regions compared to their highly immunogenic modified analogues. Binding assays with HLA-DRβ1* molecules showed that 20546 modified peptides inducing high-antibody titers (**24972**, **24320** and **24486**) bound to HLA-DRβ1*0301 molecules, while the 20570 modified analogue (**24322**) bound to HLA-DRβ1*0101. The results support including these high-immunogenic STARP-derived modified peptides as pre-erythrocytic candidates to be included in the design of a synthetic antimalarial vaccine.

1. Introduction

The Sporozoite Threonine and Asparagine Rich Protein (STARP) antigen was cloned by Fidoch et al. using *Plasmodium falciparum* malaria laboratory strains and field isolates from a wide range of endemic regions [1]. The STARP antigen has been found to be present in other *Plasmodium* species and its gene is highly conserved in *P. falciparum* strains [1,2].

Immunoflourescence and immunoelectromicroscopy assays carried out using immune sera targeting the protein's central and C-terminal region have shown that STARP is expressed on the surface of the sporozoite forms that invade hepatic cells, suggesting a role during parasite's entry to the hepatic cell and infection [1].

The transcription of the 2.0 kb STARP gene has been demonstrated by reverse PCR and Northern blot hybridization. This gene encodes a highly conserved 604-residues-long protein of about 78 kDa containing a considerable amount of asparagine and threonine residues, for which the protein receives its name [1]. STARP contains 3 central repeat regions: 1) a mosaic (M) region between residues T85 to I134 containing various degenerated small repeats, 2) Rp45, located between residues N135 and T229 which contains two 45-amino-acid-long identical tandem repeats, and 3) Rp10, constituted by 26 tandem repeat units of 10 amino acids spanning from residue N223 to N489. The central region shows limited size variations, whereas the non-repetitive N and C termini have no length variations and show low degree of polymorphism. A highly hydrophobic region is located toward the protein's C-terminal end [1–3] (Fig. 1A).

In the search for optimal vaccine candidate proteins expressed by sporozoite stages of the *P. falciparum* parasite and capable of potentiating the immune responses induced by previously reported sporozoite antigens [4,5], we have targeted our research toward the study of the STARP antigen. Twelve peptides binding with high ability to HepG2 cells were identified in STARP by Lopez et al. by performing receptor–ligand binding competition assays [6]. Three of these high-ability binding peptides (HABPs) were successively situated inside the non-repetitive N-terminal region, one of which overlapped the mosaic (M) region; whereas six HABPs were located

* Corresponding author at: Fundación Instituto de Inmunología de Colombia (FIDIC), Carrera 50, No. 26-00, Bogotá, Colombia. Tel.: +57 14815219; fax: +57 1 4815269.
E-mail address: mepatarr@mail.com (M.E. Patarroyo).

0264-410X/$ – see front matter © 2010 Published by Elsevier Ltd.
doi:10.1016/j.vaccine.2010.05.025

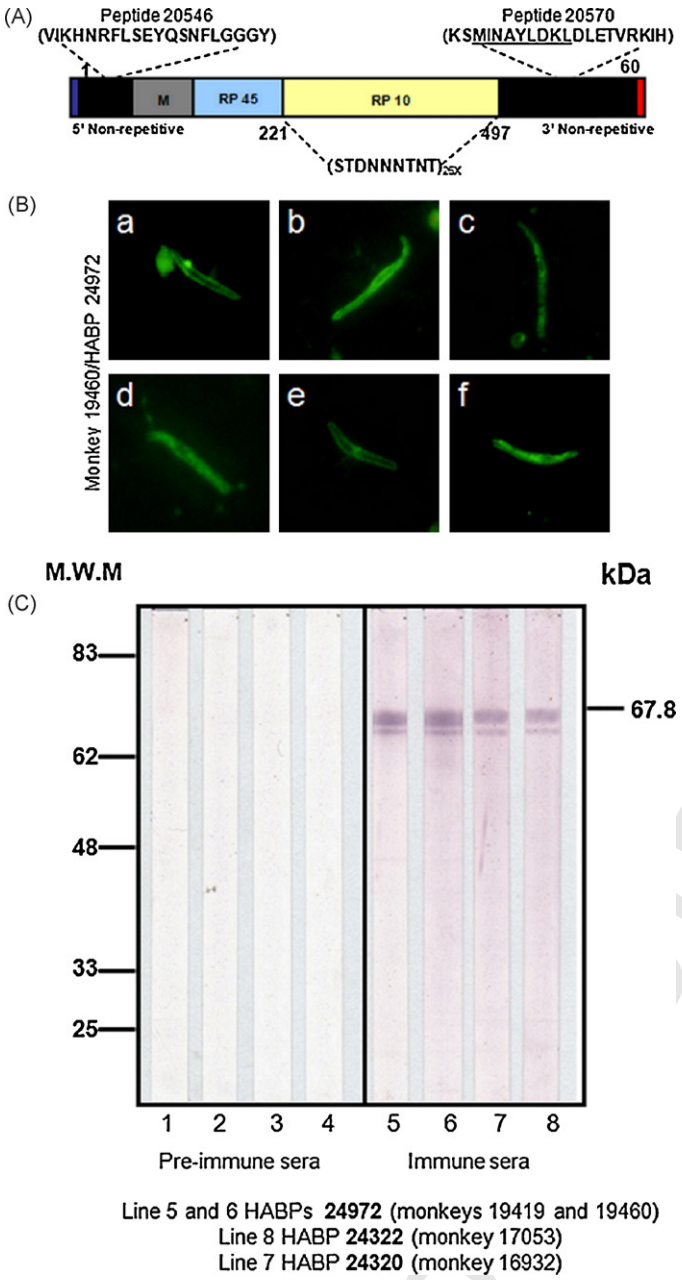

Fig. 1. (A) Schematic representation of the *Plasmodium falciparum* STARP antigen's structure showing the localization of native HABPs 20546 and 20570. (B) Sporozoite immunofluorescence patterns obtained using sera from monkey 19460 immunized with **24972** (20546) which shows recognition of membrane and granular membrane structures. (C) Western blot analysis of sera from *Aotus* monkeys immunized with native and modified STARP HABPs showing the recognition of *P. falciparum* STARP recombinant protein with a 67.8 kDa molecular weight.

in the Rp10 region of the central domain and three HABPs were found in the non-repetitive C-terminal end, one of which overlapped the Rp10 region.

For the development of the present study, we selected those STARP conserved HABPs located outside the repetitive regions M, Rp45 and Rp10 because it has been shown that repetitive sequences are highly antigenic and highly immunogenic but non-protection inducers. Therefore we choose those conserved HABPs located inside the non-repetitive N and C terminal regions: HABP 20546 (^{41}VIKHNRFLSEYQSNFLGGGY^{60}) localized inside the 5′ non-repetitive region and HABP 20570 (^{521}KSMINAYLDKLDLETVRKIH^{540}) located in the 3′ non-repetitive region. Besides binding with high capacity to HepG2, HABP 20570 contained a previously described CTL-inducing epitope (sequence underlined above and in Fig. 1A) associated to the HLA-A2.2 genetic characteristic. Both peptides presented saturable bindings with dissociation constants ranging between 18 and 219 nM and HABP 20570 cross-linked to two hepatocyte membrane proteins of about 38 and 44 kDa [6].

But it has been thoroughly shown that conserved HABPs are non-antigenic, non-immunogenic, non-protective inducers and that to render them into highly immunogenic and protective inducer peptides critical binding residues (identified by glycine analogue scanning) have to be properly modified [7–9].

We have consistently shown that such modifications are associated with the appropriate fit of these modified HABPs inside the macromolecular complex formed by Class II Major Histocompatibility molecules (MHC II) and T cell receptors (TCR), necessary to induce an effective immune response [10–13]. Based on previously published data, some residues were replaced trying to maintain their volume and mass but changing their polarity [13–15] so that they could properly fit into a particular HLA–DRβ1* molecule to be presented to the TCR. Therefore non-immunogenic natives peptides 20546 (VIKH**N**RF**LS**EYQ**SN**FLGGGY) and 20570 (KSMINAYLDK**LD**L**E**TVRKIH) were render into immunogenic-inducing peptides by replacing the critical HepG2 binding residues (in bold and underlined above) according to principles previously described [13–15]. Immunogenicity studies were performed with the above mentioned natives peptides and their corresponding modified analogues **24972**, **24320** and **24486** (modified from 20546); **24322** (modified from 20570) seeking for a correlation between their ^{1}H NMR 3D structures and their immunological activity.

The role played by STARP in the *P. falciparum* exo-erythrocytic cycle inside the human host is still unclear; however, all the aforementioned evidence supports the idea that STARP is involved in sporozoite invasion of hepatocytes and also that STARP HABPs (when being property modified) may be good candidates to be included in the design of a minimal subunit-based, multi-epitopic, multi-stage, chemically synthesized vaccine against *P. falciparum* malaria, so urgently needed.

2. Materials and methods

2.1. Peptide chemical synthesis

Native peptides 20546, 20570 and its corresponding **24972**, **24320**, **24486**, and **24322** modified analogues (shown in bold throughout the paper) were synthesized by the standard solid-phase peptide synthesis methodology [16], purified by reverse-phase HPLC and analyzed by MALDI-TOF mass spectrometry to determine their molecular masses (Autoflex Bruker Daltonics). A glycine-cysteine (GC) tag was added to the peptide's C and N termini during synthesis to allow polymerization following oxidation. The so obtained polymerized peptides were used to immunize *Aotus* monkeys.

2.2. Animals and immunization trials

Aotus monkeys were kept in stainless-steel cages at FIDIC's primate station in Leticia, Amazonas, Colombia, and maintained in strict accordance with the NIH and the Colombian Ministry of Health (Law 84/1989) guidelines for animal care, under the weekly supervision of CORPOAMAZONIA officials and a primatologist. All procedures were approved and supervised by FIDIC's Ethics Committee in Health Research (Resolution No. 008430 of 1993, Colombian Ministry of Health) and FIDIC's Primate

Please cite this article in press as: Bermúdez A, et al. 3D structure determination of STARP peptides implicated in *P. falciparum* invasion of hepatic cells. Vaccine (2010), doi:10.1016/j.vaccine.2010.05.025

Station Ethics Committee. Once studies had concluded and monkeys were in excellent health conditions, they were released back into the jungle close to the places where they had been captured.

All monkey serum samples were first tested for the presence of antibodies against air-dried fixed *P. falciparum* sporozoites and infected red blood cells (iRBCs) at the schizont stag (1:20 dilution). Monkeys testing positive were returned to the jungle without further manipulation whereas groups of 5 to 8 *Aotus* IFA-negative monkeys were immunized with 125 μg of peptide same as described in previous works [7–15].

2.3. Indirect immunofluorescence assays (IFA)

Slides containing air-dried *P. falciparum* sporozoites (3D7 strain) kindly provided by Dr. Patricia de la Vega (formerly of the Department of Microbiology, University of Maryland School of Medicine; Baltimore, USA) were used for IFA assays. The slides were blocked and processed as described elsewhere [7–15].

2.4. Western blot analysis

A total of 125 μg of *P. falciparum* recombinant STARP (kindly provided by Dr. Pierre Druilhe from the Pasteur Institute, Paris) were separated by discontinuous SDS-PAGE using 12% acrylamide gels (*w*/*v*) and transferred to nitrocellulose membranes. Nitrocellulose membrane strips were individually incubated with each monkey sera diluted 1:100 in blocking solution, washed several times and then incubated with alkaline phosphatase-conjugated goat anti-*Aotus* IgG at a 1:1000 dilution and developed with NBT/BCI.

2.5. Purifying HLA-DR molecules

Purified human molecules were obtained from DR1, WT100BIS (DRβ1*0101), DR3, COX (DRβ1*0301), DR4, BSM (DRβ1*0401), DR7 EKR (DRβ1*0701) and DR11 BM21 (DRβ1*1101) homozygous EBV-B cell lysates by affinity chromatography using anti-HLA-DR L-243 monoclonal antibodies cross-linked to protein A-Sepharose CL-4B (Amersham Pharmacia Biotech AB) as affinity support.

2.6. Peptide-binding competition assays

The ability of unlabeled peptides to compete with biotinylated indicator peptides for purified HLA-DR molecules was assessed in peptide-binding competition assays, as previously described elsewhere [17]. The biotinylated-labeled hemagglutinin (HA) peptide residues 306–318 (PKYVKQNTLKLAT) was used as control peptide for DRβ1*0101 and DRβ1*0401; *Mycobacterium tuberculosis* (MT) 65-kDa Y3–13 peptide (YKTIAFDEEARR) for DRβ1*0301, and tetanus toxin (TT) 830–843 (QYIKANSKFIGITE) for DRβ1*0701 and DRβ1*1101. Relative binding affinities were determined in competition assays, where a peptide inhibiting binding of indicator peptide to the HLA molecule being tested by more than 45% was considered good competitor.

2.7. Circular dichroism (CD) analysis

The CD spectra of the peptides were measured in 50 mM phosphate buffer, pH 7.0, and TFE–water (30:70, *v*/*v*) in a JASCO J810 spectropolarimeter using a 1-mm pathlength cuvette. CD data were expressed as mean residue ellipticity (deg cm^2 dmol^{-1}) [18].

2.8. NMR analysis and structure calculations

Ten milligrams of pure peptide were dissolved in 600 μl TFE–water (30/70, *v*/*v*) for NMR experiments. NMR spectra were recorded on a Bruker DRX-600 spectrometer at 295 K. Spectra were assigned according to double-quantum filter correlation spectroscopy (DQF-COSY) [19], total correlation spectroscopy (TOCSY)[20] and nuclear overhauser enhancement spectroscopy (NOESY) experiments [21]. 2D NMR data were processed using TOPSPIN software. NOESY spectra recorded at different temperatures (285–315 K) were used to obtain amide temperature coefficients for predicting hydrogen bonds ($-\Delta\delta H^N/\Delta T$ ppm/K). Distance Geometry (DGII) software was used for gathering a family of 50 structures. These structures were refined by using simulated annealing protocol (DISCOVER software). NOE intensities were calculated and classified into strong (1.8–2.5 Å), medium (2.5–3.5 Å) and weak (3.5–5.0 Å) range interactions (for more details see [22]). Only structures having reasonable geometry and minimum angle and distance violations were selected.

3. Results

3.1. Peptide characterization

Molecular mass determinations of HPLC-purified STARP HABPs and their corresponding modified analogues assessed by MALDI-TOF spectrometry showed a single signal for all peptides which corresponded to their expected molecular masses. The polymers used for immunization had molecular weights in the 8 kDa to 24 kDa range, as assessed by size exclusion chromatography (SEC), suggesting a variable but consistent degree of polymerization.

3.2. Immunogenicity studies

While immunization of *Aotus* monkeys with native 20546 induced no detectable antibodies as assessed by IFA and Western blot, its analogues **24972** and **24320** proved once again that specific modifications had to be performed on native HABP in order to render them into highly immunogenic modified peptides (as assessed by IFA test and Western blot), since antibody titers ranging between 1:320 and 1:1280 were induced 20 days after the first immunization and remained detectable after the 2nd immunization (as determined by IFA and Western blot). Modifications leading to obtaining peptide **24486** induced no antibody responses in *Aotus* monkeys being immunized with this modified peptide, proving once more the specificity and selectivity of the changes needed to render peptides into strong immunogens (Table 1).

The other native HABP (20570) was not immunogenic but its modified analogue **24322** induced high-antibody titers against the sporozoite, as assessed by IFA (1:320 to 1:640) In essence, the studies of immunization trials in *Aotus* monkeys confirmed that conserved HABPs are non-immunogenic (Table 1) unless they were specifically modified according to rules previously described with merozoite's conserved HABPs [23].

Monkey antisera induced by immunization with modified STARP peptide **24972** showed a strong reactivity against membrane (Fig. 1B), cytosol and perinuclear antigens in of air-dried sporozoites by IFA (see Fig. 1B), and a similar immunofluorescence pattern was observed with the antibodies induced by the other modified STARP peptides assessed in this study (data not shown). Such reactivity pattern agrees with the different localizations of microneme organelles in sporozoite forms, inside which STARP is deposited.

Fig. 1C shows the Western blot analysis of sera obtained from *Aotus* monkeys immunized with modified **24972** (lanes 5 and 6) and **24320** (lane 7), both of which were derived from 20546, and **24322** derived from HABP 20570 (lane 8). All three modified peptides show a clear recognition of the 67.8-kDa recombinant STARP protein kindly provided by Prof. Pierre Druilhe).

Please cite this article in press as: Bermúdez A, et al. 3D structure determination of STARP peptides implicated in *P. falciparum* invasion of hepatic cells. Vaccine (2010), doi:10.1016/j.vaccine.2010.05.025

Table 1
Amino acid sequences of the STARP conserved and modified HABPs (numbered according to our Institute's serial system) used for immunizing *Aotus* monkeys and whose 3D structures were determined by ^{1}H NMR.

Polymerized peptide	Peptide sequence																			PI	I_{20}	II_{10}	II_{15}	II_{20}
STARP							**P_1**			**P_4**			**P_6**			**P_9**								
20546	V	I	K	H	N	R	F	L	S	E	Y	Q	S	N	F	L	G	G	G	Y	0/5	0/5	0/5	0/5	0/5
24972	-	-	-	-	**M**	-	-	H	**V**	D	-	-	**A**	**I**	-	-	-	-	-		0/8	3(1280)	2(640)	ND	3(1280)
24320	-	-	-	-	**M**	-	-	H	**A**	D	-	-	**A**	**P**	-	-	-	-	-	-	0/8	1(640)	1(320)	1(320)	1(320)
24486	-	-	-	-	**N**	-	-	H	**V**	D	-	-	**A**	**P**	-	-	-	-	-	-	0/8	0/8	0/8	0/8	0/8
20570	K	S	M	I	N	A	Y	L	D	K	L	D	L	E	T	V	R	K	I	H	0/5	0/5	0/5	0/5	0/5
24322	-	-	-	-	-	-	-	-	-	-	H	P	-	M	-	-	-	-	-	-	0/8	3(640)	1(320)	1(320)	1(320)

Sequences are aligned according to their binding motifs and HLA-DRβ1 molecule's reading registers to Pockets 1, 4, 6 and 9 (shadowed residues). Antibody titers induced by each peptide in *Aotus* monkeys are shown to the left. PI, I_{20}, II_{10}, II_{15} and II_{20} correspond to the days when monkeys were bled and antibody titers were determined (shown in brackets).

3.3. Interaction with purified HLA-DRβ1* molecules

Binding assays to HLA-DRβ1* isolated molecules showed that native STARP 20546 binds promiscuously and with high capacity to HLA-DRβ1*0101, HLA-DRβ1*0301, HLA-DRβ1*0401 and HLA-DRβ1*0701 molecules a phenomenon very often observed when working with native, non immunogenic HAPBs. However, when modifications were performed to render this peptide into a long-lasting antibody-titer inducer (Table 1), modified HABP **24972** (analogue to 20546) bound with high activity to HLA-DRβ1*0301, (Table 2) displaying the classical binding motifs and binding registers characteristic for this molecule [24]: F7 fitting into Pocket 1, D10 into Pocket 4, Q12 into Pocket 6 and F15 into Pocket 9, suggesting that probably this modified HABP was binding preferentially to HLA-DRβ1*0301-like *Aotus* molecules to induce production of high long-lasting antibody titers in these monkeys. This genetic trait is present in ~27% of a group of 100 *Aotus* monkeys genotyped by molecular biology methods [25], and in another large of these monkeys recently genotyped (Suárez C. et al. unpublished results), a proportion similar to that of those of monkeys giving a positive immune response (~37%) when immunized with this modified peptide. The same phenomenon occurred with modified HABP **24320**, which bound to HLA-DRβ1*0301 with a lower binding capacity, inducing also lower antibody titers. Meanwhile, the modified HABP **24486** (analogue to 20546) bound simultaneously with high capacity to HLA-DRβ1*0401 and HLA-DRβ1*0701, both genetic markers showing a combined genetic frequency of ~40% in the same population of random heterozygous wild Amazonian *Aotus* monkeys from Colombia. This modified HABP did not induce any antibody titers at any point of the trial, as assessed by IFA and Western blot.

The other native STARP-derived HABP (20570) bound with high capacity to HLA-DRβ1*0301 and did not induce any antibody titers, whereas modified analogue **24322** bound to HLA-DRβ1*0101 as well as to HLA-DRβ1*0301. However, binding to HLA-DRβ1*0101 has been uncommon in our assays with different HABPs but since the classical binding register displayed by this peptide is more in agreement with binding to HLA-DRβ1*0101, where Y7 fits into pocket 1, K10 into pocket 4, P12 into pocket 6 and T15 into Pocket 9; therefore it was assigned an HLA-DRβ1*0101 binding capacity. This genetic trait it present in ~10% of the genotyped *Aotus* population [25] a similar proportion to the proportion of monkeys giving a positive immune response (~12.5%) when immunized with this **24322** modified HABP.

3.4. Structural analysis

NOESY spectra obtained for peptides 20546 and its modified analogues **24972**, **24320**, **24486**, and for peptide 20570 and its modified analogue **24322** showed sequential, short and medium range $d_{NN}(i,i+1)$ $d_{\alpha\beta}(i,i+3)$, $d_{\alpha N}(i,i+3)$, $d_{\alpha N}(i,i+4)$ NOE connectivities, low amide proton chemical shift temperature coefficients for some of the amino acids, which altogether suggest the presence of an α-helix structure (Fig. 2A). These results were consistent with

Table 2
Structural features of native conserved HABPs from the *P. falciparum* STARP and their corresponding analogues determined by ^{1}H NMR and their associated binding capacity to HLA-DRβ1* molecules.

Protein	Peptide	#	Helical structure	NOEs used	Distance (Å)	Rmsd Å	Maximum NOE violations Å	Haplotypes				
								DR1	DR52		DR53	
								% Binding			HLA-DRβ1*	
								alleles				
								0101	0301	1101	0401	0701
STARP	20546	20	S9-L16	210	20.69	0.21	0.25	**58**	**56**	43	**65**	**55**
	24972	25–19	M5-V9 and I14-G19	212	21.85	0.36	0.30	11	**76**	ND	22	14
	24320	41	K3-D10	193	–	0.21	0.22	26	**45**	27	28	–29
	24486	25	K3-Q12	202	19.25	0.23	0.30	10	**47**	–103	**90**	**52**
	20570	24	I4-T15	184	21.71	0.34	0.35	–1	**72**	–26	14	–110
	24322	24–29	M3-K10 and P12-H20	180	23.10	0.28	0.20	**48**	**64**	0	19	–90

(#) Number of superimposed structures chosen from an initial set of 50 low-energy conformers. Distance (in Å) between the HABP residues theoretically fitting into HLA-DRβ1* Pockets 1 and 9; Rmsd: root mean square deviation of the superimposition. Peptides binding to MHC Class II molecules with ≥45% activity are shown in bold.

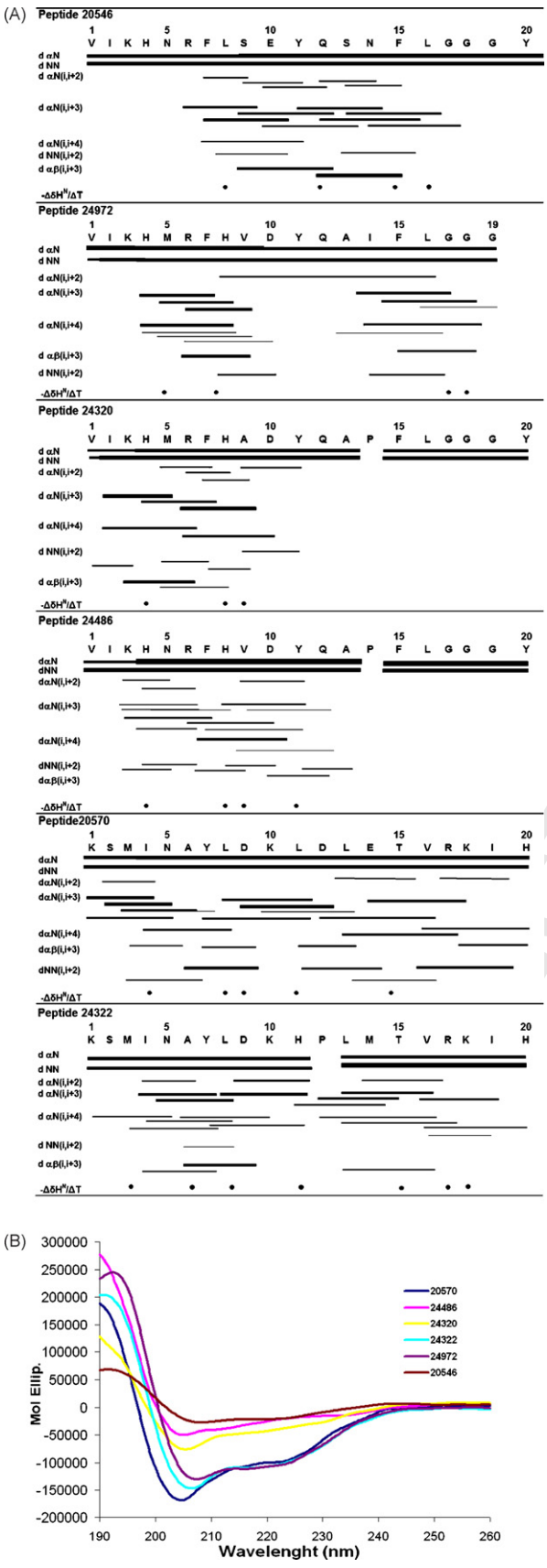

Fig. 2. (A) The most representative sequential medium range NOE connectivities used for determining the structure of native peptide 20546 and its modified analogues **24972**, **24320**, **24486**, and the structure of native 20570 and its modified analogue **24322**. Amide protons having temperature coefficients smaller than 4.0 are indicated by ●. Approximated NOE intensities are indicated by the thickness of the horizontal black bars. (B) Circular dichroism spectra of *P. falciparum* STARP peptides acquired in aqueous solution. Molar ellipticity (deg cm^2 dmol^{-1}) was plotted as a function of the wavelength (nm).

deconvolution analyses using CONTINLL, SELCON and CDSSTR programs [26,27], predicting a 50–95% content of α-helical features in the secondary structures of these peptides.

An average of 26 low energy conformers having no distance violations larger than 0.35 Å or ω angles greater than 1.4° were chosen out of the initial set of 50 structures calculated for peptide 20546 and its modified analogues **24972**, **24320**; **24486**, and for peptide 20570 and its modified analogue **24322**. Average root mean square deviations (RMSD), maximum NOE violations and the number of low energy conformers are shown in Table 2. RMSD values were obtained by superimposing backbone structures between amino acids S9–L16 in peptide 20546, M5–V9 and I14–G19 in peptide **24972**, K3–D10 in peptide **24320**, K3–Q12 in peptide **24486**, I4–T15 in peptide 20570, M3–K10 and P12–H20 in peptide **24322**. The DSSP program [28] assigned a clear α helical structure to all of these peptides (Table 2).

4. Discussion

Over the last 20 years, we have focused our efforts towards blocking red blood cell (RBC) invasion of merozoites with aim of obtaining a fully effective antimalarial vaccine. Such endeavor has comprised synthesizing and testing the RBC binding ability of thousands of peptides, as well as identificating their critical binding residues [29,30].

However, a large number of immunization studies with *P. falciparum* merozoite-derived peptides [31] demonstrated that conserved HABPs are neither antigenic, nor immunogenic or protection-inducing, a problem named by us as immunological silence. To solve this problem, critical RBC binding residues identified by glycine analogue scanning were replaced by others having the same mass and volume but opposite polarity [13] and tested in *Aotus* monkeys [32]. It was by following this strategy that we gathered a pool of potential candidate HABPs to be included in the design of a multi-epitopic, minimal subunit-based antimalarial vaccine [14,15,33].

Now that we have almost completed the functional the characterization of a large number of invasion-relevant merozoite proteins, identifying their HABPs with their critical binding residues we are now focusing our studies in proteins involved in invasion of hepatocytes by using the same strategy, seeking to identify molecules capable of blocking sporozoite's invasion of hepatic cells as the first line of defense against malaria infection and turn such non-immunogenic conserved HABPs into highly immunogenic molecules. Amongst such sporozoite proteins involved in invasion of hepatocytes is STARP, based on whose sequence we synthesized native peptides 20546 (**24972**, **24320** and **24486**) and 20570 (**24322**), together with their corresponding modified HABPs (shown above in brackets and in bold throughout this manuscript to distinguish them from the native peptides from which they were derived) and then proceeded to characterize these peptides regarding their binding ability and immunological and structural properties.

In different Nuclear Magnetic Resonance (NMR) studies performed on a large number of HABPs in 30:70 TFE–H_2O (*v*/*v*) it has been demonstrated that the tridimensional conformations of HABPs are identical to the ones displayed in the complete microbial protein when superimposing their 3D structures with the 3D structures of the protein segments where such HABPs were identified, independently of whether such structures were determined by X-ray crystallography or NMR, as indicated by the RMSD average

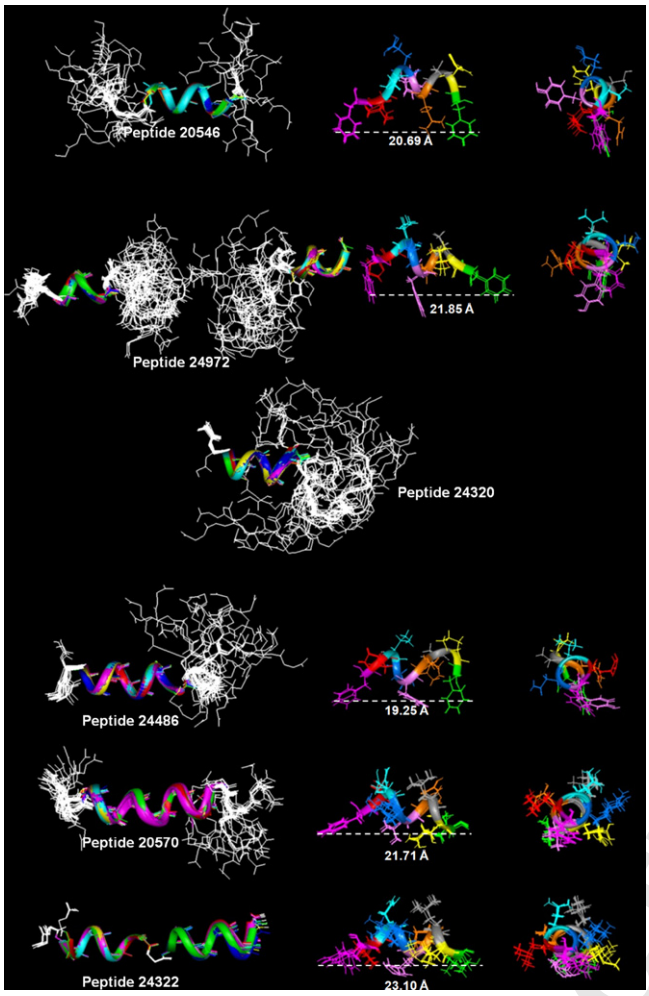

Fig. 3. Three-dimensional models of *P. falciparum* STARP peptides obtained by superimposing several of the structures obtained from an initial set of 50 structures calculated for each peptide. Left-hand and central panels show only the backbone of the molecule where well defined α helices are represented as colored ribbons. Right-hand panel: lateral chains of residues fitting into the HLA-DRβ1* molecules' pockets. Color code: fuchsia: **Pocket 1**, red: P2, turquoise: P3, blue: **Pocket 4**, pink: P5, orange: **Pocket 6**, gray: P7, yellow: P8 and green: **Pocket 9**. Pockets were assigned according to the characteristic peptide motifs and reading registers of each HLA-DRβ1* purified molecule to which these peptides bound. Peptides 20546, **24972**, **24320** and **24486** bound to HLA-DRβ1* 0301, 20570 whereas peptide **24322** bound to HLA-DRβ1* 0101.

values of 1.1 obtained in such peptide/protein superimpositions. These studies have reported α helical, β turn and random structural conformations [34] and not only α helical, therefore showing that such assay conditions help to stabilize rather than induce structural conformations [35].

In general, structural comparison between native HABPs and their modified analogue peptides showed that all modified STARP analogues presented α-helical conformations, which were different from the α-helical segments displayed by their corresponding native STARP HABPs. For instance, seventeen residues were involved in the α helical region formation of the highly immunogenic modified STARP analogue **24322** whereas only 12 amino acids displayed this structural feature in native STARP 20570, indicating that there is an extra α helix in the modified peptide.

Fig. 3 shows the ^{1}H NMR structures of native non-immunogenic peptide 20546 and its modified analogues: the antibody titer-inducing modified peptide **24972** and the modified non-immunogenic peptide**24486**. In each structure, binding motifs and binding register to HLA-DRβ1* molecules are indicated based on the results of binding assays with purified HLA-DRβ1* molecules (Table 2). The residue orientation of the highly immunogenic modified HABP **24972** can be clearly seen in the front view of these molecules (Fig. 3, right hand panel), showing how the Y11 residue (pink) in pocket 5 is downwardly orientated toward the MHC in modified HABPs **24972** and **24486** but does not have the same orientation in native HABP 20546; this same orientation is evidenced in the lateral view of the structures (Fig. 3, central panel).

Moreover, when the structure of the **24972** modified peptide is compared against the structure of the native 20546 peptide (Fig. 3, central panel), the most evident difference is observed in the distance existing between residues fitting into pocket 1 and pocket 9. Such distance is more than 1.3 Å longer in the high-antibody-titer inducing HABP **24972** (21.85 Å), which bound with high capacity to the HLA-DRβ1*0301 molecule, displaying the characteristic binding motifs and binding register for this allele: F7 in Pocket 1, D10 in Pocket 4, Q12 in Pocket 6 and F15 in Pocket 9, which is in complete agreement with the binding motifs and binding registers reported by Marsh et al. [24] for this allele. In spite to the fact that both native 20546 and highly immunogenic modified peptides **24792** and **24320** display the same binding motifs and binding registers to HLA-DRβ1*0301 molecules, reflected in the high binding capacity of all these peptides to this purified Class II molecule, striking differences are observed in HLA-DRβ1*0301 and the putative TCR contacting residues of these peptides. In Fig. 3 it can be clearly seen that in native 20546 HABP, residues fitting into Pockets 4 (E10, dark blue) and 6 (Q12, brown) are awkwardly oriented while in **24972** D10 and Q12, corresponding to residues fitting into Pockets 4 and 6 respectively of this molecule are horizontally oriented to properly fit into the canonical structure of HLA-DRβ1* 0301.

There are also differences in orientation of the lateral chain residues occupying pocket 3 (light blue) and 7 (gray), which are upwardly oriented in opposite direction to the MHC and therefore probably more available to TCR inspection, whereas the same orientation is not observed in native peptide 20546. These data suggest that peptide **24972** displays a different and probably a more appropriate structural conformation to properly fit into the HLA-DRβ1* 0301–**24972**–TCR complex and that modifications performed in residues N5/M, L8/H, S9/V, E10/D, S13/A, and N14/I altered the orientation of these residues and that such modifications shifted the immunological properties of conserved HABP 20546, rendering it into a immunogenic and high-antibody-titer inducing peptide.

A comparative analysis between structured regions of native HABPs and their modified analogues, correlated with their immunological activity, shows that native non-immunogenic HABPs contained different three-dimensional structural conformation when compared with their high-antibody-titer inducing modified analogues. Such was the case of HABP 20546 displaying an α-helix between residues S9–L16, in which modifications done to its critical residues resulted in appearance of two α-helical regions (M5–V9 and I14–G19) in its modified **24972**. In STARP modified peptides **24320** and **24486**, the N14P substitution resulted in a conformational change given that P, being an α helix breaker residue, disrupts the folding of the α helix. Even though proline is located 3 or 1 residues outside the structured region but anyhow inside the sequence of these peptides fitting into this Class II peptide binding region, it produces a conformational change by blocking the continuity of the α helix. This conformation shift might contribute to the appropriate fitting of modified **24972** inside the TCR–Peptide–MHCII complex and the improved immunogenicity shown in *Aotus* monkeys, since no strong conformational changes were evidenced.

The same behavior was evidenced with native HABP 20570 (containing an α helix between residues I4–T15) when compared to its modified high-antibody-titer inducing **24322** analogue (which displayed 2 α-helical regions between M3–K10 and P12–H20).

Please cite this article in press as: Bermúdez A, et al. 3D structure determination of STARP peptides implicated in *P. falciparum* invasion of hepatic cells. Vaccine (2010), doi:10.1016/j.vaccine.2010.05.025

This analogue bound with high affinity to purified HLA-DRβ1*0101 molecules displaying the classical binding motifs and binding registers for this molecule: Y7 in Pocket 1, K10 in Pocket 4, P12 in Pocket 6 and T15 in Pocket 9. The data suggest that when native 20570 is modified in its critical hepatocyte binding residues (L11/H in Pocket 5, D12/P in Pocket 6 and E14/M in Pocket 8), the resulting modified peptide (HABP **24322**) fits into the HLA-DRβ1*0101 molecule, rendering it capable of inducing long-lasting high-antibody titers in *Aotus* monkeys.

The results also show that native 20546 binds promiscuously to different HLA-DRβ1* molecules, whereas its modified highly immunogenic **24972** and **24320** bind preferentially and with high capacity to HLA-DRβ1*0301 molecules while its modified **24486** (non-immunogenic) binds with high capacity to another Class II molecule, HLA-DRβ1*0401. These modified peptides' immunogenic properties were tested in *Aotus* monkeys, which have proven to be an ideal experimental model due to the high similarity existing between their Class II MHC molecules and their human counterparts [25,36]. Both modified peptides (**24972** and **24320**) induced high-antibody titers, whereas the modified **24486** did not induce antibody production in *Aotus* monkeys. Their 3D structure molecular models were thus determined based on ^{1}H NMR spectral parameters and showed that all peptides presented α-helical conformations in different regions of their structure. Native peptides presented less structured regions and different localization of their α helixes when compared with their modified high-antibody-titer inducing analogues, highlighting the important role played by the peptide's structural conformation in the induction of an appropriate immune response.

Therefore, in order for a minimal subunit-based pre-erythrocytic vaccine to be effective, only conserved HABPs of liver stage proteins must be also selected. We suggest that our modified **24972** and **24322** peptides derived from conserved STARP HABPs 20546 and 20570 could be some of these epitopes given that HABP **24322** contains an amino acid sequence known to induce a CTL-associated response in individuals bearing the HLA-A2.2 genetic characteristic [37]. Furthermore, this modified analogue **24322** was capable of inducing long-lasting high anti-sporozoite antibody titers in *Aotus* monkeys, as shown by the data reported in this study.

Therefore, the results of this study show an association between the NMR structures of native and modified STARP HABPs and the antibody responses induced by these peptides in *Aotus* monkeys. The data support the inclusion of modified STARP **24972** and **24320** HABPs, together with the LSA-1 modified **24322**, as liver-stage components of a multi-antigenic, multi-stage, minimal subunit-based, chemically synthesized antimalarial vaccine.

Funding

This research has been supported by the Asociación para la Investigación Solidaria SADAR (Pamplona, Spain 2009) and the Agencia Española de Cooperación Internacional para el Desarrollo AECID (Madrid, Spain 2009). The funders had no role in the study design, data collection and analysis, decision to publish, or the preparation of the manuscript.

Acknowledgements

We would like to thank Nora Martinez for her collaborations during the translation of this manuscript. Aurora Cortes, Jamer Gomez, Vicente Amaya and Oswaldo Escobar for their assistance and collaboration during the conduction of these studies.

References

[1] Fidock DA, Bottius E, Brahimi K, Moelans II, Aikawa M, Konings RN, et al. Cloning and characterization of a novel *Plasmodium falciparum* sporozoite surface antigen, STARP. Mol Biochem Parasitol 1994;64(April (2)):219–32.
[2] Fidock DA, Sallenave-Sales S, Sherwood JA, Gachihi GS, Ferreira-da-Cruz MF, Thomas AW, et al. Conservation of the *Plasmodium falciparum* sporozoite surface protein gene, STARP, in field isolates and distinct species of Plasmodium. Mol Biochem Parasitol 1994;67(October (2)):255–67.
[3] Pasquetto V, Fidock DA, Gras H, Badell E, Eling W, Ballou WR, et al. *Plasmodium falciparum* sporozoite invasion is inhibited by naturally acquired or experimentally induced polyclonal antibodies to the STARP antigen. Eur J Immunol 1997;27(October (10)):2502–13.
[4] Bermudez A, Vanegas M, Patarroyo ME. Structural and immunological analysis of circumsporozoite protein peptides: a further step in the identification of potential components of a minimal subunit-based, chemically synthesised antimalarial vaccine. Vaccine 2008;26(December (52)):6908–18.
[5] Patarroyo ME, Cifuentes G, Rodriguez R. Structural characterisation of sporozoite components for a multistage, multi-epitope, anti-malarial vaccine. Int J Biochem Cell Biol 2008;40(3):543–57.
[6] Lopez R, Garcia J, Puentes A, Curtidor H, Ocampo M, Vera R, et al. Identification of specific Hep G2 cell binding regions in *Plasmodium falciparum* sporozoite-threonine-asparagine-rich protein (STARP). Vaccine 2003;21(June (19–20)):2404–11.
[7] Espejo F, Cubillos M, Salazar LM, Guzman F, Urquiza M, Ocampo M, et al. Structure, immunogenicity, and protectivity relationship for the 1585 malarial peptide and its substitution analogues. Angew Chem Int Ed Engl 2001;40(December (24)):4654–7.
[8] Purmova J, Salazar LM, Espejo F, Torres MH, Cubillos M, Torres E, et al. NMR structure of *Plasmodium falciparum* malaria peptide correlates with protective immunity. Biochim Biophys Acta 2002;1571(May (1)):27–33.
[9] Salazar LM, Alba MP, Torres MH, Pinto M, Cortes X, Torres L, et al. Protection against experimental malaria associated with AMA-1 peptide analogue structures. FEBS Lett 2002;527(September (1–3)):95–100.
[10] Bermudez A, Cifuentes G, Guzman F, Salazar LM, Patarroyo ME. Immunogenicity and protectivity of *Plasmodium falciparum* EBA-175 peptide and its analog is associated with alpha-helical region shortening and displacement. Biol Chem 2003;384(October–November (10–11)):1443–50.
[11] Cifuentes G, Patarroyo ME, Urquiza M, Ramirez LE, Reyes C, Rodriguez R. Distorting malaria peptide backbone structure to enable fitting into MHC class II molecules renders modified peptides immunogenic and protective. J Med Chem 2003;46(May (11)):2250–3.
[12] Cubillos M, Alba MP, Bermudez A, Trujillo M, Patarroyo ME. *Plasmodium falciparum* SERA protein peptide analogues having short helical regions induce protection against malaria. Biochimie 2003;85(July (7)):651–7.
[13] Cifuentes G, Bermudez A, Rodriguez R, Patarroyo MA, Patarroyo ME. Shifting the polarity of some critical residues in malarial peptides' binding to host cells is a key factor in breaking conserved antigens' code of silence. Med Chem 2008;4(May (3)):278–92.
[14] Cifuentes G, Espejo F, Vargas LE, Parra C, Vanegas M, Patarroyo ME. Orientating peptide residues and increasing the distance between pockets to enable fitting into MHC-TCR complex determine protection against malaria. Biochemistry 2004;43(June (21)):6545–53.
[15] Alba MP, Salazar LM, Purmova J, Vanegas M, Rodriguez R, Patarroyo ME. Induction and displacement of an helix in the 6725 SERA peptide analogue confers protection against *P. falciparum* malaria. Vaccine 2004;22(March (9–10)):1281–9.
[16] Houghten RA. General method for the rapid solid-phase synthesis of large numbers of peptides: specificity of antigen-antibody interaction at the level of individual amino acids. Proc Natl Acad Sci USA 1985;82(August (15)):5131–5.
[17] Frayser M, Sato AK, Xu L, Stern LJ. Empty and peptide-loaded class II major histocompatibility complex proteins produced by expression in Escherichia coli and folding in vitro. Protein Expr Purif 1999;15(February (1)):105–14.
[18] Chen YH, Yang JT, Martinez HM. Determination of the secondary structures of proteins by circular dichroism and optical rotatory dispersion. Biochemistry 1972;11(October (22)):4120–31.
[19] Rance M, Sorensen OW, Bodenhausen G, Wagner G, Ernst RR, Wuthrich K. Improved spectral resolution in cosy 1H NMR spectra of proteins via double quantum filtering. Biochem Biophys Res Commun 1983;117(December (2)):479–85.
[20] Bax A, Davis DG. MLEV-17 based two dimensional homonuclear magnetization transfer spectroscopy. J Magn Reson 1985:65.
[21] Jenner J, Meier BH, Backman P, Ernst RR. Investigation of enhance processes by two-dimensional NMR spectroscopy. J Chem Phys 1979;71:4546–5427.
[22] Bermudez A, Alba P, Espejo F, Vargas LE, Parra C, Rodriguez R, et al. Fitting modified HRP-I peptide analogue 3D structure into HLA-DR molecules induces protection against *Plasmodium falciparum* malaria. Int J Biochem Cell Biol 2005;37(February (2)):336–49.
[23] Patarroyo ME, Patarroyo MA. Emerging rules for subunit-based, multiantigenic, multistage chemically synthesized vaccines. Acc Chem Res 2008;41(March (3)):377–86.
[24] Marsh SG, Parham P, Barber LD. The HLA fact book; 2000.
[25] Suarez CF, Patarroyo ME, Trujillo E, Estupinan M, Baquero JE, Parra C, et al. Owl monkey MHC-DRB exon 2 reveals high similarity with several HLA-DRB lineages. Immunogenetics 2006;58(July (7)):542–58.

[26] Sreerama N, Venyaminov SY, Woody RW. Estimation of the number of alpha-helical and beta-strand segments in proteins using circular dichroism spectroscopy. Protein Sci 1999;8(February (2)):370–80.
[27] Sreerama N, Woody RW. Estimation of protein secondary structure from circular dichroism spectra: comparison of CONTIN, SELCON, and CDSSTR methods with an expanded reference set. Anal Biochem 2000;287(December (2)):252–60.
[28] Kabsch W, Sander C. Dictionary of protein secondary structure: pattern recognition of hydrogen-bonded and geometrical features. Biopolymers 1983;22(December (12)):2577–637.
[29] Rodriguez LE, Urquiza M, Ocampo M, Suarez J, Curtidor H, Guzman F, et al. *Plasmodium falciparum* EBA-175 kDa protein peptides which bind to human red blood cells. Parasitology 2000;120(March (Pt 3)):225–35.
[30] Urquiza M, Rodriguez LE, Suarez JE, Guzman F, Ocampo M, Curtidor H, et al. Identification of *Plasmodium falciparum* MSP-1 peptides able to bind to human red blood cells. Parasite Immunol 1996;18(October (10)):515–26.
[31] Patarroyo ME, Cifuentes G, Bermudez A, Patarroyo MA. Strategies for developing multi-epitope, subunit-based, chemically synthesized anti-malarial vaccines. J Cell Mol Med 2008;12(October (5B)):1915–35.
[32] Rodriguez R, Moreno A, Guzman F, Calvo M, Patarroyo ME. Studies in owl monkeys leading to the development of a synthetic vaccine against the asexual blood stages of *Plasmodium falciparum*. Am J Trop Med Hyg 1990;43(October (4)):339–54.
[33] Espejo F, Bermudez A, Torres E, Urquiza M, Rodriguez R, Lopez Y, et al. Shortening and modifying the 1513 MSP-1 peptide's alpha-helical region induces protection against malaria. Biochem Biophys Res Commun 2004;315(March (2)):418–27.
[34] Rodriguez LE, Curtidor H, Urquiza M, Cifuentes G, Reyes C, Patarroyo ME. Intimate molecular interactions of *P. falciparum* merozoite proteins involved in invasion of red blood cells and their implications for vaccine design. Chem Rev 2008;108(September (9)):3656–705.
[35] Patarroyo ME, Cifuentes G, Martinez NL, Patarroyo MA. Atomic fidelity of subunit-based chemically-synthesized antimalarial vaccine components. Prog Biophys Mol Biol 2010;102(January (1)):38–44. Q1
[36] Nino-Vasquez JJ, Vogel D, Rodriguez R, Moreno A, Patarroyo ME, Pluschke G, et al. Sequence and diversity of DRB genes of Aotus nancymaae, a primate model for human malaria parasites. Immunogenetics 2000;51(March (3)):219–30.
[37] BenMohamed L, Thomas A, Druilhe P. Long-term multiepitopic cytotoxic-T-lymphocyte responses induced in chimpanzees by combinations of *Plasmodium falciparum* liver-stage peptides and lipopeptides. Infect Immun 2004;72(August (8)):4376–84.

Please cite this article in press as: Bermúdez A, et al. 3D structure determination of STARP peptides implicated in *P. falciparum* invasion of hepatic cells. Vaccine (2010), doi:10.1016/j.vaccine.2010.05.025

6. CAPÍTULO 2

The high immunogenicity induced by modified sporozoites' malarial peptides depends on their phi (ϕ) and psi (ψ) angles.

Conociendo la importancia que tienen las moléculas HLA-DRβ1*(99) en la respuesta inmune en el tema de vacunas, péptidos modificados pertenecientes a la proteína STARP y CSP del *P. falciparum* fueron seleccionados para realizar un ensayo de inmunización y una evaluación de su conformación estructural entre moléculas HLA-DRβ1*. Teniendo en cuenta el registro de unión a estas moléculas, se realizó la superposición del péptido de interés y se identificó que la distancia interatómica entre los átomos de los residuos más lejanos que ajustan entre el bolsillo 1 al bolsillo 9 es mayor siempre en los péptidos modificados inductores de anticuerpos que en los nativos, así como el número de interacciones de puentes de hidrógeno entre el esqueleto del péptido y las cadenas laterales de la molécula HLA-DRβ1* probablemente estabilizando el complejo formado (MHCII-péptido) y permitiendo posiblemente la activación del receptor de células T e induciendo una respuesta inmune. Adicionalmente el análisis de los ángulos diedros φ y ψ de los péptidos del estudio proporcionó como resultado una tendencia a una conformación del tipo $PPII_L$ suministrando un posible complemento a dicha respuesta.

Biochemical and Biophysical Research Communications xxx (2012) xxx–xxx

Contents lists available at SciVerse ScienceDirect

Biochemical and Biophysical Research Communications

journal homepage: www.elsevier.com/locate/ybbrc

The high immunogenicity induced by modified sporozoites' malarial peptides depends on their phi (ϕ) and psi (ψ) angles

Manuel E. Patarroyo[a,b,*], Adriana Bermudez[a,c], Martha P. Alba[a,c]

[a] Fundación Instituto de Inmunología de Colombia (FIDIC), Bogotá, Colombia
[b] Universidad Nacional de Colombia, Bogotá, Colombia
[c] Universidad del Rosario, Bogotá, Colombia

ARTICLE INFO

Article history:
Received 12 October 2012
Available online xxxx

Keywords:
Plasmodium falciparum
Antimalarial-vaccine
Pre-erythrocyte stage
HLADRβ* molecules
ϕ and ψ angles

ABSTRACT

The importance of CSP- and STARP-derived ϕ and ψ dihedral angles in mHABP structure was analysed by ^{1}H NMR in the search for molecules which can be included as components of a first-line-of-defence *Plasmodium falciparum* sporozoite multi-epitope vaccine against the most lethal form of human malaria. Most of the aforementioned dihedral angles were left-hand-like polyproline type II ($PPII_L$) structures whilst others had right-hand-like α-helix (α_R), thus allowing mHABPS to fit better into MHCII molecules and thereby form an appropriate pMHCII complex and also establish the H-bonds which stabilise such complex and by this means induce an appropriate immune response. This information has great implications for vaccine development, malaria being one of them.

1. Introduction

Developing a totally effective and definitive vaccine against the main parasite causing human malaria (*Plasmodium falciparum*, producing ~200 million cases and 1.2 million deaths annually) [1] needs highly immunogenic components in its first line-of-defence, such as molecules from the parasite's sporozoite (the parasite form which invades liver cells after being inoculated during an infected *Anopheles* mosquito's bite) [2].

However, obtaining enough amounts of sporozoites for biological, biochemical, functional and immunological studies from the mosquito's salivary glands where they are localised is not an easy task but rather a very difficult one. It is equally impossible to culture sporozoites *in vitro* [2,3] and a lack of *Anopheles* mosquito strains which have been adapted for infecting *Aotus* monkeys further hampers developing a totally effective vaccine against this stage and thus against this deadly disease.

Our institute has thus opted for defining the principles or rules for developing second-line-of-defence vaccines by working with the merozoite, the parasite's infective form which invades the red blood cells (RBCs). This is easily cultured and can be obtained in large amounts from infected blood *in vivo* or *in vitro* [4] for biological, biochemical and immunological studies. Such rules can then be applied to developing a totally effective vaccine against the sporozoite stage.

Our institute has also taken advantage of having access to the *Aotus* monkey which is an appropriate experimental model for studying merozoites; it has a ~90–100% identical immunological system to that of humans [5]. These monkeys can be easily infected by intravenous route and such monkeys' blood can be monitored daily regarding the development of the disease (or parasitaemia) by simple methods such as Giemsa staining or fluorescence (Acridine Orange) or molecular biology (PCR).

Plasmodium falciparum genome encodes ~5600 proteins, ~50 of which have been found to be involved in merozoite invasion of RBC in elegant proteome studies [6] and it has been calculated that a similar number of sporozoite proteins is involved in invasion of hepatocytes [7]. Our group has identified conserved amino acid sequences having high specific binding capacity to both RBC and hepatocytes which are involved in the invasion of such cells, called conserved **h**igh **a**ctivity **b**inding **p**eptides (cHABPs). Their critical residues have been identified, as well as fundamental residues establishing H-bonds with other cHABPs or with receptor molecules [8] for designing modified HABPs (mHABPs) according to thoroughly-described previously established principles and rules [9–11] and thus converting such immunologically silent cHABPs into highly immunogenic, protection-inducing mHABPs.

Based on such principles and rules, our group has identified cHABPs from ~20 sporozoite proteins [12,13] which have been recognised to date as being involved in sporozoite traverse of endothelial and Kuppfer cells to reach and invade hepatocytes, the circumsporozoite protein (CSP) [14] and the sporozoite threonine- and asparagine-rich protein (STARP).

* Corresponding author at: Fundación Instituto de Inmunología de Colombia (FIDIC) Bogotá, Colombia. Fax: +57 1 4815269.
E-mail address: mepatarr@gmail.com (M.E. Patarroyo).

0006-291X/$ - see front matter © 2012 Elsevier Inc. All rights reserved.
http://dx.doi.org/10.1016/j.bbrc.2012.10.088

The modifications made to sporozoite cHABPs have led to developing mHABPs inducing high antibody titres when inoculated into *Aotus* monkeys, as determined by immunofluorescence antibody test (IFA), using sporozoites from infected mosquitoes salivary glands or by Western blot (WB) or ELISA test using their respective recombinant proteins.

Ascertaining these cHABP and mHABP 3D structure by ^{1}H NMR has led to showing that such modifications provide a better fit into the trimolecular complex formed by molecules from the major histocompatibility complex class II-peptide-T-cell receptor (MHCII-p-TCR) [15].

The accompanying paper by our group has shown that merozoite-derived mHABPs which were highly immunogenic and induced protection against experimental challenge in *Aotus* monkeys had a specific 3D structure which was associated with left-handed-polyproline type II ($PPII_L$) and/or left-handed α-helix (α_L) physical–chemical characteristics [16], with defined ϕ and ψ torsion angles ensuring a perfect fit into the MHCII-p-TCR complex, to induce a highly immunogenic, protection-inducing response [15].

This manuscript has thus been aimed at describing the development and analysis of CSP-derived [17,18] and STARP-derived mHABPs [19,20] to include them as first-line-of-defence components (the sporozoite) in a totally effective and definitive multi-epitope, multistage minimal subunit-based, chemically-synthesised [9,12] antimalarial vaccine.

2. Materials and methods

Peptide synthesis, *Aotus* immunizations, mHABPs' 3D structure determined by 1H NMR and superimposition studies onto HLA-DRβ1* molecules have been previously reported and have been summarised in a previous accompanying paper [21]. Sporozoites for IFA studies were purchased from Sanaria Inc. (Bethesda. USA). WB analysis was performed with STARP, CSP-N-terminal construct 2 and CSP-C-terminal recombinant proteins which were kindly provided by Professors Pierre Druille (Institute Pasteur, France), Mauricio Calvo Calle (Boston University) and Manuel Alfonso Patarroyo (FIDIC), respectively.

3. Results and discussion

3.1. Immunological studies

It has been thoroughly demonstrated [9] that cHABPs must be specifically modified to render them highly immunogenic and protection-inducing mHABPs against intravenous experimental challenge with a highly virulent *Aotus*-adapted *P. falciparum* strain, thereby opening the way forward for vaccine development (i.e., malaria).

Unfortunately, the Santa Lucia strain (the only *P. falciparum* strain adapted to *Anopheles* mosquitoes for transmitting malarial infection via sporozoites to *Aotus* monkeys via direct mosquito bites) gives very weird and irreproducible results, leaving immunogenicity (as assessed by different methods) as the only way to determine a sporozoite protein-induced humoral immune response.

The most relevant protein in sporozoite invasion (CSP) has two non-antigenic, non-immunogenic cHABPs (4383 and 4388 according to our institute's serial numbering system) [17]; they have become highly immunogenic when they have been properly modified (mHABP are indicated in bold numbers from this point onwards whilst native cHABPs are not shown in bold but in parenthesis) [18]. These were **25608** (4383) and **32958** (4388) which induced very high antibody titres as assess by IFA (Fig. 1B) [18] and reacted with sporozoite membrane, as determined by double immunofluorescence (**25608** shown in red in Fig. 1C and **32958** in Fig. 1D).

STARP, another very important molecule in sporozoite invasion, contained highly relevant cHABP 20546 [19] which, when properly modified as **24320,** became highly immunogenic in *Aotus* monkeys as assessed by IFA titres (Fig. 1B) and Western blot (WB) [20]. **24320** mHABP reacted with sporozoite membrane and small intracytoplasmatic structures (Fig. 1C and D green), probably corresponding to the micronemes where it is deposited before translocation to the membrane. STARP ranked second in importance in a prospective study using protein microarrays carried out in Mali regarding Ab response to *P. falciparum* before and after the malaria season in such hyper-endemic area [22]; the importance of identifying this mHABP as a component in a fully-protective multistage, multi-epitope antimalarial vaccine can thus be seen.

The fact that some regions of these highly immunogenic mHABPs (also protection-inducing against merozoites) could adopt configurations different to the canonical $PPII_L$, such as the α_L region in **10014.35** or α_R in **24320.18**, has suggested that some other transitional structures could fit into the MHCII PBR to be presented to the TCR to induce an appropriate immune response as long as they could form a stable MHCII-p-TCR complex [22].

These *Aotus*' sera also reacted with their corresponding recombinant proteins or their fragments in WB in such a way that anti-**25608** sera recognised 36 kDa MW CSP N-terminal construct 2 where only the last 5 residues were present [18], **32958** reacted with 10 kDa CSP C-terminal fragment (including residues 283–379 where 4383 cHABP was present) and anti-**24320** reacted with the complete 68 kDa recombinant STARP molecule [20] (Fig. 1E).

Amino-acid replacements in these cHABPs clearly induced modifications in their peptides' 3D structure, changing 4383 random structure into a mHABP having a type II-β-turn in **25608**. By the same token, 4388 random structure became changed in **32958** into a mHABP having a type I-β-turn [18] and the α-helix from S9-to L16 in 20546 became displaced to K3 to D10 in **24320** [20].

The aforementioned modifications involved some other biological implications associated with changes in their immunological behaviour, such as binding to HLA-DRβ1* molecules (Fig. 1B); i.e., CSP 4383 did not bind to any of the HLA-DRβ1* purified molecules studied here, but **25608** had high binding capacity (58%) to HLA-DRβ1*0401, also displaying the characteristic binding motifs and binding registers for this molecule. Something similar occurred with cHABP 4388 which did not bind to any HLA-DRβ1* purified molecule but **32958** carrying both HLA-DRβ1*0101 and HLA-DRβ1*0401 binding motifs and registers, simultaneously bound to them with high capacity (65% and 52%, respectively) [18]. The latter was chosen for superposition studies; STARP cHABP 20546 was highly promiscuous regarding its binding to HLA-DRβ1* purified molecules, binding to practically all of them, (Fig. 1B) but mHABP **24320** displaying the binding motifs and registers characteristic of HLA-DRβ1*0301 and HLA-DRβ1*0101 binding to both (even though weakly so to the latter) [20]. High HLA-DRβ1*0101 binding capacity was assumed for technical reasons.

3.2. Structural characteristics

Previous papers with highly immunogenic, protection-inducing, merozoite protein-derived mHABPs [9] and sporozoite protein-derived mHABPs [12,18,20,23] have shown that the distance between the furthest atoms capable of fitting into HLA-DRβ1* pockets 1 to 9 was 27.50 Å for **25608.37**, 27.10 Å for **32958.2** and 21.35 Å for **24320.18** conformers (Fig. 2A, D, G), this being a perfect distance to fit into MHCII molecules' most distant and relevant pockets.

Since steric restriction has been recognised as the major organisational force in proteins, and the amide bond being planar, each

Please cite this article in press as: M.E. Patarroyo et al., The high immunogenicity induced by modified sporozoites' malarial peptides depends on their phi (φ) and psi (ψ) angles, Biochem. Biophys. Res. Commun. (2012), http://dx.doi.org/10.1016/j.bbrc.2012.10.088

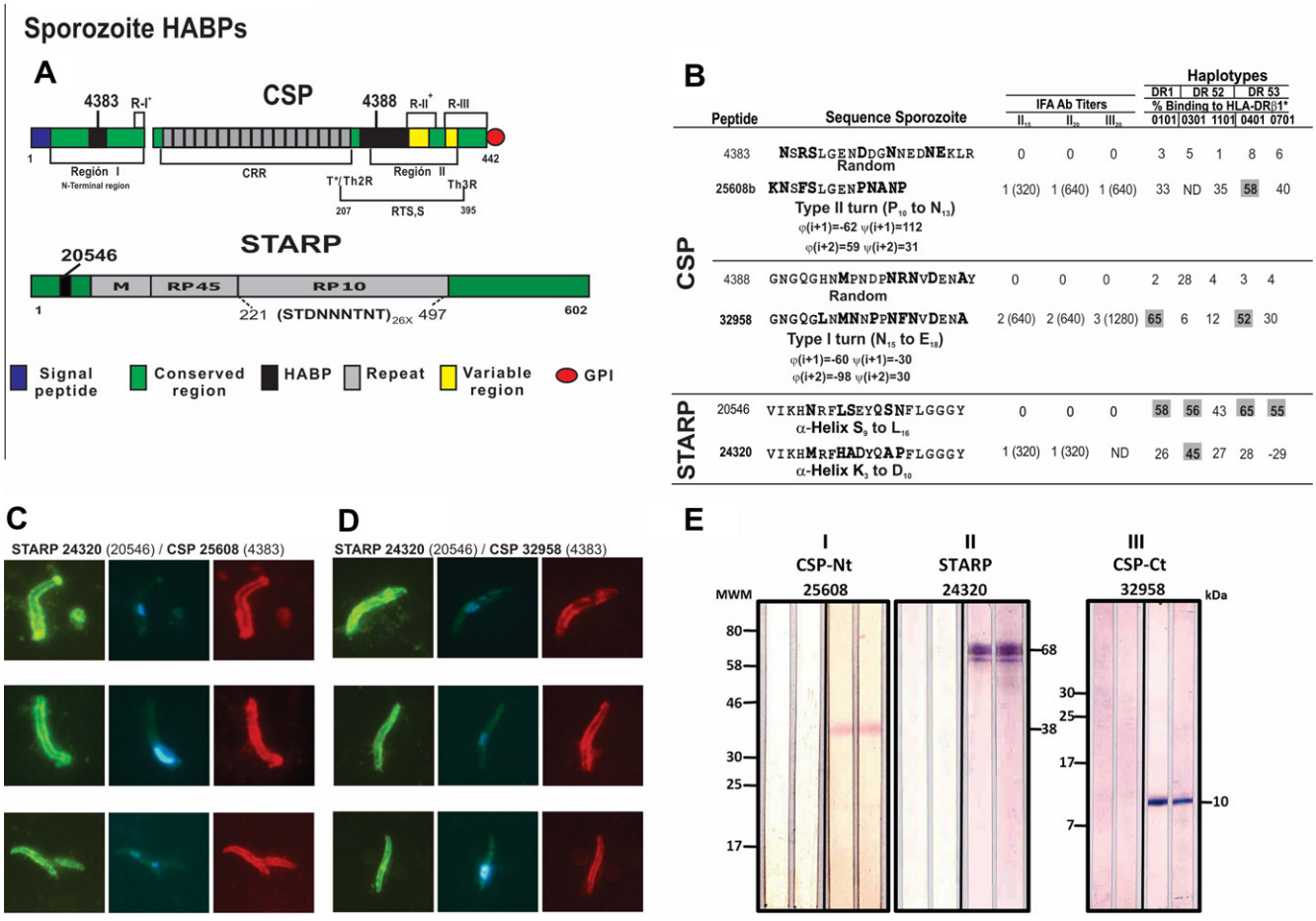

Fig. 1. (A) CSP and STARP molecule schematic representation according to the colour code below, showing cHABP localisation in vertical black bars; the bar length corresponds to approximate molecular weight. (B) CSP and STARP with their corresponding amino acid sequences and structural features elucidated by ^{1}H NMR; antibody titres as assessed by IFA against cHABP- and mHABP-induced sporozoites (in bold). Their capacity to bind to HLA-DRβ1* purified allele molecules where >50% binding (shadowed) was considered positive. (C) and (D) Double immunofluorescence (IFA) assays for sporozoite protein patterns and localisation, determined with high antibody titre sera produced in *Aotus* monkeys immunised with mHABPs. *Aotus* antibodies against STARP-modified HABP **24320** (20546) used at 1:40 dilution, detected with fluorescein isothiocyanate (FITC)-labelled goat purified IgG directed against *Aotus* IgG (1:100 dilution) displaying a green membrane fluorescence and small intracytoplasmatic dots inside the sporozoite. *Aotus* anti-CSP mHABP **25608** (4383) and anti-**32958** (4388) reactivity (serum dilution 1:100) detected by purified goat IgG anti-*Aotus* IgG conjugate with rhodamine isothyocynate (RITC), diluted 1:10, showing red membrane fluorescence. For reference, the localisation of the sporozoite's nucleus detected by 4,6 diamino-2phenylindole (DAPI) (bright blue). Sporozoites were purchased from Sanaria Inc: Bethesda USA. (E) Western blot analysis showing *Aotus* monkey reactivity. In panel I, sera from monkeys immunised with **25608** (4383), reacting with recombinant CSP construt 2 having 35 kDa MW; in panel II **24320** (20560) immunised monkeys' sera reactivity with rSTARP (68 kDa MW) and panel III anti **32958** (4388) monkey sera reacting with rCSP C-terminal (10 kDa MW).

peptide has only two degrees of freedom: ϕ and ψ; this is limited by atom clashes which "disallow" their minimal energy configurations. The two dihedral angles in question were thus obtained from ^{1}H NMR information choosing these mHABPs' lowest energy conformer (numbered according to our institute's serial number, followed by a dot and its corresponding conformer number) to identify their role in immunogenicity and protection (as shown in the accompanying paper) induced by these mHABPs in our endeavour to ensure a logical and rational methodology for fully-protective, definitive vaccine development.

Two contiguous left-handed polyproline II-like helices ($PPII_L$) were clearly identified in the CSP-derived **25608.37** conformer (Fig. 2B, highlighted in green), ϕ angles ranging from −91.8° to −46.5° (−93.5 ± 25° canonical range) and +149.4° to +85.1° for the ψ angles (+135 ± 20° canonical range) [24–28]. Such angles formed part of a sequence also displaying a $PPII_L$-like structure three residues upstream, thereby confirming, together with the other two mHABPs, the elegant work by Jardetzky et al., [29] that the predominant structures bindings to class II molecules display $PPII_L$-like structural characteristics.

Modifying the HLA-DRβ1*0401 molecule according to the amino-acid sequence differences found in the *Aotus* [15] in HLA-DRβ1*0422 led to 12 H-bonds (<4.0 Å distance) spontaneous formation when the **25608.37** conformer was superimposed onto HLA-DRβ1*0422 (Fig. 2C and Table 1) without any further manipulation, keeping in mind that these two molecules' 3D structures were determined by two different methodologies (^{1}H NMR for mHABPs and X-ray crystallography for HLA-DRβ1* molecules). The foregoing striking and outstanding finding confirmed that mHABPs must be properly modified to render them highly immunogenic, thereby fitting perfectly well into MHCII molecules, as elegantly shown by other groups and that such interaction largely depends on mHABPs structural conformation as dictated by ϕ and ψ dihedral angle rotations.

25608.37 formed five 9–11-member ring bidentate H-bonds with Sα53, Nβ82, Qα9, Nα62 and Kβ71 and established a single H-bond between Nα69 and Wβ61 (Fig. 2C and Table 1), anchoring it very stably to HLA-DRβ1*0422 to induce a very high immune response, as assessed by different immunological methods. It is worth mentioning that, although HLA-DRβ1*0422 occurs very frequently in the *Aotus* population (~20%), it is relatively rare in humans (<5%).

The **32958.2** conformer also displayed two sequential $PPII_L$ structures (Fig. 2E, highlighted in green) involving residues p2N

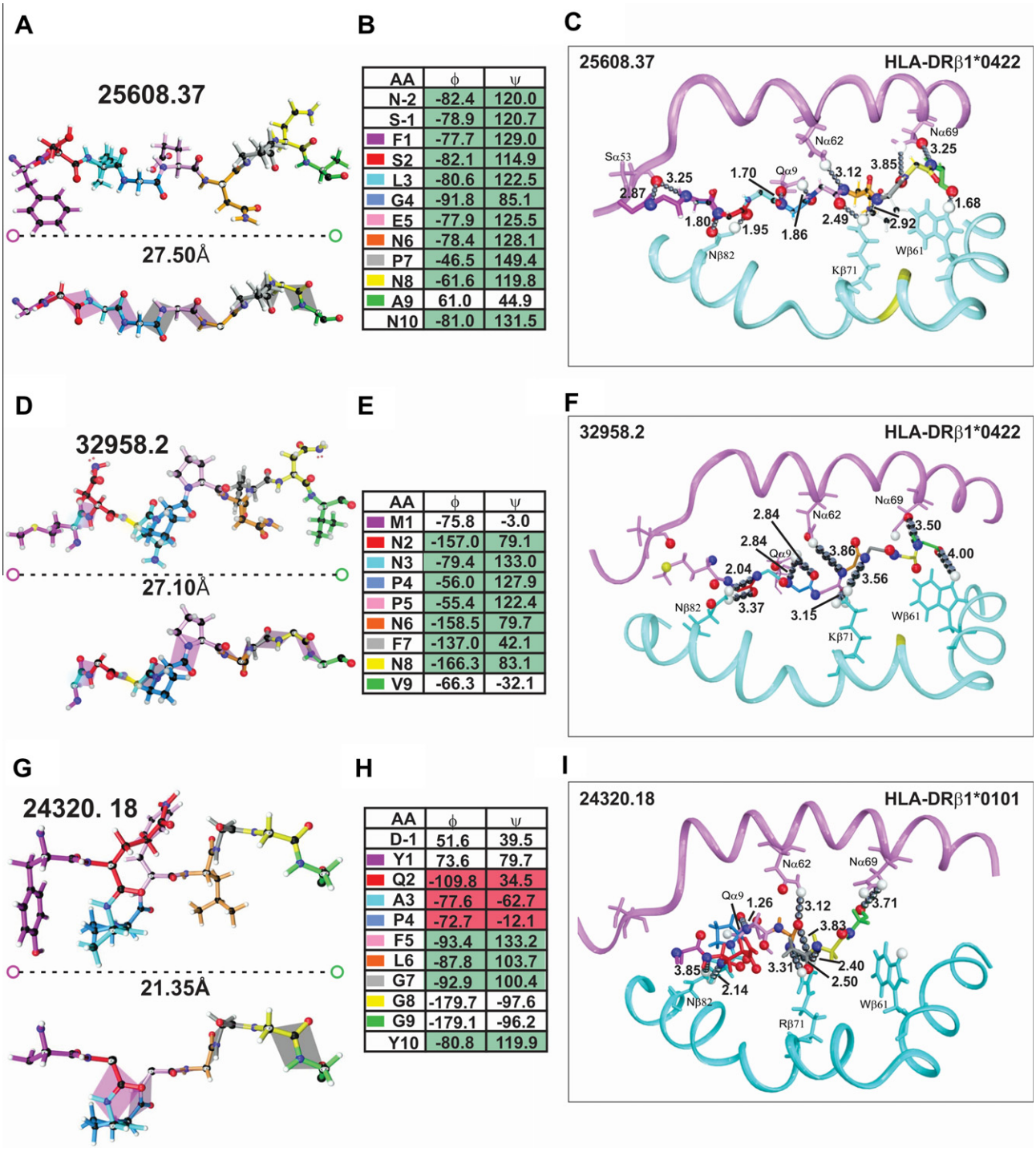

Fig. 2. Left panel: Lowest energy conformer 3D structure determined by 1H NMR, identified by our serial number followed by dot and corresponding conformer number (A) CSP **25608**.37 (4383), (D) CSP **32958**.2 (4388) and (G) STARP **24320**.18 (25608). Central panel: B, E, H dihedral angles ϕ and ψ for the corresponding conformer. Right panel: C, F, I superimposition of mHABPs determined by ^{1}H NMR on HLA-DRβ1* molecules and their inter-atomic distances between peptide backbone and HLA-DR lateral chain atoms. (C) **25608**.37 and (F) **32958**.2 on HLA-DRβ1*0422 and (I) **24320**.18 on HLA-DRβ1*0101.

to p5P within the first $PPII_L$ segment, containing four residues, and p6N to p8N within the second one containing three residues, both being characteristic of $PPII_L$-helices [24]; their ϕ and ψ dihedral angles very closely followed the characteristics for the $PPII_L$ structures described in the accompanying article.

Eight H-bonds and one van der Waals (vdW) interaction were established between **32958**.2 backbone atoms and HLA-DRβ1*0422 lateral chains' atoms when **32958**.2 was superimposed onto the same HLA-DRβ1*0422 3D structure (Fig. 2F and Table 1).

Three bidentate 9–11-member ring H-bonds [28] were spontaneously formed between Nβ82 with p2N, Qα9 with p4P and Kβ71 with p5P and p7F while Nα62, Nα69 and Wβ61 formed individual H-bonds with p5P, p9V and p9V, respectively (Fig. 2F and Table 1); this led to a very stable pMHCII complex involving **32958.2** being formed, partly explaining this mHABP's very high immunogenicity.

The situation with STARP-derived **24320.18** conformer was slightly different as this mHABP was shorter than the other two, (21.35 Å), confirming that the inter-atom distance between the

Please cite this article in press as: M.E. Patarroyo et al., The high immunogenicity induced by modified sporozoites' malarial peptides depends on their phi (ϕ) and psi (ψ) angles, Biochem. Biophys. Res. Commun. (2012), http://dx.doi.org/10.1016/j.bbrc.2012.10.088

Table 1
Atoms involved in H-bond formation between mHABPs and their corresponding HLA-DRβ1* molecule lateral chains. Distances shown for these H-bonds in Å are represented by silver dots.

A.			B.			C.		
	P1 P9 KNSFSLGENPNANP			P1 P9 GNGQGLNMNNPPNFNVDENA			P1 P9 VIKHMRFHADYQAPFLGGGY	
HLA-DRb1*0422	**25608.37**	Distance Å	HLA-DRb1*0422	**32958.2**	Distance Å	HLA-DRβ1*0101	**24320.18**	Distance Å
Sα53:O	HN:S-1	3.81	Nβ82:Hδ21	N:N2	2.04	Nβ82:Hδ21	N:A3	2.14
Sα53:O	HN:F1	3.67	Nβ82:Hδ22	O:N2	3.37	Nβ82:Hδ22	N:Q2	3.85
Nβ82:Hδ21	O:S2	1.95	Qα9:Hε22	N:P4	2.84	Qα9:Hε22	N:P5	1.26
Nβ82:Oδ1	HN:S2	1.8	Qα9:Hε22	O:P4	2.84	Nα62:Hδ22	O:L6	3.12
Qα9:Oε1	HN:G4	1.7	Nα62:Hδ22	N:P5	3.86	Nβ69:Hδ21	O:G9	3.71
Qα9:Hε22	O:G4	1.86	Nα69:Oδ1	HN:V9	3.1	Rβ71:HH21	O:L6	3.83
Nα62:Hδ21	O:P7	3.85	Kβ71:HH11	N:F7	3.56	Rβ71:HH21	N:G8	2.4
Nα62:Hδ22	N:N6	3.12	Kβ71:HH13	O:P5	3.15	Rβ71:HH21	N:G7	2.5
Nα69:Oδ1	HN:A9	2.44	Wβ61:Hε1	O:V9	4	Rβ71:HH12	N:G7	3.31
Kβ71:HH11	N:P7	2.92						
Kβ71:HH12	O:E5	2.49						
Wβ61:Hε1	O:A9	1.68						

furthest atoms fitting into p1 and p9 was 23.5 ± 2.5 Å, as we have thoroughly shown for merozoite-derived mHABPs [9].

The dihedral angles in this mHABP adopted a particular conformation involving a typical $PPII_L$ from p5F to p7G (−93.4° to −87.8° in ϕ and +133.2° to +100.4° in ψ) [27] (Fig. 2H, highlighted in green); however, as in some merozoite highly-immunogenic, protection-inducing mHABPs reported in the accompanying paper, there was a deviation from this rule with other structures different to $PPII_L$.

24320.18 mHABP conformer had a right-handed-like α-helix (α_R) region having ϕ −109.8° to −72.7° to and ψ −62.7° to +34.5° (Fig. 2H, highlighted in pink), such angles corresponded to this helical structure spanning p2Q to p4P, suggesting that some other structures besides the canonical $PPII_L$ structure [29] could be implicated in the binding to HLA-DRβ1* molecules to form an appropriate pMHCII complex and thereby induce an appropriate immune response. Hypothetically, such non-canonical structures could have high segmental atomic mobility in some areas (as occurs with Ab reacting regions in a protein) [30] thereby partly explaining their promiscuity in binding to HLA-DRβ1* molecules as another mechanism to escape immune pressure.

Nine H-bonds were spontaneously formed when **24320.18** was superimposed onto HLA-DRβ1*0101 3D structure without any modifications having been made, as explained before (Fig. 2I and Table 1). One was a bidentate 9-member ring H-bond between Nβ82 lateral chain atoms and p2Q and p3A and a very complex chain of H-bonds between Rβ71 and p5L and consecutive glycines p7G and p8G; the others consisted of three individual H-bonds established between Qα9 with p5P, Nα62 with p6L and Nα69 with p9G, showing that other structures than $PPII_L$ could also activate a high immune response, as shown for this mHABP.

In support of such molecule segmental atomic mobility we could cite Porter and Rosen's argument [31] for a new folding pathway of proteins where consecutive intermediates could successfully maintain an unbroken series of intra-molecular H-bonds. $PPII_L$ is frequently found in conditions following an H-bond low energy pathway (preserving intermediates) traversing a progressive continuum from β-turns to 3_{10}, to α_R-helices (α) through a bridge region defined by an area having $\phi = -80$ and $\psi = 30$, in such a way that the proposed low energy pathway would follow a sequence of events regarding their ϕ and ψ angles: $PPII_L$ (−60; 150) ↔ inverse γ-turn (−75; 80), hybrid turn (h) (−90; 35), bridge turn (b) (−90; 0.0), α-helices (α) (60; −40). This would facilitate switching handedness from left to right, without breaking any H-bonds and thus partly explaining $PPII_L$ transition into an α_R-helix, as occurred in **24320.18** mHABP; such situation was much more observable in ^{1}H NMR structures as occurred with our HABPs which are in solution than in rigid crystal structures as determined by X-ray crystallography.

This, and the accompanying paper, have clearly demonstrated that these principles or rules can be universally applied based on the following: (a) they deal with mHABPs derived from different proteins, performing different biological functions, (b) they are derived from different *P. falciparum* stages (sporozoites and merozoites) infecting different cell types and (c) when properly modified, they bind to different HLA-DRβ1* alleles corresponding to different haplotypes covering most of the genetic traits controlling specific humoral immune responses: HLA-DRβ1*0101 represents the HLA DR1 haplotype (including HLA-DRβ1*0101, 0104, 1001, etc.), HLA-DRβ1*0301 represents HLA DR52 (including HLA-DRβ1*03, 08, 11, 12, 13, 14) alleles and HLA-DRβ1*04 represents HLA DR53 (including HLA-DRβ1*04, 07, 09). The data presented here could thus be applied to any vaccine.

Physical–chemical rules determined by ϕ and ψ dihedral angles could thus be applied to a logical and rational methodology for a definitive minimal subunit-based, multi-epitope, multistage, chemically-synthesised, fully-protective vaccine, an antimalarial vaccine being one of them.

Acknowledgments

We would like to thank Mr. Jason Garry or reviewing this manuscript and making appropriate corrections to the use of English.

References

[1] C.J. Murray, L.C. Rosenfeld, S.S. Lim, K.G. Andrews, K.J. Foreman, D. Haring, N. Fullman, M. Naghavi, R. Lozano, A.D. Lopez, Global malaria mortality between 1980 and 2010: a systematic analysis, Lancet 379 (2012) 413–431.
[2] P. Sinnis, A. Coppi, A long and winding road: the Plasmodium sporozoite's journey in the mammalian host, Parasitol. Int. 56 (2007) 171–178.
[3] R. Menard, V. Heussler, M. Yuda, V. Nussenzweig, Plasmodium pre-erythrocytic stages: what's new?, Trends Parasitol 24 (2008) 564–569.
[4] W. Trager, J.B. Jensen, Human malaria parasites in continuous culture, Science 193 (1976) 673–675.
[5] C.F. Suarez, M.E. Patarroyo, E. Trujillo, M. Estupinan, J.E. Baquero, C. Parra, R. Rodriguez, Owl monkey MHC-DRB exon 2 reveals high similarity with several HLA-DRB lineages, Immunogenetics 58 (2006) 542–558.
[6] Z. Bozdech, M. Llinas, B.L. Pulliam, E.D. Wong, J. Zhu, J.L. DeRisi, The transcriptome of the intraerythrocytic developmental cycle of *Plasmodium falciparum*, PLoS Biol. 1 (2003) E5.
[7] L. Florens, M.P. Washburn, J.D. Raine, R.M. Anthony, M. Grainger, J.D. Haynes, J.K. Moch, N. Muster, J.B. Sacci, D.L. Tabb, A.A. Witney, D. Wolters, Y. Wu, M.J. Gardner, A.A. Holder, R.E. Sinden, J.R. Yates, D.J. Carucci, A proteomic view of the *Plasmodium falciparum* life cycle, Nature 419 (2002) 520–526.
[8] M.E. Patarroyo, G. Cifuentes, C. Pirajan, A. Moreno-Vranich, M. Vanegas, Atomic evidence that modification of H-bonds established with amino acids critical for

host-cell binding induces sterile immunity against malaria, Biochem. Biophys. Res. Commun. 394 (2010) 529–535.
[9] M.E. Patarroyo, A. Bermudez, M.A. Patarroyo, Structural and immunological principles leading to chemically synthesized, multiantigenic, multistage, minimal subunit-based vaccine development, Chem. Rev. 111 (2011) 3459–3507.
[10] L.M. Salazar, M.P. Alba, H. Curtidor, A. Bermudez, E.V. Luis, Z.J. Rivera, M.E. Patarroyo, Changing ABRA protein peptide to fit into the HLA-DRbeta1*0301 molecule renders it protection-inducing, Biochem. Biophys. Res. Commun. 322 (2004) 119–125.
[11] M.P. Alba, L.M. Salazar, L.E. Vargas, M. Trujillo, Y. Lopez, M.E. Patarroyo, Modifying RESA protein peptide 6671 to fit into HLA-DRbeta1* pockets induces protection against malaria, Biochem. Biophys. Res. Commun. 315 (2004) 1154–1164.
[12] H. Curtidor, M. Vanegas, M.P. Alba, M.E. Patarroyo, Functional, immunological and three-dimensional analysis of chemically synthesised sporozoite peptides as components of a fully-effective antimalarial vaccine, Curr. Med. Chem. 18 (2011) 4470–4502.
[13] J.E. Garcia, A. Puentes, M.E. Patarroyo, Developmental biology of sporozoite-host interactions in *Plasmodium falciparum* malaria: implications for vaccine design, Clin. Microbiol. Rev. 19 (2006) 686–707.
[14] S. Kappe, T. Bruderer, S. Gantt, H. Fujioka, V. Nussenzweig, R. Menard, Conservation of a gliding motility and cell invasion machinery in Apicomplexan parasites, J. Cell Biol. 147 (1999) 937–944.
[15] M.A. Patarroyo, A. Bermudez, C. Lopez, G. Yepes, M.E. Patarroyo, 3D Analysis of the TCR/pMHCII complex formation in monkeys vaccinated with the first peptide inducing sterilizing immunity against human malaria, PLoS One 5 (2010) e9771.
[16] M. Novotny, G.J. Kleywegt, A survey of left-handed helices in protein structures, J. Mol. Biol. 347 (2005) 231–241.
[17] J.E. Suarez, M. Urquiza, A. Puentes, J.E. Garcia, H. Curtidor, M. Ocampo, R. Lopez, L.E. Rodriguez, R. Vera, M. Cubillos, M.H. Torres, M.E. Patarroyo, *Plasmodium falciparum* circumsporozoite (CS) protein peptides specifically bind to HepG2 cells, Vaccine 19 (2001) 4487–4495.
[18] A. Bermudez, M. Vanegas, M.E. Patarroyo, Circumsporozoite components of a multiantigenic, subunit-based, synthetic, antimalarial vaccine, Vaccine 26 (2008) 6908–6918.
[19] R. Lopez, J. Garcia, A. Puentes, H. Curtidor, M. Ocampo, R. Vera, L.E. Rodriguez, J. Suarez, M. Urquiza, A.L. Rodriguez, C.A. Reyes, C.G. Granados, M.E. Patarroyo, Identification of specific Hep G2 cell binding regions in *Plasmodium falciparum* sporozoite-threonine-asparagine-rich protein (STARP), Vaccine 21 (2003) 2404–2411.
[20] A. Bermudez, M.P. Alba, M. Vanegas, M.E. Patarroyo, 3D structure determination of STARP peptides implicated in *P. falciparum* invasion of hepatic cells, Vaccine 28 (2010) 4989–4996.
[21] M.E. Patarroyo, A. Moreno-Branich, A. Bermudez, Phi (Φ) and psi (Ψ) angles in malarial peptide bonds determine sterile protective immunity, Biochem. Biophys. Res. Commun. (in Press) Q3
[22] P.D. Crompton, M.A. Kayala, B. Traore, K. Kayentao, A. Ongoiba, G.E. Weiss, D.M. Molina, C.R. Burk, M. Waisberg, A. Jasinskas, X. Tan, S. Doumbo, D. Doumtabe, Y. Kone, D.L. Narum, X. Liang, O.K. Doumbo, L.H. Miller, D.L. Doolan, P. Baldi, P.L. Felgner, S.K. Pierce, A prospective analysis of the Ab response to *Plasmodium falciparum* before and after a malaria season by protein microarray, Proc. Natl. Acad. Sci. USA 107 (2010) 6958–6963.
[23] M.E. Patarroyo, A. Bermudez, A. Moreno-Branich, Towards the development of fully-protective *P. falciparum* anti-malarial vaccine, Expert Rev. (in Press)
[24] R.V. Pappu, G.D. Rose, A simple model for polyproline II structure in unfolded states of alanine-based peptides, Protein Sci. 11 (2002) 2437–2455.
[25] W.G. Han, J. Jalkanen, M. Elstener, S. Suhai, Theoretical study of aqueous N-acetyl-l-alanine N′-methylamide: structures and Raman, VCD, and ROA spectra, J. Phys. Chem. B 102 (1998) 2587–2602.
[26] Z. Shi, K. Chen, Z. Liu, N.R. Kallenbach, Conformation of the backbone in unfolded proteins, Chem. Rev. 106 (2006) 1877–1897.
[27] J.C. Horng, R.T. Raines, Stereoelectronic effects on polyproline conformation, Protein Sci. 15 (2006) 74–83.
[28] A.A. Adzhubei, M.J. Sternberg, Left-handed polyproline II helices commonly occur in globular proteins, J. Mol. Biol. 229 (1993) 472–493.
[29] T.S. Jardetzky, J.H. Brown, J.C. Gorga, L.J. Stern, R.G. Urban, J.L. Strominger, D.C. Wiley, Crystallographic analysis of endogenous peptides associated with HLA-DR1 suggests a common, polyproline II-like conformation for bound peptides, Proc. Natl. Acad. Sci. USA 93 (1996) 734–738.
[30] J.A. Tainer, E.D. Getzoff, H. Alexander, R.A. Houghten, A.J. Olson, R.A. Lerner, W.A. Hendrickson, The reactivity of anti-peptide antibodies is a function of the atomic mobility of sites in a protein, Nature 312 (1984) 127–134.
[31] L.L. Porter, G.D. Rose, Redrawing the Ramachandran plot after inclusion of hydrogen-bonding constraints, Proc. Natl. Acad. Sci. USA 108 (2011) 109–113.

7. CAPÍTULO 3

Binding activity, structure, and immunogenicity of synthetic peptides derived from Plasmodium falciparum CelTOS and TRSP proteins.

En la búsqueda de nuevos antígenos importantes en la interacción patógeno-hospedero, las proteínas CelTOS y TRSP del esporozoito (primera línea de defensa contra la infección por *Plasmodium*) han mostrado tener un papel relevante, la primera en el paso de los esporozoitos a través de diferentes células (17) hasta llegar a la célula hepática que posteriormente invadirá, y la segunda implicada en la infección de la misma célula blanco (69). En este trabajo se identificaron 4 péptidos nativos de alta capacidad de unión a células HepGII y HeLa, 3 provenientes de la proteína CelTOS uno de la proteína TRSP. Estos péptidos fueron modificados de acuerdo a reglas ya preestablecidas, fueron usados en estudios de respuesta inmune en monos *Aotus* y analizados estructuralmente mediante RMN de ^{1}H, encontrando que los péptidos modificados de la proteína CelTOS tienen fragmentos α helicales con la misma longitud, pero diferente orientación en las cadenas laterales de los residuos en la posición 2, 3 y 7 en el contexto de moléculas HLA-DRβ1* y para los péptidos de TRSP el nativo fue más estructurado que los modificados con también algunos cambios de orientación de las cadenas laterales de algunos aminoacidos que probablemente podrían estar interviniendo en las propiedades inmunogénicas. Las modificaciones hechas en los péptidos conservados de las proteínas CelTOS y TRSP han generado péptidos que han presentado un leve cambio conformacional, convirtiéndolos en inmunogénicos, comparados con los nativos que no lo son.

Amino Acids
DOI 10.1007/s00726-011-1087-8

ORIGINAL ARTICLE

Binding activity, structure, and immunogenicity of synthetic peptides derived from *Plasmodium falciparum* CelTOS and TRSP proteins

Hernando Curtidor · Gabriela Arévalo-Pinzón · Adriana Bermudez · Dayana Calderon · Magnolia Vanegas · Liliana C. Patiño · Manuel A. Patarroyo · Manuel E. Patarroyo

Received: 25 May 2011 / Accepted: 30 August 2011

Abstract Several sporozoite proteins have been associated with *Plasmodium falciparum* cell traversal and hepatocyte invasion, including the cell-traversal protein for ookinetes and sporozoites (CelTOS), and thrombospondin-related sporozoite protein (TRSP). CelTOS and TRSP amino acid sequences have been finely mapped to identify regions specifically binding to HeLa and HepG2 cells, respectively. Three high-activity binding peptides (HABPs) were found in CelTOS and one HABP was found in TRSP, all of them having high α-helical structure content. These HABPs' specific binding was sensitive to HeLa and HepG2 cells' pre-treatment with heparinase I and chondroitinase ABC. Despite their similarity at three-dimensional (3D) structural level, TRSP and TRAP HABPs located in the TSR domain did not compete for the same binding sites. CelTOS and TRSP HABPs were used as a template for designing modified sequences to then be assessed in the *Aotus* monkey experimental model. Antibodies directed against these modified HABPs were able to recognize both the native parasite protein by immunofluorescence assay and the recombinant protein (expressed in *Escherichia coli*) by Western blot and ELISA assays. The results suggested that these modified HABPs could be promising targets in designing a fully effective, antimalarial vaccine.

Keywords *Plasmodium falciparum* · Sporozoite · CelTOS · TRSP · Peptide · Vaccine

Introduction

Highly specialized invasive forms of *Plasmodium falciparum* (the parasite causing the most lethal form of malaria) recognize, invade, and infect two target cells in human hosts: hepatocytes and red blood cells (RBC) (Kappe et al. 2004; Garcia et al. 2006; Cowman and Crabb 2006). *P. falciparum* sporozoites (larvae-like structures) injected into the skin during the bite of an infected female *Anopheles* mosquito travel through the bloodstream to the liver during the first phase of human malaria infection where they cross the sinusoidal layer through Disse's space and Kupffer cells to invade their primary target: the hepatic cell (Sinnis and Coppi 2007). Two highly relevant proteins participating in such host–pathogen interactions have been widely studied: the circumsporozoite protein (CSP) and the thrombospondin-related anonymous protein (TRAP) (Akhouri et al. 2008; Rathore et al. 2003); both have been shown to mediate sporozoite motility, host-cell recognition, cell traversal, binding, and entry to host cells. These proteins thus constitute targets for intensive research in designing vaccines acting against this deadly disease's pre-erythrocyte stage (Bermudez et al. 2008; Bongfen et al. 2009; Cifuentes et al. 2008; Khusmith et al. 1991; Kumar et al. 2006). Several studies have shown that sporozoite proteins promote the malaria parasite crossing the dermis and the liver's sinusoidal wall prior to invading the

H. Curtidor (✉) · G. Arévalo-Pinzón · A. Bermudez · D. Calderon · M. Vanegas · L. C. Patiño · M. A. Patarroyo · M. E. Patarroyo
Fundación Instituto de Inmunología de Colombia FIDIC, Carrera 50 No. 26-20, Bogotá, Colombia
e-mail: hernando_curtidor@fidic.org.co

H. Curtidor · G. Arévalo-Pinzón · A. Bermudez · D. Calderon · M. Vanegas · L. C. Patiño · M. A. Patarroyo
Universidad del Rosario, Calle 14 No. 6-25, Bogotá, Colombia

M. E. Patarroyo
Universidad Nacional de Colombia, Carrera 45 No. 26-85, Bogotá, Colombia

Journal : Large 726 | Dispatch : 20-9-2011 | Pages : 14
Article No. : 1087 | LE | TYPESET
MS Code : duplicationof1074 | CP | DISK

hepatocytes; SPECT-1 and SPECT-2 are two such sporozoite microneme proteins as they are essential for cell traversal and are expressed in the micronemes and then translocated to the sporozoite surface (Ishino et al. 2004, 2005; Kaiser et al. 2004a; Yuda and Ishino 2004).

Knowledge regarding sporozoite biology, chemistry, and function during this first invasion phase has been limited for several years, mainly due to the small number of sporozoite and pre-erythrocyte forms available, as well as a lack of an in vitro system for producing sporozoites. A large number of attractive molecules from each parasite stage have recently been identified due to the complete *P. falciparum* genome, proteome, and transcriptome having been analyzed (Florens et al. 2002; Gardner et al. 2002; Kaiser et al. 2004b). These molecules are currently being studied as alternatives for developing more efficient malaria control mechanisms.

Two novel sporozoite proteins from among this promising array have been recently associated with sporozoite cell traversal via liver macrophages (Kupffer) and hepatic cell recognition and infection, namely the *cel*l-*t*raversal protein for *o*okinetes and *s*porozoites (CelTOS) and the *t*hrombospondin-*r*elated *s*porozoite *p*rotein (TRSP) (Kaiser et al. 2004b; Kariu et al. 2006; Labaied et al. 2007).

CelTOS is translocated to the sporozoite surface and then mediates parasite infectiveness. It is a 25-kDa protein which is expressed in micronemes from both mosquito midgut and mammalian liver-infective sporozoites (Kariu et al. 2006). Targeted disruption of the *celtos* gene has demonstrated in vitro this protein product's direct participation in parasite transversal to HeLa cells and cellular barriers in both mosquitoes and vertebrates (Kariu et al. 2006), since *celtos*-null sporozoites have been shown to have reduced infectivity in mice ~~by sporozoite count~~, whilst in vitro experiments have shown that cell-passage ability becomes almost abolished. Interestingly, sporozoite infectivity was restored in Kupffer cell-depleted rats, suggesting that CelTOS main function is specifically related to sporozoite host-cell traversal ability, possibly by interacting with host-cell molecules on the membrane (Kariu et al. 2006). Interestingly, it has been reported that immunization with Pf CelTOS elicits protection in mice against heterologous challenge with *Plasmodium berghei* and that CelTOS-specific antibodies can inhibit *P. falciparum* sporozoite invasion of hepatocytes in vitro and also *P. falciparum* sporozoite motility in vitro (Bergmann-Leitner et al. 2010), thereby highlighting CelTOS' potential as a promising vaccine candidate.

The TRSP protein was identified in differential transcriptome analysis of *Plasmodium yoelii* sporozoites (Kaiser et al. 2004b) as being a 18-kDa protein (163 amino acids long), containing a characteristic signal sequence within its primary structure, a *C*-terminal hydrophobic region which could serve as a membrane anchor domain (Labaied et al. 2007) and a *t*hrombo*s*pondin type 1 *r*epeat (TSR) domain. This TSR domain is characteristic of the *P. falciparum* TRAP protein family which has been found in several surface proteins involved in ookinete and sporozoite motility, as well as in host cell binding and invasion (Kaiser et al. 2004b; Pradel et al. 2002; Tucker 2004). TRSP has a unique distribution pattern by contrast with other micronemes and surface proteins, suggesting that TRSP is located in the sporozoite rhoptries. Unfortunately, no sporozoite rhoptry-specific proteins have been identified so far, thus precluding co-localization studies confirming this hypothesis (Kaiser et al. 2004b; Labaied et al. 2007). Interestingly, in vitro and in vivo knockout assays with the *Plasmodium berghei* TRSP homolog have indicated an important role for this protein in hepatocyte invasion; this would also reinforce this protein's potential as an antimalarial vaccine component (Labaied et al. 2007).

Identifying specific *Plasmodium* protein-derived antigens participating in host–pathogen interactions in all parasite stages is a highly relevant step for ensuring a logical and rational development strategy for designing a fully effective antimalarial vaccine (Patarroyo et al. 2008a; Cowman et al. 2002). A vaccine is urgently needed for protecting around 3.2 billion people living in high-risk areas, as well as preventing the 300 million cases, and more than 2 million deaths caused by this disease every year (Snow et al. 2005; Hay et al. 2010).

Entire sequences have been synthesized as short synthetic peptides (20-mer-long) regarding CelTOS' relevance for the necessary cell passage for crossing the sinusoidal layer and TRSP during hepatocyte invasion; each peptide's ability to bind to HeLa (in vitro model for parasite cell-traversal ability) or HepG2 cells (hepatic cell line for sporozoite invasion) has also been assessed. **H**igh-**a**ctivity **b**inding **p**eptides (HABPs) have thus been identified by using a robust, highly specific and sensitive methodology which has been tailor-made for this purpose. Specific binding has been determined in binding assays by using radiolabeled and non-radiolabeled peptide. The data have been analyzed by using bimolecular interaction theory which has led to finding that high-affinity binding regions recognize around 2,000 binding sites per cell and that they have nanomolar dissociation constants (Patarroyo and Patarroyo 2008; Rodriguez et al. 2008).

This has led to identifying and characterizing a new set of minimal subunit-based, chemically synthesized sporozoite peptides mediating CelTOS interaction with HeLa cells, as well as TRSP interaction with HepG2 cells, in turn, constituting interesting targets for blocking sporozoite invasion during cell-traversal and hepatic infection stages as components of a chemically synthesized, multi-epitope, multistage, minimal subunit-based, fully effective antimalarial vaccine.

Journal : Large 726 | Dispatch : 20-9-2011 | Pages : 14
Article No. : 1087 | ☐ LE | ☐ TYPESET
MS Code : duplicationof1074 | ☑ CP | ☑ DISK

Materials and methods

Peptide synthesis and radiolabeling

The *t*-Boc strategy was used for synthesizing 20-mer-long (Merrifield 1963; Houghten 1985), non-overlapping peptides from *P. falciparum* 3D7 strain CelTOS (**PFL0800c**), and TRSP (**PFA0200w**) protein sequences, taken from the PlasmoDB database (http://plasmodb.org/plasmo/). Synthesized peptides were named according to our institute's sequential numbering system (Fig. 1). A tyrosine residue was added to the *C*-terminal of those peptides which did not contain this residue in their sequence to enable radiolabeling.

Regarding immunization studies, peptide polymers were obtained after CG had been added to the *N*- and *C*-termini to allow peptide polymerization. HPLC-purified peptides were incubated for 15 min with 5 μL $Na^{125}I$ (100 mCi/mL, MP Biomedicals) and 15 μL chloramine-T (2.75 mg/mL) for radiolabeling (Curtidor et al. 2008b). The reaction was stopped by adding 15 μL sodium metabisulfite (2.25 mg/mL). Radiolabeled peptides were purified on a Sephadex G-10 column and analyzed in an Auto Gamma Counter Cobra II (Packard).

HepG2 and HeLa cells

HeLa cells were cultured in RPMI 1640 medium supplemented with 10% fetal bovine serum (Gibco) and antibiotic/antimycotic mixture (Gibco). Likewise, HepG2 cells were cultured in DMEM medium supplemented with non-

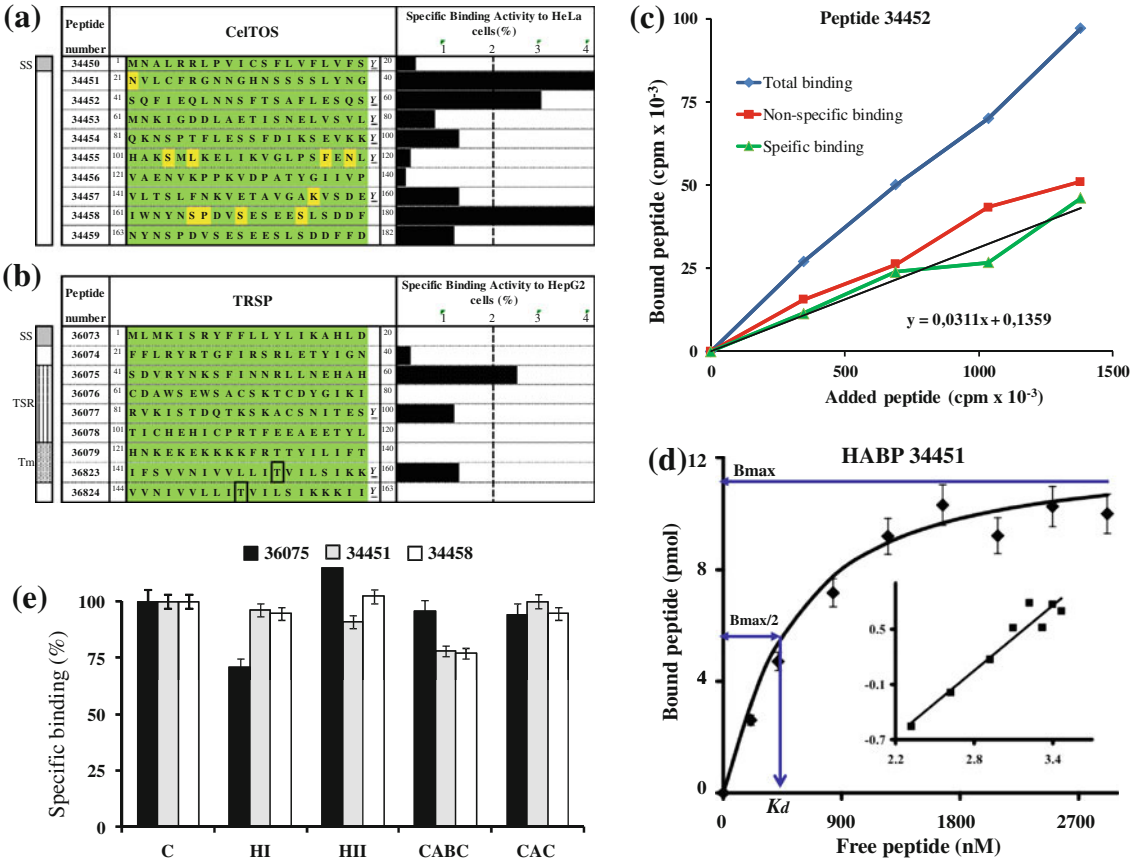

Fig. 1 Receptor-ligand assays. Each peptide's binding activity is represented by the length of the black bars shown in front of each amino acid sequence: **a** CelTOS and **b** TRSP. Peptides presenting a ≥2% binding activity cut-off point were considered to be HABPs. CelTOS and TRSP schematic representation, indicating signal sequence position (SS), transmembrane domains (Tm), and thrombospondin-related type I domain (TSR). Two cysteine residues were replaced by threonine (*black rectangles*) in TRSP peptides 36823 and 36824 due to polymerization issues during peptide synthesis. Conserved protein regions are shown in *green* and variable regions are shown in *yellow*. **c** Total, non-specific, and specific binding for peptide 34452. The slope from trend line in specific binding indicates 3.1% specific binding, meaning that peptide 34452 is a HABP. cpm: counts per minute. **d** HABP 34451 saturation curve. Increasing amounts of radio-labeled peptide were added in the presence or absence of unlabeled peptide. The curve represents specific binding. In the Hill plot (interior), the abscissa is log *F* and the ordinate is log(*B*/*B* max − *B*), *F* being free peptide, *B* the amount of bond peptide and *B* max the maximum amount of bound peptide. B_{max} is used for calculating K_d and number of sites per cell (Attie and Raines 1995; Rodriguez et al. 2008). **e** The effect of HeLa and HepG2 cell treatment with heparinase I (HI), heparinase II (HII), chondroitinase (CABC), and chondroitinase AC (CAC) on CelTOS and TRSP HABP binding activity. Peptides binding to untreated cells were used as binding (100%) control (C)

Journal : Large 726 Dispatch : 20-9-2011 Pages : 14
Article No. : 1087 LE TYPESET
MS Code : duplicationof1074 CP DISK

essential amino acids (Gibco) and bovine pancreas insulin (Sigma). Cells were incubated at 37°C in a 5% CO_2 atmosphere. After a confluent layer became formed, cells were dissociated using 0.05% EDTA–PBS. Before being used, cells were collected by adding EDTA–PBS and centrifuging; they were then washed with incomplete medium and their viability and concentration were assessed in a Neubauer chamber using trypan blue staining.

CelTOS and TRSP peptide binding assays

HeLa and HepG2 cell binding assays were conducted in triplicate, as described elsewhere (Curtidor et al. 2008b; Lopez et al. 2001). Briefly, increasing concentrations (0–560 nM) of radiolabeled CelTOS- and TRSP-derived synthetic peptides were incubated for 1 h with HeLa or HepG2 cells (1.2×10^6 cells), respectively, in the absence (total binding) or presence (unspecific binding, 140-fold excess) of unlabeled peptide. Cells were recovered from the reaction mixture by spinning at $8{,}000 \times g$ for 5 min through a 60:40 dioctyl phthalate/dibutyl phthalate cushion (1.015 g/mL) and cell-associated radioactivity was quantified by gamma counter. HABPs were defined as being peptides having a ≥0.02 ratio (2% specific binding) according to previously established criteria, keeping in mind that specific binding activity (specific binding activity = total binding − unspecific binding) at four increasing logarithmic concentrations defines the specifically bound peptide (pmol) per added peptide (pmol) ratio (Curtidor et al. 2008b; Rodriguez et al. 2008).

Modified binding assays involving a wider range of concentrations (0–3,200 nM) were carried out to determine the HABP binding equilibrium constants for the interactions established between CelTOS and TRSP HABPs with HepG2 and HeLa cells, respectively. Samples were incubated and separated from the mixture reaction (the same used in binding assays); cell-associated radioactivity was analyzed by gamma counter. The experimental data so obtained was analyzed using saturation function (bound ligand concentration compared with total and or free ligand); Hill coefficients (cooperativity), dissociation constants (K_d), and number of sites per cell could thus be obtained (Attie and Raines 1995; Rodriguez et al. 2008).

Binding to enzyme-treated cells and cross-competition assays

Each cell line was suspended in HBS buffer and treated independently for 1 h with 500 μU/mL of heparinase I (HI; CAS 9025-39-2, Sigma), heparinase II (HII; CAS 149371-12-0, Sigma), chondroitinase AC (CAC; CAS 9047-57-8, Sigma), and chondroitinase ABC (CABC; CAS 9024-13-9, Sigma) at 37°C. Treated cells were then washed and assessed in the same way as conventional binding assays, using untreated cells as positive control.

Cross-competition assays were also carried out between TRSP HABP and a TRAP-derived peptide. Briefly, 24 nM of ^{125}I-labeled-HABP 36075 was incubated for 90 min with HepG2 cells (1×10^6) in the presence of unlabeled TRAP HABP 3289 at three concentrations (6, 20 and 80 μM). Cells were then washed before cell-bound radiolabeled peptides were quantified (as described above).

Circular dichroism (CD) and nuclear magnetic resonance (NMR) spectroscopy, and structural calculation

CelTOS and TRSP HABP secondary structures were analyzed by ~~(~~CD~~)~~. HPLC-purified peptides' spectra were recorded at 20°C in 30% *v/v* trifluoroethanol (TFE), using a 1-cm optical path length thermostated quartz cell. All spectra were acquired in a Jasco J-810 equipment (JASCO Inc.) by averaging three sweeps taken at 20 nm/min. Data were processed by Spectra Manager software and analyzed with CONTINLL, SELCON and CDSSTR deconvolution software (Sreerama and Woody 2000).

For NMR experiments, ten milligrams of HPLC purified HABP 36075 was dissolved in 500 μL 30% *v/v* TFE (Roccatano et al. 2002). Resonance assignments were obtained from two-dimensional TOCSY, DQF-COSY, and NOESY spectra and sequences were assigned following standard procedure (Wüthrich New York 1986). All experiments were carried out using a Bruker DRX-500 MHz spectrometer at 295 K.

Accelrys software was used for determining HABP 36075 structure. NOE peaks (selected from NOESY data sets obtained at 400 ms) were integrated and converted into distance restraints; such restraints were grouped as being strong, medium, and weak, corresponding to 1.8–2.5, 2.5–3.5, and 3.5–5.0 Å distance restraints, respectively. Hydrogen bond constraints were introduced for slow peptide NH exchange rate; distance ranges involving these likely NH–O hydrogen bonds were set at 1.8–2.5 Å. Havel and Wuthrich's DGII distance geometry software was used for producing 50 starting structures (Havel and Wuthrich 1985).

Aotus monkey immunization with CelTOS and TRSP modified HABPs

CelTOS-derived HABPs 34451 and 34458 and TRSP-derived HABP 36075 were used as templates for designing analog peptides **38138** (CG^{21}NV***HT***FRGDN**V**HNSSSSL^{40}GC), **38140** (CG^{161} IWNYNS***D***DVSESEESLSDDF^{180}GC) and **38148** (CG^{41}SD***V***RYNKSFINN***RL***LNEHAH^{60}GC), respectively, following thoroughly described physicochemical

Journal : Large 726 | Dispatch : 20-9-2011 | Pages : 14
Article No. : 1087 | LE | TYPESET
MS Code : duplicationof1074 | CP | DISK

principles (Patarroyo and Patarroyo 2008). Please note that modified peptides and modified residues are written in italics and highlighted in bold.

Analog peptides were used for subcutaneously immunizing groups of 5–8 *Aotus* monkeys which were kept in our field station in Leticia (Amazonas, Colombia); animal care and handling were in line with Colombian Institute of Health guidelines which was strictly supervised by the competent Colombian environmental authority (CORPOAMAZONIA), as previously described (Curtidor et al. 2007; Cifuentes et al. 2009). The immunization scheme was as follows: 125 μg peptide dissolved in distilled water was homogenized with 250 μL Freund's complete adjuvant (FCA) for the first dose administered on day zero and with 250 μL Freund's incomplete adjuvant (FIA) for the second and third doses administered on days 20 and 40, respectively. Each monkey was immunized with 200 μL of the peptide emulsion and control monkeys were immunized with saline solution and CFA or FIA on the same days. Blood was obtained from the femoral vein.

Extracting *P. falciparum* genomic DNA and PCR amplification

Human RBCs (200 μL) parasitized with either *P. falciparum* FCB-2 (Colombia), or PAS-2 (unknown origin) or FVO (Vietnam) strains (30% parasitemia) were obtained from an asynchronous culture, maintained as described elsewhere (Lambros and Vanderberg 1979). Erythrocytes were lysed afterwards using 0.2% saponin and genomic DNA (gDNA) from each strain was extracted using an UltraClean DNA blood isolation kit (MO BIO, Carlsbad, CA).

Genes encoding CelTOS and TRSP proteins in the *P. falciparum* 3D7 reference strain (PFL0800c and PFA0200w, respectively) were analyzed for designing specific primer sets for amplifying HABP-encoding regions. A single primer set was designed for each protein using Gene Runner v3.05; sequences were CelTOS-F (5′-CGTATTAC GTTTGTTTGTTTG-3′) and CelTOS-R (5′-AAATTAGCA CACACATATATAC-3′) amplifying the region encoding HABPs 34451, 34452 and 34458, as well as TRSP-F (5′-GG CTTTATCCGTTCACGAC-3′), and TRSP-R (5′-TGATCT GTGCTTATTTTTACTC-3′) amplifying the HABP 36075-encoding region. The HABP 33577-encoding region in *P. falciparum* integral membrane protein *Pf*25-IMP was included as a positive PCR control; it was amplified using DIR1 and REV1 primers (Curtidor et al. 2008a).

DNA regions were amplified in 50 μL reaction mixture using 1.25U BioTaqTM DNA polymerase (Bioline, London, UK). The following thermocycling profile was used for all primer sets: an initial denaturing step at 95°C for 5 min, followed by 35 cycles consisting of: 1 min of annealing at 56°C, 1 min of extension at 72°C, and 1 min denaturing at 95°C, followed by a final extension cycle at 72°C for 5 min. The same reaction conditions were established using DNase- and RNase-free water instead of DNA as negative control. Amplification products were purified using a Wizard PCR preps kit (Promega, Madison, WI) and sequenced using their corresponding forward and reverse primers.

Recombinant protein cloning and expression

The *P. falciparum* FCB-2 strain CelTOS (residues 25–182) and TRSP (residues 39–138) putative protein encoding regions were amplified from genomic DNA using the following specific primers: forward-CelTOS: 5′-ATGTTCAG AGGAAACAACGGA-′3, reverse-CelTOS: 5′-ATCGAAA AAATCATCTGATA-3′, forward-TRSP: 5′-ATGCTTATG AAAATTTCAAG-3′ and reverse-TRSP: 5′-GATTAAAA TATATGTTGTTCG-3′. PCR products were cloned in pE XP5-CT/TOPO expression vector (Invitrogen) which adds a polyhistidine (6-His) tag at proteins' *C*-terminus to facilitate further purification and detection. Recombinant plasmid integrity was corroborated by an ABI PRISM 310 automatic genetic analyzer (PE Applied Biosystems). ClustalW was used for comparing FCB2 strain sequencing results with those for the 3D7 reference strain through nucleotide and amino acid alignment (Thompson et al. 2002).

Recombinant proteins were expressed in *E. coli* BL21-AI cells after being induced with 0.2% L-arabinose. Harvested cell pellets were solubilized in denaturing lysis buffer (6 M Urea, 10 mM sodium phosphate, 10 mM Tris–Cl, 15 mM Imidazole) supplemented with protease inhibitors (100 mM PMSF, 0.5 M EDTA, 1 mg/mL leupeptin, 100 mM iodoacetamide) and 1 mg/mL lysozyme. The clear supernatant was applied to a pre-equilibrated Ni–NTA agarose column (Qiagen) to purify the recombinant protein by solid-phase affinity chromatography, as has been previously described (Mongui et al. 2010). The presence of both CelTOS (r*Pf*CelTOS) and TRSP recombinant proteins (r*Pf*TRSP) was verified by SDS–PAGE and Western blot (WB) using peroxidase-coupled monoclonal anti-polyhistidine antibodies (Mongui et al. 2010). Recombinant proteins were thoroughly dialyzed against PBS pH 7.5 and the amount of protein was determined by Micro BCA Protein Assay kit (Thermo Scientific).

Enzyme-linked immunosorbent assay (ELISA) with recombinant proteins

r*Pf*CelTOS and r*Pf*TRSP recognition and antibody titers were determined by ELISA. In brief, 96-well plates coated with 5 μg/mL r*Pf*CelTOS or r*Pf*TRSP were incubated with

Journal : Large 726 Dispatch : 20-9-2011 Pages : 14
Article No. : 1087 LE TYPESET
MS Code : duplicationof1074 CP DISK

modified peptide-immunized *Aotus* monkey sera (1:100 initial dilution), followed by twofold serial dilutions in the entire row of wells. Anti-CelTOS sera and anti-TRSP sera final dilutions were 1:6,400 and 1:3,200, respectively. Peroxidase-coupled anti-Aotus IgG (1:10,000) was used as secondary antibody and immunoreactivity was revealed using a TMB Microwell peroxidase substrate system kit (KPL Laboratories, WA, USA), according to the manufacturer's instructions. *Aotus* monkey antibody titers were determined by successive twofold dilutions of primary antibody, until reaching an A450 value equal to pre-immune sera value ± 2SD.

Indirect immunofluorescence assays (IFA) and WB analysis

P. falciparum 3D7 strain sporozoite air-dried slides, fixed with 2% BSA in PBS (kindly provided by Dr. Patricia de la Vega) were used for assessing the reactivity of *Aotus* monkey sera immunized with CelTOS (**38138**, **38140**) and TRSP (**38148**) analog peptides. Slides were incubated for 30 min with monkey sera at 1:40 dilution. Pre-immune sera from all monkeys were used as negative controls. Fluorescence was observed using the F(ab)2 fragment from affinity purified goat anti-monkey IgG:rhodamine isothiocyanate (TRITC) conjugate in 1:100 dilution (appearing as red by fluorescence microscopy). Anti-CSP serum produced in an *Aotus* monkey was used as primary antibody at a 1:100 dilution for CelTOS co-localization studies and then detected with goat anti-*Aotus* IgG conjugated to fluorescein isothiocyanate (FITC) at a 1:100 dilution (appearing as green).

r*Pf*CelTOS or r*Pf*TRSP was separated by 12% SDS–PAGE in non-reducing conditions and then transferred to a nitrocellulose membrane for WB analysis. Membranes were blocked with 5% skimmed milk in PBS-0.05% Tween and washed thrice with PBS-0.05% Tween. Nitrocellulose strips were individually incubated with monkey sera diluted 1:100 in blocking solution, washed several times, incubated with goat anti-*Aotus* IgG conjugated to alkaline phosphatase (AP) at 1:1000 dilution, and finally developed with NBT/BCIP (Vector Laboratories).

Results

CelTOS and TRSP peptides interacted with HeLa and HepG2 cells, respectively

Three HABPs were found in CelTOS which had high specific HeLa cell binding activity and affinity: 34451 (^{21}NVLCFRGNNGHNSSSSLYNG^{40}), 34452 (^{41}SQFIEQLNNSFTSAFLESQSY^{60}) and 34458 (^{161}IWNYNSPDVSESEESLSDDF^{180}). The first two were located in the CelTOS *N*-terminal region and the latter was located towards its *C*-terminal (Fig. 1a). Only one HepG2 cell-binding HABP was identified in TRSP, namely 36075 (^{41}SDVRYNKSFINNRLLNEHAH^{60}), which was located towards its TSR domain's *N*-terminal region (Fig. 1b). Figure 1c shows as an example of the plots obtained for peptide 34452 total, non-specific and specific binding. The specific binding plot slope (0.311) indicated 3.1% specific binding, meaning that peptide 34452 was considered to be a HABP (Fig. 1a).

CelTOS HABPs had high-affinity HeLa cell interactions, as shown by their dissociation constants (K_d) which came within the nanomolar range (500 nM for HABP 34451 and 680 nM for HABP 34458) and recognized around 7,200,000 (HABP 34451) and 139,000 (HABP 34458) sites per cell. Hill coefficients (n_H) obtained from saturation curves were higher than 1 for both HABPs (1.18 for HABP 34451 and 1.90 for HABP 34458), suggesting these peptides' positive cooperative effect on CelTOS-mediated cell-traversal activity. Figure 1d shows HABP 34451 saturation curve and Hill plot. CelTOS HABP 34452 and TRSP HABP 36075 binding did not reach saturation in the conditions being assessed here, due perhaps to a larger number of binding sites per cell for these peptides.

CelTOS and TRSP HABPs bound differentially to enzyme-treated HeLa and HepG2 cells

HI-, HII-, CAC- and CABC-treated HepG2, and HeLa cells weakly affected CelTOS and TRSP HABP binding. TRSP HABP 36075 HepG2 cell binding was weakly affected by HI treatment, whereas CelTOS HABP 34451 and 34452 HeLa cell binding was slightly sensitive to CABC (less than 24% for each HABP) (Fig. 1e).

CelTOS and TRSP HABP polymorphism assessed in different strains

CelTOS and TRSP HABP-encoding regions from FCB-2, PAS-2 and FVO strains were amplified by PCR, as described above. Two different sized amplification products (850 and 291 bp) were observed for CelTOS and TRSP, respectively, agreeing with expected sizes. The control primers amplified a single band of around 438 bp (Curtidor et al. 2008a) (Fig. 2a).

CelTOS nucleotide and amino acid sequences from the three aforementioned *P. falciparum* strains were aligned with those from the 3D7 (Airport malaria, Amsterdam, The Netherlands) and Dd2 (Thailand) reference strains, while TRSP sequences were only compared with the 3D7 reference strain; ClustalW software was used for all alignments (Combet et al. 2000). The CelTOS sequence had 12 nucleotide changes (8 single

Journal : Large 726 | Dispatch : 20-9-2011 | Pages : 14
Article No. : 1087 | LE | TYPESET
MS Code : duplicationof1074 | CP | DISK

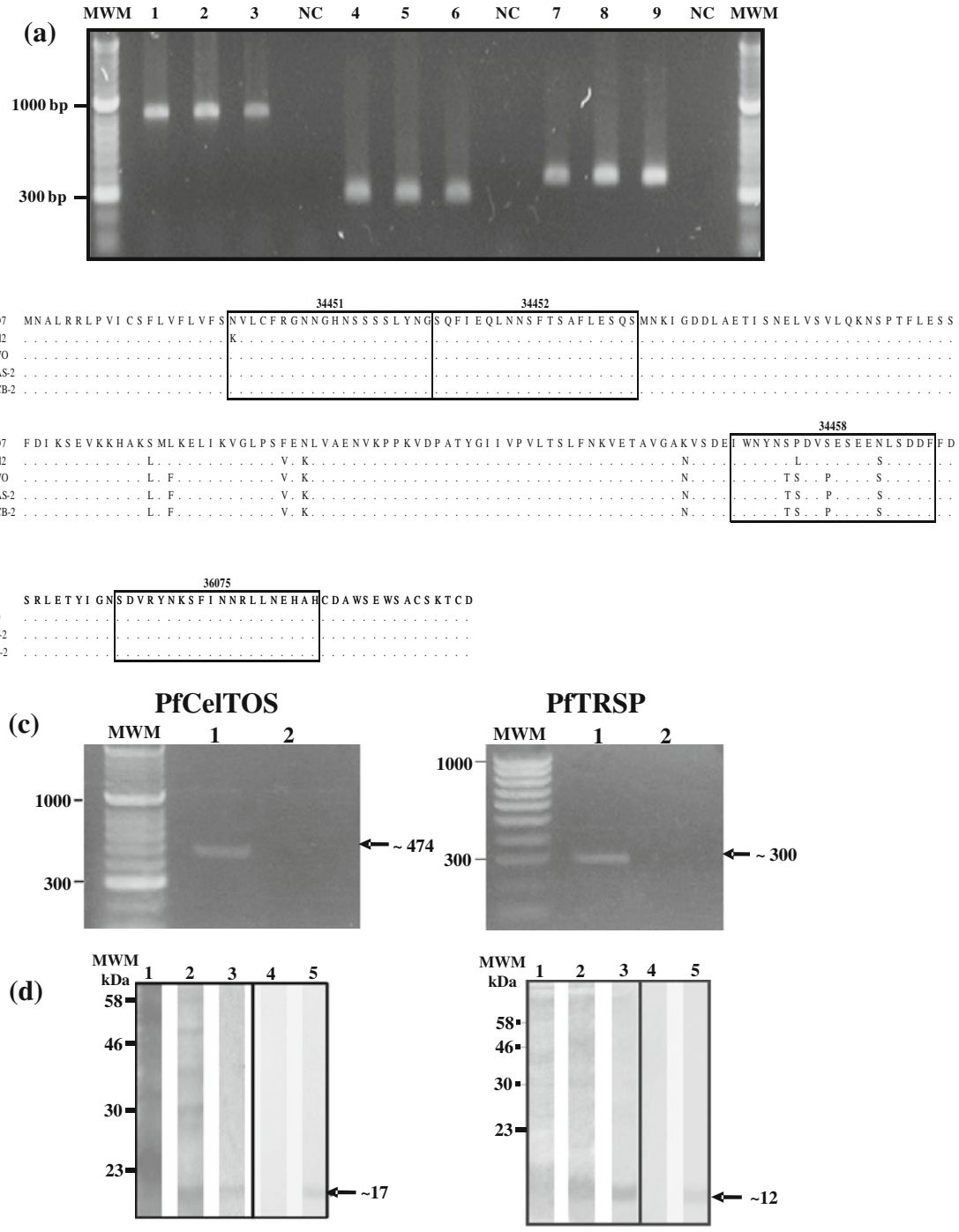

Fig. 2 Molecular biology assays. **a** *Lanes 1*, 2, and *3*, PCR amplification of the region encoding FCB-2, FVO and PAS-2 strain gDNA CelTOS HABPs 34451, 34452, and 34458, respectively. *Lanes 4, 5,* and *6*: amplification of FCB-2, FVO, and PAS-2 strain gDNA TRSP HABP 36075, respectively. *Lanes 7*, *8,* and *9*: positive control (*Pf*25-IMP) for the FCB-2, FVO and PAS-2 strains, respectively. NC: PCR negative control. **b** CelTOS (*top*) and TRSP (*down*) amino acid sequence alignment from different *P. falciparum* strains using MEGA 4 software (Tamura et al. 2007). FCB-2, FVO and PAS-2 strains were sequenced and compared with other strains reported in Broad Institute projects (http://www.broadinstitute.org/), as well as in the PlasmoDB database (http://plasmodb.org/plasmo/). HABPs are enclosed within *black boxes*. **c** PCR amplification of genes encoding *P. falciparum* CelTOS and TRSP in the FCB-2 strain. MWM: molecular weight marker. *Lane (1)* CelTOS (*left*) and TRSP (*right*), PCR of genomic DNA. *Lane (2)* negative control. **d** SDS–PAGE and Western blot of *P. falciparum* CelTOS (*left*) and TRSP (*right*) purified proteins. *Lane (1)* non-induced bacterial lysate. *Lane (2)* L-arabinose-induced bacterial lysate. *Lane (3)* SDS–PAGE of purified protein. *Lane (4)* Western blot of non-induced lysate and *Lane (5)* Western blot of purified protein using anti-polyhistidine monoclonal antibody

Journal : Large 726 Dispatch : 20-9-2011 Pages : 14
Article No. : 1087 LE TYPESET
MS Code : duplicationof1074 CP DISK

and 2 double non-synonymous substitutions, therefore producing a shift in 10 amino acid residues). Strain-specific polymorphisms in HABP regions described below, with their positions, have been numbered regarding the 3D7 reference strain. T to G nucleotide substitution was observed in HABP 34451 *N*-terminus in position 63 in the Dd2 strain, shifting asparagine to lysine in residue 21. Four nucleotide substitutions were found in HABP 34458-encoding sequences: one T to A substitution in position 496, shifting serine (S) to threonine (T) in residue 166 in FCB-2, PAS-2 and FVO strains, (2) a double substitution in nucleotide positions 499 (from T to C) and 500 (from C to T), shifting proline (P) to leucine (L) in residue 167 in the Dd2 strain and to serine (S) in the FCB-2, PAS-2 and FVO strains, (3) a T to C mutation in position 508, shifting serine (S) to proline (P) in residue 170 in FCB-2, PAS-2 and FVO and (4) a G to A substitution was found in position 524, shifting (S) to asparagine (N) in residue 175 in the Dd2, FCB-2, PAS-2, and FVO strains. The other substitutions were found outside HABP-encoding sequences (Fig. 2b).

Amino acid sequences obtained from the three *P. falciparum* strains for TRSP HABP 36075 were seen to be 100% identical to the reference sequence; no substitutions were found in the nucleotide sequence (Fig. 2b).

Recombinant protein production

celtos and *trsp* gene amplification revealed specific ~474 bp and ~300 bp bands, respectively (Fig. 2c). Recombinant protein expression was observed after L-arabinose induction, a single ~17 kDa band being detected with r*Pf*CelTOS anti-polyhistidine monoclonal antibody (Fig. 2d), thereby agreeing with this protein's predicted molecular weight without signal peptide (Kariu et al. 2006). The anti-polyhistidine monoclonal antibody detected a single specific ~12 kDa band (Fig. 2d) for r*Pf*TRSP, in agreement with the expected molecular weight for the recombinant protein fragment so obtained. Proteins were purified and dialyzed against PBS to ensure that denaturing agents had been completely removed and also allow protein folding.

TRAP HABP 3289 did not compete for HABP 36075 binding sites

Cross-competition assays with TRSP HABP 36075 and previously-identified TRAP HABP 3289 (Lopez et al. 2001) showed that TRAP HABP did not specifically compete for TRSP HABP 36075 binding sites when using different competitor peptide concentrations.

CelTOS and TRSP HABPs had similar secondary structure features

High α-helix content in CelTOS 34451, 34452, and TRSP 36075 HABP structures was determined by CD spectroscopy; two characteristic minima were observed in all spectra at 206 and 221 nm and one maximum at 190 nm (Fig. 3a). Spectra deconvolution with SELCON, CONTINLL and CDSSTR software showed greater than 80% α-helix content in agreement with these results. By contrast, HABP 34458 mostly presented 200 nm minimum random elements, agreeing with the low α-helical element content obtained in CD deconvolution results.

NMR HABP 36075 structure determination

NOESY spectra showed that dαN (i, i + 1) sequence signals were stronger than intra-residue cross-peaks. The presence of dNN cross-peaks indicated a significant population of conformations in the α-region of ΦΨ space, as well as some medium-range dα*β* (i, i + 3), dαN (i, i + 3), and dαN (i, i + 4) NOE connectivity, suggesting the presence of an α-helical structure between residues N11–H20 and a helical trend between K7-I10 (Fig. 3b).

Twenty-four modeled structures (from the original 50) whose distance violations were no greater than 0.25 Å and whose ω angles were greater than 1.5° were chosen. An average 0.24 Å RMSD (Root Mean Square Deviation) was obtained for the main-chain atoms by superimposing structures between residues N6-H20 with a consensus structure having the lowest total energy. Secondary structure analysis showed the presence of an α-helix between residues N11-H20; this structural feature was confirmed by medium-range NOEs and by dihedral Φ and Ψ angles for each residue in the helical region, adopting equal values (approximately −60° and 45°, respectively). A helical trend was observed between residues K7-I10 (Fig. 3c).

Immunoassays

Recognizing native protein by anti-HABP modified antibodies

One monkey out of eight immunized with analog peptide **38138** (34451) and three more monkeys immunized with analog **38140** (34458) developed specific antibodies which strongly reacted with small sporozoite intracytoplasmic structures by immunofluorescence (Fig. 4ai, aii, red), suggesting microneme location, as has been previously reported for this protein. The reactivity obtained with the *Aotus* anti-CSP molecule displayed a green fluorescence pattern on the periphery, suggesting a membrane location (Fig. 4ai, aii, green).

Journal : Large 726 | Dispatch : 20-9-2011 | Pages : 14
Article No. : 1087 | LE | TYPESET
MS Code : duplicationof1074 | CP | DISK

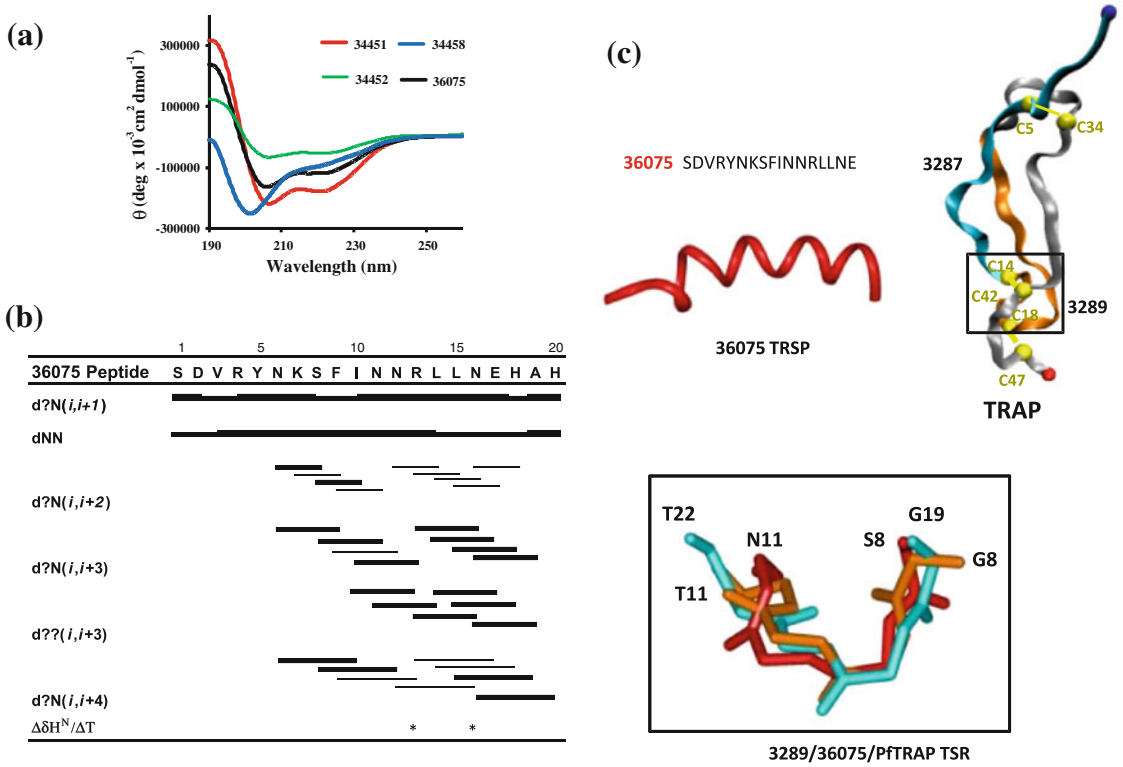

Fig. 3 CelTOS and TRSP HABP structural characteristics. **a** Circular dichroism spectra for CelTOS HABPs 34451, 34452 and 34458, and TRSP HABP 36075, recorded in 30% TFE. **b** Summary of sequential and medium-range NOE connectivity for HABP 36075, represented by line thickness. Temperature coefficient values less than 4.0 used in the calculation are indicate as *asterik*. **c** Ribbon representation of HABP 36075 determined by NMR is shown in *red*. The 3D structure for the TRS domain in TRAP protein (PDB 2BBX) is shown in *silver*, while regions where peptides 3287 and 3289 sequences are located are shown in *blue* and *orange*, respectively. At the *bottom*, backbone representation from HABP 3289 (*orange*) and 36075 (*red*) 3D structures (determined by NMR) superimposed on PfTRAP-TSR β-turn ^{258}GKGT^{261} fragment backbone (*blue*) (PDB 2BBX)

Aotus antibodies raised against TRSP analog peptide **38148** (36075) revealed an internal bilobulated staining pattern, suggesting its location in sporozoite rhoptries; however, sporozoite rhoptry-specific proteins have not been reported to date (Fig. 4aiii). Unfortunately, double-staining with anti-CSP and TRSP was not carried out because of the scarcity of sporozoite slides.

Antibodies against CelTOS and TRSP protein analog peptides recognized recombinant proteins by ELISA and WB

Specific antibody titers against r*Pf*CelTOS and r*Pf*TRSP were obtained by successive dilutions of monkey sera immunized with analog peptides **38138** (34451), **38140** (34458), and **38148** (36075); 1:400 titers were found for the single monkey immunized with peptide **38138** and titers ranging from 1:800 to 1:6,400 were found for monkeys immunized with peptide **38140** (Fig. 4b). Titers ranging from 1:800 to 1:3,200 for TRSP modified HABP **38148** (36075) were found for all six monkeys assessed in this study (Fig. 4b, right).

A ~17 kDa band was detected by WB when the same monkey sera inoculated with CelTOS analog peptides **38138** (34451) and **38140** (34458) was incubated with r*Pf*CelTOS (Fig. 4c). ~36 kDa and ~54 kDa bands were detected in some cases which could have corresponded to the dimerized and trimerized recombinant protein; this resulted from a lack of reduction/alkylation treatment of the sample prior to electrophoresis. Likewise, monkey sera inoculated with TRSP analog peptide **38148** (36075) recognized a specific ~12 kDa band and a very weak ~27 kDa band which could have corresponded to the dimerized recombinant protein (Fig. 4c).

Discussion

Hepatocyte invasion by *Plasmodium falciparum* sporozoites represents the initial stage in the most lethal form of human malaria. Sporozoites must overcome natural barriers to reach their host/target cell (the hepatocyte), including circumventing the liver's sinusoidal barrier and Disse's space via Kupffer cells (Sinnis and Coppi 2007). Along

Journal : Large 726 Dispatch : 20-9-2011 Pages : 14
Article No. : 1087 LE TYPESET
MS Code : duplicationof1074 CP DISK

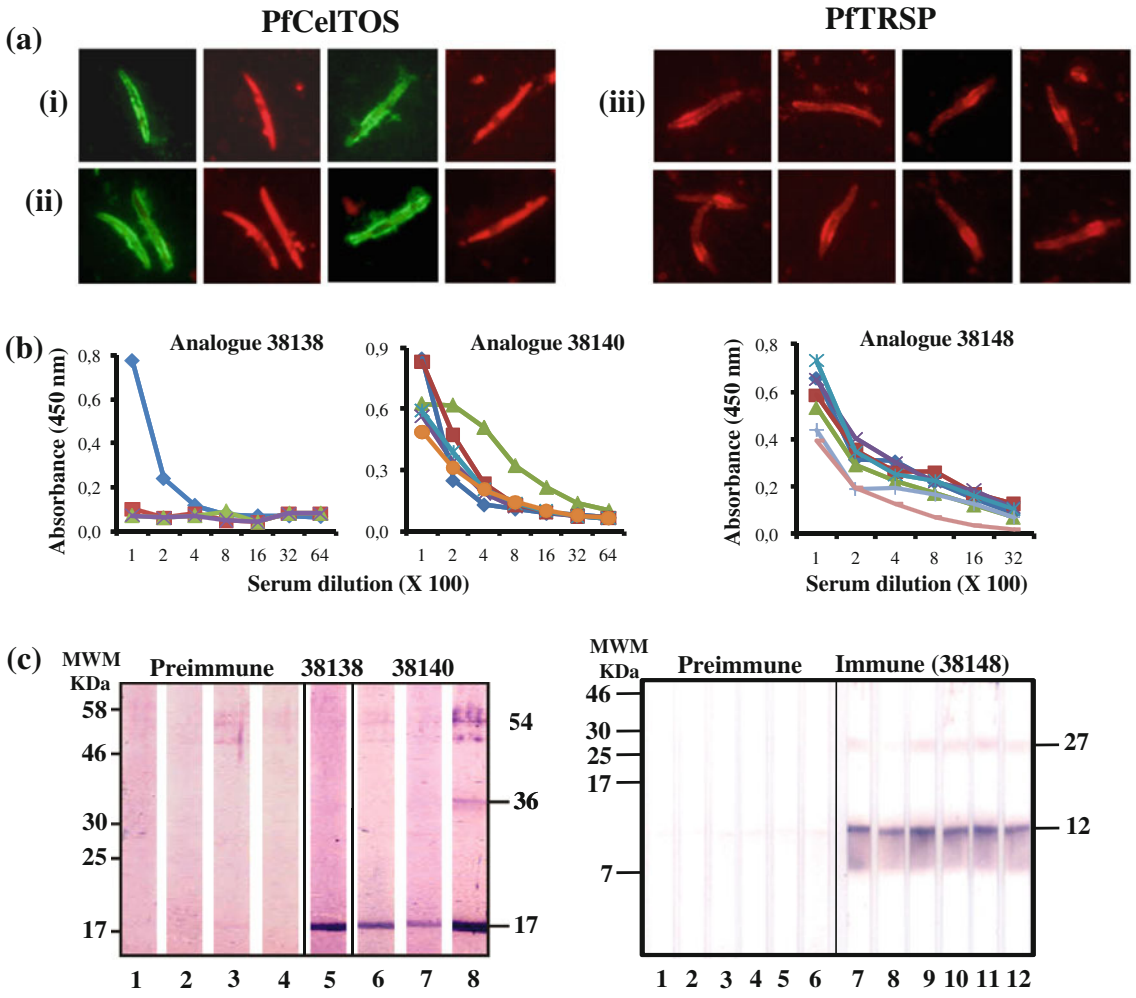

Fig. 4 Immunological assays. **a** *Aotus* monkey sera immunized with modified HABPs recognized CelTOS and TRSP in *P. falciparum* sporozoites by immunofluorescence. A dual indirect fluorescence assay carried out with antisera produced in *Aotus* monkeys (specific for CSP, gives *green fluorescence*) showed microneme labeling (*small dots*) and also the protein's presence on membrane. Antibodies against CelTOS-derived analog peptides (i) **38138** and (ii) **38140** revealed small intracytoplasmic dots similar to micronemes. (iii) TRSP protein detection with antibodies against analog peptide **38148**, showing an internal bilobed staining pattern. **b** Immunized monkeys' antibody titers were determined using ELISA with CelTOS analog peptides **38138** and **38140,** and TRSP **38148**. Two monkeys' sera dilutions starting at 1:100 are shown, until reaching the target's absorbance ±2SD. *Each line* represents a monkey assessed here. **c** Western blot assays. *Left panel*: r*Pf*CelTOS recognition *Lane 1–4*: Pre-immune serum. *Lane 5*: Hyper-immune monkey serum immunized with **38138** peptide analog. *Lane 6–8*: hyper-immune monkey sera immunized with analog peptide **38140**. *Right panel*: *Lanes 1–6*: Pre-immune serum. *Lanes 7–12*: recognition of r*Pf*TRSP protein by monkey sera immunized with **38148** peptide analog

with CSP, TRAP and SPECT 1 and 2, two new proteins have been recently described as they are directly involved in sporozoite cell-traversal and hepatic cell invasion: CelTOS and TRSP, respectively (Kaiser et al. 2004b; Kariu et al. 2006; Labaied et al. 2007; Bergmann-Leitner et al. 2010). These new proteins represent attractive targets to be used as templates for designing a multi-stage, multiepitope, minimal subunit-based, chemically synthesized, fully antimalarial vaccine.

A highly robust, sensitive, and specific methodology has thus been designed using 20-mer non-overlapping synthetic peptides in binding assays; this has led to identifying *P. falciparum* protein HABPs interacting with host cells (Garcia et al. 2006; Rodriguez et al. 2008). Efforts having been focused on conserved HABPs due to *P. falciparum* proteins' tremendous genetic polymorphism as a commonly used mechanism for microbes and parasites to evade host immune response.

Every conserved HABP identified so far represents a potential target to be specifically modified to activate an appropriate immune response capable of blocking host–pathogen interactions, i.e. to produce a protective immune response against *P. falciparum* challenge in the *Aotus* model (Cifuentes et al. 2009; Patarroyo et al. 2008a; Patarroyo and Patarroyo 2008). Complete CelTOS and TRSP sequences have been finely mapped using HeLa and

Journal : Large 726 Dispatch : 20-9-2011 Pages : 14
Article No. : 1087 LE TYPESET
MS Code : duplicationof1074 CP DISK

HepG2 cells, respectively, for identifying specific regions involved in binding to host cells. *N*-terminal peptides 34451 (^{21}NVLCFRGNNGHNSSSSLYNG^{40}) and 34452 (^{41}SQFIEQLNNSFTSAFLESQS*Y*^{60}), and *C*-terminal peptide 34458 (^{161}IWNYNSPDVSESEESLSDDF^{180}) have been identified as HABPs in CelTOS while only TSR domain peptide 36075 (^{41}SDVRYNKSFINNRLLNEHAH^{60}) has been identified as a HABP in TRSP (Fig. 1a, b). Interestingly, two consecutive HABPs were found: 34451 and 34452. An overlapping peptide involving sequences from both these HABPs may also bind to HeLa cells (Lopez et al. 2001; Patarroyo et al. 2008b).

Polymorphism analysis of regions where HABPs were located identified ten non-synonymous substitutions. Four changes within these (shown in bold) were located in CelTOS semi-conserved HABP 34458 (^{161}IWNYN**SP**DV**S**ESEE**S**LSDDF^{180}) (Fig. 2b). HABP 34451 had just one *N*-terminal residue substitution regarding the Dd2 strain and the other strains assessed here. By contrast, no changes were observed in the TRSP nucleotide and protein sequence when the 3D7 reference strain was compared with the FCB-2 (Colombia), PAS-2 (unknown origin), and FVO (Vietnam) strains (Fig. 2b). Sequence conservation in these potential vaccine antigens is thus an important issue in blocking *P. falciparum* parasites' exquisite immune evasion pathways (Patarroyo and Patarroyo 2008; Hisaeda et al. 2005).

CelTOS and TRSP protein HABPs' specific binding was determined after HepG2 (for TRSP) and HeLa (CelTOS) cells had been pre-treated with HI, HII, CAC, and CABC to assess the nature of their receptors. CelTOS HABP 34451 and 34458 binding was found to be moderately sensitive to HeLa cell treatment with CABC, CABC activity being mainly directed towards dermatan sulfate and chondroitin-6-, -4-, and -4,6- sulfate (Pradel et al. 2002). Interestingly, it has been reported that CABC has great potential for inhibiting recombinant CSP binding to Kupffer cells, thereby indicating a CSP chondroitin sulfate-dependent interaction during cell traversal (Pradel et al. 2002). The results thus suggest CelTOS HABP interaction with chondroitin sulfate-containing receptors on HeLa cell surface, which could be closely related to dermatan sulfate-like molecules (Fig. 1e); however, additional assays should be performed to confirm such interaction.

Several studies have reported that the TSR domain is involved in protein–protein interactions (Tucker 2004) and that it can also be found in different sporozoite proteins such as CSP (Suarez et al. 2001), TRAP (Lopez et al. 2001), *P. falciparum* secreted protein with altered thrombospondin repeat (*Pf*SPATR) (Curtidor et al. 2008b) and *Plasmodium* thrombospondin-related apical merozoite protein (PTRAMP) (Thompson et al. 2004). Studies using the well-described methodology for identifying specific HepG2 cell binding regions have reported that HABPs 3287 and 3289 were found in the TRAP TRS domain (Lopez et al. 2001; Patarroyo et al. 2008b), having poor amino acid sequence similarity with TRSP 36075. However, HABP 36075 binding was slightly sensitive to HI treatment (which cleaves heparin-like oligosaccharides into heparan sulfate, exhibiting a high degree of sulfation and epimerization to iduronic acid) (Fig. 1e); this is similar behavior to that displayed in TRAP heparin sulfate-dependent binding to HepG2 cells. A 1.1 Å RMSD region was observed between TRSP S8-N11 amino acids and TRAP 3289 G8-T11 when ~~TRAP HABP 3287~~ 3D structure was superimposed on TRSP HABP 36075 3D structure, suggesting similar structural characteristics (Fig. 3c). A 1.69 Å RMSD was observed when *P. falciparum* TRAP TSR 3D structure (PDB 2BBX) was superimposed on conserved HABP 36075 structure (determined by NMR) in the corresponding region (data not shown).

Previous studies have reported a 1.55 Å RMSD when TRS protein domain 3D structure was superimposed on conserved HABP 3289 structure in the region corresponding to distorted type III β-turn structures in both molecules (Patarroyo et al. 2008b). However, cross-competition assays revealed that, despite similar structural characteristics and binding to heparan sulfate proteoglycans, HABP 3289 (which also binds specifically to HepG2 cells) did not compete for HABP 36075 binding sites on HepG2 cells (data not shown). This suggested that even though there was structural resemblance between proteins from the same family, both HABPs were involved in different invasion pathways, recognizing subtle receptor differences, as has been widely documented for other molecules (Mayer et al. 2004).

On the other hand, it has been reported that the PfTRAP TSR domain contains a heparin-binding site located in the *N*-terminal half of the structure (Tossavainen et al. 2006) and that conserved tryptophans (WDEW) together with stacked arginines (RSRKRE) are involved in domain folding (Tossavainen et al. 2006). Interestingly, the TRSP 36076 peptide, whose sequence includes conserved tryptophans (^{64}WSEW^{67}), but not arginines, and is homologous to the TRAP TSR domain *N*-terminal portion, does not have cell specific binding. Raw data analysis has also indicated that the peptide–cell interaction was non-specific (data not shown). The foregoing shows how minimal changes in sequence can dramatically affect function, this being the basis for our approach.

Previous data have shown that knowledge regarding HABP structure and that of their modified peptides has led to correlating immunological activity with protection against experimental malarial challenge in *Aotus* spp monkeys. A strong immunogenicity-structure association has been widely reported for regions derived from several

Journal : Large 726 Dispatch : 20-9-2011 Pages : 14
Article No. : 1087 LE TYPESET
MS Code : duplicationof1074 CP DISK

P. falciparum merozoite-associated proteins (Reyes et al. 2007) and more recently for the sporozoite-related liver stage antigen-1 (LSA-1), the sporozoite and liver stage antigen (SALSA), CSP and TRAP (Patarroyo et al. 2008b; Bermudez et al. 2008; Cifuentes et al. 2009). This evidence has led to determining CelTOS and TRSP HABP structural content by CD along with NMR for HABP 36075. HABPs 34451, 34452, and 36075 mainly contain α-helical elements in their secondary structures, having two minima at 208 and 220 nm (Fig. 3a). HABP 36075 NMR studies have confirmed the presence of α-helical structures between residues N11-H20 and helical tendency between K7-I10 (Fig. 3b, c). A displacement has been observed in HABP 34458 spectrum (200 nm minima), indicating the presence of some other structural features, such as random coil elements. These results agreed with deconvolution analysis using CONTINLL, SELCON and CDSSTR software, revealing 40% α-helical features for HABP 34458 compared with >95% α-helical elements for HABPs 34451, 34452, and 36075 (Fig. 3a). Such results are relevant since previous studies have shown that specific structural modifications made on α-helical HABPs have been able to induce protective immune responses in *Aotus* monkeys when immunized with these modified merozoite HABPs (Patarroyo and Patarroyo 2008; Patarroyo et al. 2008a).

Conserved HABPs derived from the relevant proteins observed in *P. falciparum* merozoite and sporozoite stages are poorly immunogenic and do not induce protection. These HABPs have been used as templates for designing analog peptides to break this immunologic code of silence by substituting critical binding amino acids (determined by glycine analog scanning) for others having the same mass but different polarity, according to previously described physicochemical and biological principles (Patarroyo et al. 2008a). Such detailed changes lead to structural modifications in these analog peptides, thereby allowing a better fit into immune systems molecules and thus improving their immunological characteristics (Patarroyo et al. 2008a).

CelTOS-derived analog peptides **38138** (34451) and **38140** (34458) and TRSP-derived analog **38148** (36075) were thus designed and inoculated in *Aotus* monkeys to determine their immunogenic properties. Immunofluorescence assays showed that antibodies against modified peptides were able to recognize CelTOS protein as small intracytoplasmic dots, suggesting a micronemal pattern (Fig. 4a red) and TRSP showed a bilobed pattern (Fig. 4a iii, red), suggesting its location in sporozoite rhoptries. Sera from the same *Aotus* monkeys immunized with these CelTOS- or TRSP-derived modified HABPs have specifically recognized both ~17 kDa r*Pf*CelTOS and ~12 kDa r*Pf*TRSP proteins by WB. Therefore, specific modifications made to HABPs from the different proteins assessed here were able to induce antibodies in the *Aotus* spp. experimental model which recognized recombinant protein by ELISA and WB and native protein in sporozoites using immunofluorescence. These results stress the importance of complete structural and immunologic analysis for all *P. falciparum* HABPs for developing multi-epitope, multi-stage, minimal subunit-based, chemically synthesized vaccines to ensure obtaining complete protection against malaria (Patarroyo et al. 2008a; Patarroyo and Patarroyo 2008). Unfortunately, it was only discovered that native peptide 34458 had genetic polymorphism when polymorphism studies had been completed (as described above), thereby allowing this HABP to be classified as variable according to our strict conservation definition standards and also rule out the possibility of using **38140** modified analog as a component of a minimal subunit-based, synthetic antimalarial vaccine.

This study has thus determined the profile for all CelTOS and TRSP amino acid sequence-derived peptides binding to HeLa and HepG2 cells, respectively, leading to conserved HABPs mainly displaying α-helical features being identified. These HABPs also established high-affinity interactions with heparan-like or dermatan sulfate-containing host-cell surface receptors which have been reported to play an important role in recognition by *P. falciparum* sporozoite molecules during hepatic cell traversal and invasion. CelTOS and TRSP HABP-derived modified peptides have been rendered highly immunogenic in the *Aotus* model; they have been able to recognize the recombinant protein in both its native and denatured conformation. Taken as a whole, these results support including these modified CelTOS and TRSP HABPs when designing vaccine components for a multi-stage, multi-epitope, minimal subunit-based, fully-protective antimalarial vaccine, as part of a logical and rational methodology for vaccine development.

Acknowledgments We would like to thank Jason Garry for translating this manuscript.

Conflict of interest The authors declare no conflict of interest. The authors alone are responsible for the content and writing of this manuscript.

References

Akdi RR, Sharma A, Malhotra P, Sharma A (2008) Role of *Plasmodium falciparum* thrombospondin-related anonymous protein in host-cell interactions. Malar J 7:63

Attie A, Raines R (1995) Analysis of receptor-ligand interactions. J Chem Educ 72:119–124

Bergmann-Leitner ES, Mease RM, De La Vega P, Savranskaya T, Polhemus M, Ockenhouse C, Angov E (2010) Immunization with pre-erythrocytic antigen CelTOS from *Plasmodium*

falciparum elicits cross-species pro1tection against heterologous challenge with *Plasmodium berghei*. PLoS ONE 5 (8):e12294. doi:10.1371/journal.pone.0012294

Bermudez A, Vanegas M, Patarroyo ME (2008) Structural and immunological analysis of circumsporozoite protein peptides: a further step in the identification of potential components of a minimal subunit-based, chemically synthesised antimalarial vaccine. Vaccine 26(52):6908–6918

Bongfen SE, Ntsama PM, Offner S, Smith T, Felger I, Tanner M, Alonso P, Nebie I, Romero JF, Silvie O, Torgler R, Corradin G (2009) The *N*-terminal domain of *Plasmodium falciparum* circumsporozoite protein represents a target of protective immunity. Vaccine 27(2):328–335

Cifuentes G, Bermudez A, Rodriguez R, Patarroyo MA, Patarroyo ME (2008) Shifting the polarity of some critical residues in malarial peptides' binding to host cells is a key factor in breaking conserved antigens' code of silence. Med Chem 4(3):278–292

Cifuentes G, Vanegas M, Martinez NL, Pirajan C, Patarroyo ME (2009) Structural characteristics of immunogenic liver-stage antigens derived from *P. falciparum* malarial proteins. Biochem Biophys Res Commun 384(4):455–460

Combet C, Blanchet C, Geourjon C, Deleage G (2000) NPS@: network protein sequence analysis. Trends Biochem Sci 25(3):147–150

Cowman AF, Crabb BS (2006) Invasion of red blood cells by malaria parasites. Cell 124(4):755–766. doi:S0092-8674(06)00181-4[pii] 10.1016/j.cell.2006.02.006

Cowman AF, Baldi DL, Duraisingh M, Healer J, Mills KE, O'Donnell RA, Thompson J, Triglia T, Wickham ME, Crabb BS (2002) Functional analysis of *Plasmodium falciparum* merozoite antigens: implications for erythrocyte invasion and vaccine development. Philos Trans R Soc Lond B Biol Sci 357(1417):25–33. doi:10.1098/rstb.2001.1010

Curtidor H, Torres MH, Alba MP, Patarroyo ME (2007) Structural modifications to a high-activity binding peptide located within the PfEMP1 NTS domain induce protection against *P. falciparum* malaria in Aotus monkeys. Biol Chem 388(1):25–36. doi: 10.1515/BC.2007.003

Curtidor H, Arevalo G, Vanegas M, Vizcaino C, Patarroyo MA, Forero M, Patarroyo ME (2008a) Characterization of *Plasmodium falciparum* integral membrane protein Pf25-IMP and identification of its red blood cell binding sequences inhibiting merozoite invasion in vitro. Protein Sci 17(9):1494–1504. doi: ps.036251.108[pii]10.1110/ps.036251.108

Curtidor H, Garcia J, Vanegas M, Puentes F, Forero M, Patarroyo ME (2008b) Identification of peptides with high red blood cell and hepatocyte binding activity in the *Plasmodium falciparum* multistage invasion proteins: PfSPATR and MCP-1. Biochimie 90(11–12):1750–1759. doi:10.1016/j.biochi.2008.08.003

Florens L, Washburn MP, Raine JD, Anthony RM, Grainger M, Haynes JD, Moch JK, Muster N, Sacci JB, Tabb DL, Witney AA, Wolters D, Wu Y, Gardner MJ, Holder AA, Sinden RE, Yates JR, Carucci DJ (2002) A proteomic view of the *Plasmodium falciparum* life cycle. Nature 419(6906):520–526

Garcia JE, Puentes A, Patarroyo ME (2006) Developmental biology of sporozoite–host interactions in *Plasmodium falciparum* malaria: implications for vaccine design. Clin Microbiol Rev 19(4):686–707

Gardner MJ, Hall N, Fung E, White O, Berriman M, Hyman RW, Carlton JM, Pain A, Nelson KE, Bowman S, Paulsen IT, James K, Eisen JA, Rutherford K, Salzberg SL, Craig A, Kyes S, Chan MS, Nene V, Shallom SJ, Suh B, Peterson J, Angiuoli S, Pertea M, Allen J, Selengut J, Haft D, Mather MW, Vaidya AB, Martin DM, Fairlamb AH, Fraunholz MJ, Roos DS, Ralph SA, McFadden GI, Cummings LM, Subramanian GM, Mungall C, Venter JC, Carucci DJ, Hoffman SL, Newbold C, Davis RW, Fraser CM, Barrell B (2002) Genome sequence of the human malaria parasite *Plasmodium falciparum*. Nature 419(6906): 498–511

Havel TF, Wuthrich K (1985) An evaluation of the combined use of nuclear magnetic resonance and distance geometry for the determination of protein conformations in solution. J Mol Biol 182(2):281–294

Hay SI, Okiro EA, Gething PW, Patil AP, Tatem AJ, Guerra CA, Snow RW (2010) Estimating the global clinical burden of *Plasmodium falciparum* malaria in 2007. PLoS Med 7 (6):e1000290. doi:10.1371/journal.pmed.1000290

Hisaeda H, Yasutomo K, Himeno K (2005) Malaria: immune evasion by parasites. Int J Biochem Cell Biol 37(4):700–706. doi: 10.1016/j.biocel.2004.10.009

Houghten RA (1985) General method for the rapid solid-phase synthesis of large numbers of peptides: specificity of antigen–antibody interaction at the level of individual amino acids. Proc Natl Acad Sci USA 82(15):5131–5135

Ishino T, Yano K, Chinzei Y, Yuda M (2004) Cell-passage activity is required for the malarial parasite to cross the liver sinusoidal cell layer. PLoS Biol 2(1):E4

Ishino T, Chinzei Y, Yuda M (2005) A Plasmodium sporozoite protein with a membrane attack complex domain is required for breaching the liver sinusoidal cell layer prior to hepatocyte infection. Cell Microbiol 7(2):199–208

Kaiser K, Camargo N, Coppens I, Morrisey JM, Vaidya AB, Kappe SH (2004a) A member of a conserved *Plasmodium* protein family with membrane-attack complex/perforin (MACPF)-like domains localizes to the micronemes of sporozoites. Mol Biochem Parasitol 133(1):15–26

Kaiser K, Matuschewski K, Camargo N, Ross J, Kappe SH (2004b) Differential transcriptome profiling identifies *Plasmodium* genes encoding pre-erythrocytic stage-specific proteins. Mol Microbiol 51(5):1221–1232

Kappe SH, Buscaglia CA, Nussenzweig V (2004) Plasmodium sporozoite molecular cell biology. Annu Rev Cell Dev Biol 20:29–59

Kariu T, Ishino T, Yano K, Chinzei Y, Yuda M (2006) CelTOS, a novel malarial protein that mediates transmission to mosquito and vertebrate hosts. Mol Microbiol 59(5):1369–1379

Khusmith S, Charoenvit Y, Kumar S, Sedegah M, Beaudoin RL, Hoffman SL (1991) Protection against malaria by vaccination with sporozoite surface protein 2 plus CS protein. Science 252(5006):715–718

Kumar KA, Sano G, Boscardin S, Nussenzweig RS, Nussenzweig MC, Zavala F, Nussenzweig V (2006) The circumsporozoite protein is an immunodominant protective antigen in irradiated sporozoites. Nature 444(7121):937–940. doi:nature05361[pii]10.1038/nature 05361

Labaied M, Camargo N, Kappe SH (2007) Depletion of the *Plasmodium berghei* thrombospondin-related sporozoite protein reveals a role in host cell entry by sporozoites. Mol Biochem Parasitol 153(2):158–166

Lambros C, Vanderberg JP (1979) Synchronization of *Plasmodium falciparum* erythrocytic stages in culture. J Parasitol 65(3):418–420

Lopez R, Curtidor H, Urquiza M, Garcia J, Puentes A, Suarez J, Ocampo M, Vera R, Rodriguez LE, Castillo F, Cifuentes G, Patarroyo ME (2001) *Plasmodium falciparum*: binding studies of peptide derived from the sporozoite surface protein 2 to Hep G2 cells. J Pept Res 58(4):285–292

Mayer DC, Mu JB, Kaneko O, Duan J, Su XZ, Miller LH (2004) Polymorphism in the *Plasmodium falciparum* erythrocyte-binding ligand JESEBL/EBA-181 alters its receptor specificity. Proc Natl Acad Sci USA 101(8):2518–2523

Merrifield RB (1963) Solid phase peptide synthesis. I. The synthesis of a tetrapeptide. J Am Chem Soc 85:2149–2154

Mongui A, Angel DI, Moreno-Perez DA, Villarreal-Gonzalez S, Almonacid H, Vanegas M, Patarroyo MA (2010) Identification and characterization of the *Plasmodium vivax* thrombospondin-related apical merozoite protein. Malar J 9:283. doi:10.1186/1475-2875-9-283

Patarroyo ME, Patarroyo MA (2008) Emerging rules for subunit-based, multiantigenic, multistage chemically synthesized vaccines. Acc Chem Res 41(3):377–386

Patarroyo ME, Cifuentes G, Bermudez A, Patarroyo MA (2008a) Strategies for developing multi-epitope, subunit-based, chemically synthesized anti-malarial vaccines. J Cell Mol Med 12(5B):1915–1935

Patarroyo ME, Cifuentes G, Rodriguez R (2008b) Structural characterisation of sporozoite components for a multistage, multi-epitope, anti-malarial vaccine. Int J Biochem Cell Biol 40(3):543–557

Pradel G, Garapaty S, Frevert U (2002) Proteoglycans mediate malaria sporozoite targeting to the liver. Mol Microbiol 45(3):637–651

Rathore D, Hrstka SC, Sacci JB Jr, De la Vega P, Linhardt RJ, Kumar S, McCutchan TF (2003) Molecular mechanism of host specificity in *Plasmodium falciparum* infection: role of circumsporozoite protein. J Biol Chem 278(42):40905–40910

Reyes C, Patarroyo ME, Vargas LE, Rodriguez LE, Patarroyo MA (2007) Functional, structural, and immunological compartmentalisation of malaria invasive proteins. Biochem Biophys Res Commun 354(2):363–371

Roccatano D, Colombo G, Fioroni M, Mark AE (2002) Mechanism by which 2, 2, 2-trifluoroethanol/water mixtures stabilize secondary-structure formation in peptides: a molecular dynamics study. Proc Natl Acad Sci USA 99(19):12179–12184. doi:10.1073/pnas.182199699

Rodriguez LE, Curtidor H, Urquiza M, Cifuentes G, Reyes C, Patarroyo ME (2008) Intimate molecular interactions of *P. falciparum* merozoite proteins involved in invasion of red blood cells and their implications for vaccine design. Chem Rev 108(9):3656–3705

Sinnis P, Coppi A (2007) A long and winding road: the Plasmodium sporozoite's journey in the mammalian host. Parasitol Int 56(3):171–178

Snow RW, Guerra CA, Noor AM, Myint HY, Hay SI (2005) The global distribution of clinical episodes of *Plasmodium falciparum* malaria. Nature 434(7030):214–217

Sreerama N, Woody RW (2000) Estimation of protein secondary structure from circular dichroism spectra: comparison of CONTIN, SELCON, and CDSSTR methods with an expanded reference set. Anal Biochem 287(2):252–260

Suarez JE, Urquiza M, Puentes A, Garcia JE, Curtidor H, Ocampo M, Lopez R, Rodriguez LE, Vera R, Cubillos M, Torres MH, Patarroyo ME (2001) *Plasmodium falciparum* circumsporozoite (CS) protein peptides specifically bind to HepG2 cells. Vaccine 19(31):4487–4495

Tamura K, Dudley J, Nei M, Kumar S (2007) MEGA4: Molecular Evolutionary Genetics Analysis (MEGA) software version 4.0. Mol Biol Evol 24 (8):1596–1599. doi:10.1093/molbev/msm092

Thompson JD, Gibson TJ, Higgins DG (2002) Multiple sequence alignment using ClustalW and ClustalX. Curr Protoc Bioinformatics Chapter 2:Unit 2 3. doi:10.1002/0471250953.bi0203s00

Thompson J, Cooke RE, Moore S, Anderson LF, Janse CJ, Waters AP (2004) PTRAMP; a conserved Plasmodium thrombospondin-related apical merozoite protein. Mol Biochem Parasitol 134(2):225–232. doi:10.1016/j.molbiopara.2003.12.003

Tossavainen H, Pihlajamaa T, Huttunen TK, Raulo E, Rauvala H, Permi P, Kilpelainen I (2006) The layered fold of the TSR domain of *P. falciparum* TRAP contains a heparin binding site. Protein Sci 15(7):1760–1768. doi:15/7/1760[pii]10.1110/ps.052068506

Tucker RP (2004) The thrombospondin type 1 repeat superfamily. Int J Biochem Cell Biol 36(6):969–974

Wüthrich K (New York 1986) NMR of proteins and nucleic acids. Wiley

Yuda M, Ishino T (2004) Liver invasion by malarial parasites—how do malarial parasites break through the host barrier? Cell Microbiol 6(12):1119–1125

8. CAPÍTULO 4

Protective immunity provided by a new modified SERA protein peptide: its immunogenetic characteristics and correlation with 3D structure.

SERA 5 es una proteína del merozoíto con repetición de serinas que se expresa en grandes cantidades específicamente en etapas finales de trofozoito y esquizonte (138) (segunda línea de defensa contra la infección por *Plasmodium*). Modificaciones hechas al péptido conservado 6754, ha generado el péptido 23426 que induce anticuerpos y protección contra el reto experimental. El péptido nativo 6754 presentó una conformación al azar por RMN de ^{1}H, mientras el péptido modificado 23426 presentó una estructura de giro β tipo V entre V3 a L6. De acuerdo al registro de unión HLA-DRβ1*0401, el péptido 23426 tiene una distancia de 24.31 Å entre los átomos más lejanos entre el P1 y el P9, mayor al presentado por el péptido modificado 22892 que induce anticuerpos pero no protege contra el reto experimental, así como orientaciones de las cadenas laterales diferentes cambiando probablemente las propiedades inmunológicas y complementando el conjunto de péptidos elegidos como candidatos para el diseño de una vacuna contra malaria.

Amino Acids
DOI 10.1007/s00726-011-1061-5

ORIGINAL ARTICLE

Protective immunity provided by a new modified SERA protein peptide: its immunogenetic characteristics and correlation with 3D structure

Adriana Bermúdez · Armando Moreno-Vranich · Manuel E. Patarroyo

Received: 30 May 2011 / Accepted: 9 August 2011

Abstract The serine repeat antigen (SERA) protein is a leading candidate molecule for inclusion as a component in a multi-antigen, multi-stage, minimal subunit-based, chemically synthesised anti-malarial vaccine. Peptides having high red blood cell binding affinity (known as HABPs) have been identified in this protein. The 6733 HABP was located in the C-terminal portion of the 47-kDa fragment while HABP 6754 was located in the C-terminal region of the 56-kDa fragment. These conserved HABPs failed to induce an immune response. Critical red blood cell binding residues and/or their neighbours (assessed by glycine-analogue scanning) were replaced by others having the same mass, volume and surface but different polarity, rendering some of them highly immunogenic when assessed by antibody production against the parasite or its proteins and protection-inducers against experimental challenge with a highly infectious *Aotus* monkey-adapted *Plasmodium falciparum* strain. This manuscript presents some modified HABPs as vaccine candidate components for enriching our tailor-made anti-malarial vaccine repertoire, as well as their 3D structure obtained by ^{1}H-NMR displaying a short-structured region, differently from the native ones having random structures.

Keywords SERA 5 · NMR · Structure · Malaria vaccine

A. Bermúdez · A. Moreno-Vranich · M. E. Patarroyo (✉)
Fundación Instituto de Inmunología de Colombia (FIDIC),
Carrera 50 No. 26-00, Bogotá, Colombia
e-mail: mepatarr@mail.com

A. Bermúdez
Universidad del Rosario, Bogotá, Colombia

M. E. Patarroyo
Universidad Nacional de Colombia, Bogotá, Colombia

Introduction

The *Plasmodium falciparum* serine repeat antigen (SERA) protein family consists of a group of six closely related proteins (SERA 1–6); including the SERA-5 molecule (synthesised as a 111-kDa precursor) which has been studied in depth and which has been considered as a potential erythrocyte-stage vaccine candidate. SERA proteins are expressed during late trophozoite and schizont maturation stages where they undergo proteolytic processing by the *Pf* subtilisin 1 (*Pf*SUB-1) enzyme prior to the merozoite release and invasion of red blood cells (RBCs). Such proteolytic processing gives rise to a 47-kDa N-terminal fragment, a soluble 56-kDa inner domain fragment having a significant active serine-protease homologous region and an 18-kDa C-terminal portion. The 47- and 18-kDa fragments contain cysteine-rich domains, both remaining associated by disulphide bridges and forming a soluble 73-kDa hybrid protein fragment in non-reducing conditions (Sato et al. 2005). The 47-kDa fragment N-terminal is further processed into two 25-kDa fragments; one of these is attached to the 18-kDa fragment by a disulphide bridge (Fig. 1a), remaining bound to the merozoite membrane. The 56-kDa fragment is further processed in its C-terminal region and a 6-kDa peptide is removed to yield a 50-kDa fragment having putative serine-like activity. Although its exact function is still not very clear, SERA is the target of in vivo parasite antibodies before and after merozoite release; its recognition leads to merozoite agglutination and their subsequent dispersion obstruction. Such evidence strongly supports considering SERA as a good candidate to be included in a multi-antigenic anti-malarial vaccine.

In previous studies (Puentes et al. 2000), 49 non-overlapping 20 residue-long peptides encompassing the whole SERA protein were synthesised; six native peptides showed

Journal : Large 726 | Dispatch : 17-8-2011 | Pages : 12
Article No. : 1061 | ☐ LE | ☐ TYPESET
MS Code : AMAC-D-11-00212 | ☑ CP | ☑ DISK

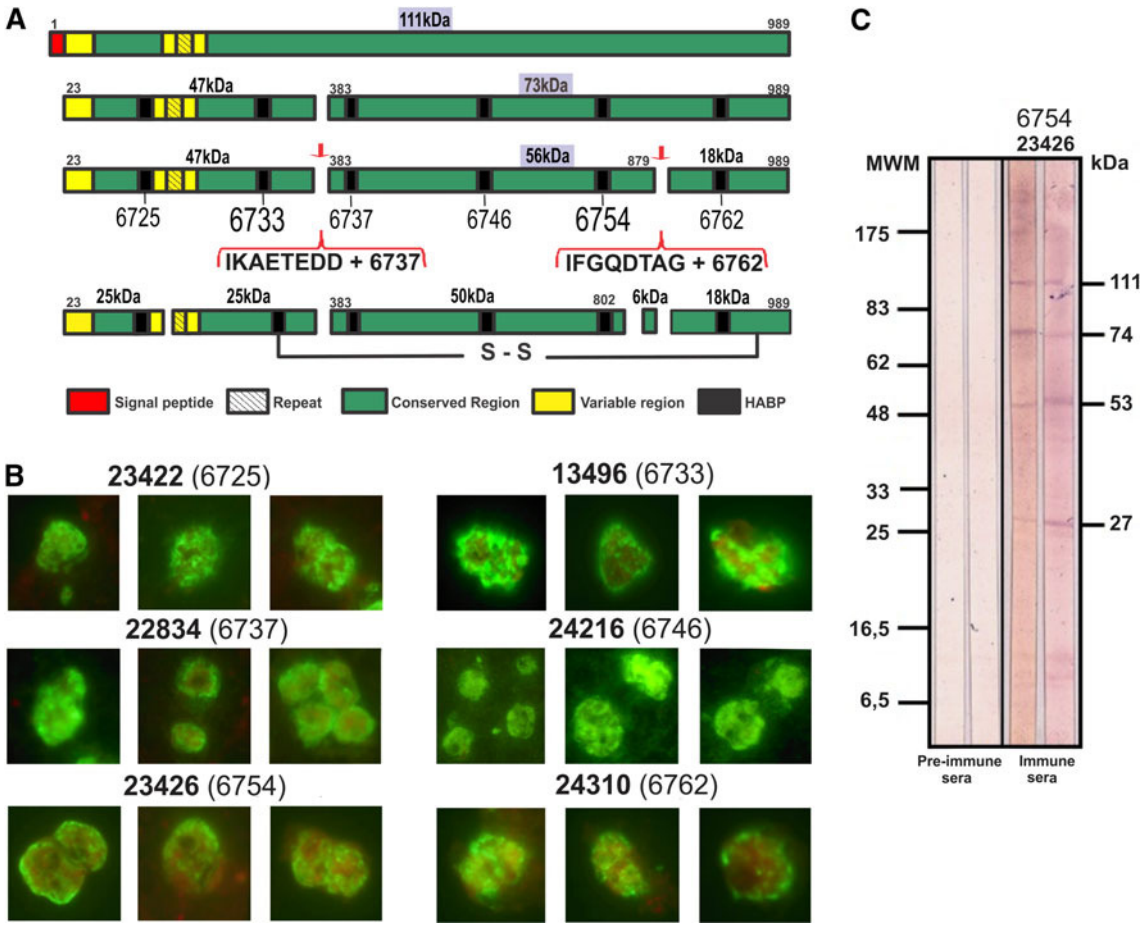

Fig. 1 **a** Schematic representation of the *P. falciparum* SERA protein involved in RBC invasion. The cleavage sites and their corresponding amino acid sequences have been indicated by *red arrows* together with HABPs 6725, 6733, 6737, 6746, 6754 and 6762 localizations, represented by *black vertical bars* (peptides identified as HABPs are indicated by our Institute's serial numbering system). *Bar length* shows approximate molecular weights and putative cleavage places and fragments. *Green fragments* show conserved amino acid sequences while *yellow regions* show variable amino acid sequences. The signal peptide is shown in *red*. **b** Immunofluorescence patterns shown by sera from protected *Aotus* monkeys, immunised with SERA protein-derived HABPs. These modified analogues (shown in *bold*) were derived from previously reported conserved HABPs (shown *inside parenthesis*) and the ones included in this manuscript. **c** Western blot analysis of sera from *Aotus* monkeys immunised with modified analogue **23426,** derived from conserved HABP 6754. The recognition of protein bands agreed with proteins' theoretical weight from which their amino acid sequences or their cleavage products were derived. Molecular weight markers are shown to the *left* in kDa, while the molecular weights of recognised bands are shown to the *right*

high binding capacity to RBCs, named high-activity binding peptides (HABPs): 6725 (Alba et al. 2004), 6733 (this paper), 6737 (Cubillos et al. 2003), 6746 (Alba et al. 2003), 6754 (this paper) and 6762 (Salazar et al. 2008). They were numbered according to our institute's peptide coding system, meaning that their localisation (Fig. 1a, black bars) in the protein's amino acid sequence has been written in small superscript numbers. Native HABP numbers will be shown throughout this document in normal script whilst their modified analogues will be shown in bold (the effect of modified HABPs being the main emphasis of this paper). Immunological and structural studies from some of these native peptides and their modified HABPs have been previously reported, with the exception of peptides 6733 (^{321}YALGS**D**IPEKCDT**L**LAS**NC**FLS^{340}) and 6754 (Y^{749}K**K**VQNLCG**D**DTADHAVNI**V**G^{768}) along with their critical RBC-binding residues (assessed by glycine-analogue scanning, shown in bold and underlined above). These have been localised in the 47- and 56-kDa fragments, respectively, and form the focus of this manuscript. These native HABPs have been used in the attempt to induce antibodies against the *P. falciparum* parasite, as well as protective immunity against experimental challenge with this parasite but giving negative results, as has happened with previous experimental data for all conserved HABPs derived from most merozoite proteins studied so far (Patarroyo and Patarroyo 2008; Patarroyo et al. 2011). Critical binding residues and some of their neighbours were thus replaced by others

Journal : Large 726 Dispatch : 17-8-2011 Pages : 12
Article No. : 1061 LE TYPESET
MS Code : AMAC-D-11-00212 CP DISK

having the same mass, volume and surface, but opposite polarity, as thoroughly described beforehand (Cifuentes et al. 2008). This rendered some of these modified HABPs highly immunogenic, as assessed by antibodies production against the parasite or its proteins, and protection induction against challenge with a highly infectious *P. falciparum* strain adapted to *Aotus* monkeys (a primate species highly susceptible to human malaria).

Our previous studies have also identified modified peptides derived from other SERA-conserved HABPs [6725 (Alba et al. 2004), 6737 (Cubillos et al. 2003), 6746 (Alba et al. 2003) and 6762 (Salazar et al. 2008)] which were able to induce high immune responses and protective immunity, highlighting them as strong vaccine candidates. The present manuscript has concentrated on studying native peptides 6733 and 6754 (which displayed random configuration 3D structures as determined by CD and ^{1}H-NMR studies) known to be involved in RBC invasion due to the aforementioned studies. This paper highlights the importance of HABP **23426** (KKVQNLTGDDTADLATNIVG) which was modified from native peptide 6754; the modified HABP displayed a type V (γ-turn structure) as evidenced by ^{1}H-NMR and the modifications made were T7C, L14H and T16V. Since the immune response against malaria is genetically controlled by the major histocompatibility complex region II (MHC II), it was found that this peptide bound with higher affinity to HLA DRβ1*0401 molecules than to the other HLA molecules involved in this study.

A very relevant aspect concerns the fact that HABP **23426** induced high antibody titres and protected *Aotus* monkeys against experimental challenge. Molecular modelling studies of this peptide in the HLA DRβ1*0403 molecule showed that 12 H-bonds were established between **23426** backbone and MHCII molecule lateral chains atoms, suggesting that these atomic features would be relevant in an immune response generated by this modified peptide in *Aotus* monkeys. This HABP has thus been considered a good candidate for being a component in an antimalarial vaccine.

Materials and methods

Solid-phase peptide synthesis

Native peptides and their corresponding modified analogues (shown in bold type throughout the paper) 6733 (**13496**) and 6754 (**22892**, **23426**) were synthesised by the standard solid-phase peptide synthesis method, (Merrifield 1963), purified by reverse-phase HPLC and their molecular masses were determined by MALDI-TOF mass spectrometry (Autoflex Bruker Daltonics). Glycine-cysteine (GC) were added to the C- and N-terminals of all peptides used for immunisation studies to polymerise them by an oxidation reaction; this established disulphide bonds amongst them and guaranteed the formation of high-molecular-weight polymers (8–24 kDa) for immunisation purposes.

Animals

Naïve, spleen-intact *Aotus* monkeys from the Colombian Amazon basin, which had been kept in our monkey colony in Leticia, were used for this trial; this non-human primate has proved to be very susceptible to experimental infection with the highly infective *Aotus*-adapted *P. falciparum* FVO strain (Rodriguez et al. 1990). The animals were housed in strict accordance with the Colombian Institute of Health's (INS) animal guidelines and the Colombian Ministry of Health laws (84/1989). They were supervised by expert biologists and veterinarians from Colombian wild-life authorities (CORPOAMAZONIA) and by FIDIC's Primate Station Ethics Committee. Monkey sera were tested by immunofluorescence assay (IFA) for the presence of anti-*P. falciparum* parasite antibodies at 1:20 dilution; monkeys seen to have positive sera at this point were returned to the jungle without further manipulation.

Immunisation and challenge

Groups of 5–9 *Aotus* monkeys (depending on availability) were immunised with 125 μg peptide, as described in previous work (Bermudez et al. 2007). Blood samples were obtained before each immunisation (day 0, 20, 40) and 20 days after the third immunisation for immunological studies. Immunised and control *Aotus* monkeys were intravenously infected with 100,000 *P. falciparum* FVO-strain infected RBCs which had been freshly obtained from another infected monkey. This dose is known to be 100% infective for these monkeys (Rodriguez et al. 1990).

Parasitaemia assessment

Blood parasitaemia levels were monitored daily for 15 days using Acridine Orange staining to reveal parasitaemia levels. Protection was defined as the total absence of parasites in blood during these 15 days. Non-protected monkeys developed evident parasitaemia on day 5 or 6, $\geq$5% levels being reached between days 8 and 10. The infected monkeys received treatment with anti-malarial drugs; they were kept in quarantine until complete cure had been ensured and then released back into the jungle, directly supervised by CORPOAMAZONIA officials.

Immunofluorescence antibody (IFA) testing

Synchronised late-stage schizonts from a continuous *P. falciparum* culture (FCB-2 strain) were washed and

Journal : Large 726 | Dispatch : 17-8-2011 | Pages : 12
Article No. : 1061 | LE | TYPESET
MS Code : AMAC-D-11-00212 | CP | DISK

treated as described earlier (Rodriguez et al. 1990). The slides on which the dry parasites had been mounted were blocked for 10 min with 1% non-fat milk and incubated for 30 min with increasing dilutions of monkey sera for antibody analysis, starting at 1:40 dilution. Reactivity was observed by fluorescence microscopy using the F(ab′)2 fragment from a 1:100 diluted goat affinity purified IgG anti-monkey IgG–FITC conjugate. Pre-immune sera from all monkeys were used as negative controls.

Western blotting

Late-stage schizonts from continuous *P. falciparum* cultures, exhibiting 20% parasitaemia, were collected, washed in sterile PBS and RBCs lysed with 0.2% saponine solution with vigorous vortexing for 45 s. The pellet was washed twice with large volumes of PBS to remove haemoglobin and erythrocyte debris. The enriched schizont pellet was further lysed with Laemmli's buffer and 5% SDS. The soluble proteins were separated in a discontinuous SDS-PAGE system using 7.5–15% acrylamide (w/v) gradient, transferred to nitrocellulose membranes and then blocked with TBS-T (0.02 M Tris–HCl, pH 7.5, 0.05 M NaCl, 1% Tween-20) and 5% skimmed milk (blocking solution) for 1 h and cut into strips. Each strip was individually incubated with monkey sera diluted 1:200 in blocking solution, washed several times with TBS-T and then incubated with goat anti *Aotus* IgG, alkaline phosphatase (AP) conjugated at 1:1,000 dilution and developed with NBT/BCIP (Blake et al. 1984).

HLA-DR molecule affinity purification

Purified human molecules were obtained from WT100BIS (DRβ1*0101), COX (DRβ1*0301), BSM (DRβ1*0401), EKR (DRβ1*0701) and DR11 BM21 (DRβ1*1101) homozygous EBV-transformed B cell lysates by affinity chromatography, using anti-HLA-DR mAb L-243 cross-linked to protein A Sepharose CL-4B (Amersham Pharmacia Biotech AB) as affinity support.

Peptide-binding competition assays

Peptide-binding competition assays measured unlabelled peptides' ability to compete with biotinylated indicator peptides in binding to purified HLA-DR molecules, as previously described (Sinigaglia et al. 1991; Vargas et al. 2003). Biotinylated-labelled haemagglutinin HA peptide 306-318 (PKYVKQNTLKLAT) was used as control peptide for DRβ1*0101, DRβ1*0301, DRβ1*0401 and Gly-Phe-Lys-$(Ala)_7$ ($GFKA_7$) for DRβ1*1101 and DRβ1*0701.

Purified HLA-DR molecules were diluted in freshly prepared binding buffer containing 100 mM citrate/phosphate buffer (pH 7), 0.15 mM NaCl, 4 mM EDTA, 4% NP-40, 4 mM PMSF and 40 µg/ml for each of the following: soybean trypsin inhibitor, antipain, leupeptin and chymostatin. About 90 µl of HLA-DR molecule (0.1 µM) was added to Eppendorf tubes, together with 30 µl biotinylated-labelled peptide (5 µM) in DMSO:PBS (1:4) for direct binding assay; an additional 250 µM was added for the competition assay. After 24 h of incubation at room temperature, the peptide/class II complexes were transferred to ELISA well-plates (NuncImmuno Modules Maxisorp Loose Brand product, Denmark) which had been coated with a 10-µg/ml anti-HLA-DR mAb-L-243 solution and subsequently blocked with PBS containing 5% bovine serum albumin. Plates were washed with PBS, 0.05% Tween-20 after 2 h incubation at room temperature. After incubation with alkaline phosphatase-labelled streptavidine (Vector Laboratories, Burlingame, CA), labelled peptide/HLA-DR complexes were revealed with 4-nitrophenyl-phosphate substrate (Kirkegaard and Perry Laboratories, MD, USA). A Titertek MC Multi-scan ELISA reader (Labsystems, Franklin, Mass) with 405 nm filter was used for determining peptide binding to HLA-DR molecules by measuring optical density (OD). Relative binding affinity for other peptides was determined by competition assay; according to this assay, a good competitor was a peptide which was able to inhibit indicator peptide binding to the HLA molecule being tested by more than 50%.

Circular dichroism (CD)

A JASCO J-810 spectropolarimeter was used to take spectra for native HABP 6733 and 6754, their modified and corresponding monomers and polymers; the spectra were smoothed using JASCO software. The peptide sample was analysed in 500 µl TFE-water mixtures (30:70, v/v) using a 1-mm path-length rectangular cell (Greenfield 1996). Measurements were taken at 20°C and expressed in terms of mean residue ellipticity (deg $cm^2/dmol$). The spectra were measured between 190 and 250 nm using 0.2 nm spectra bandwidth and 10 nm/min scan speed.

NMR analysis and structural calculations

Seven to ten milligram of HPLC purified peptides was dissolved in 600 µl TFE-water (30/70 v/v) for NMR experiments. NMR spectra were recorded on a Bruker DRX-600 spectrometer at 295°K. Double-quantum filter correlation spectroscopy (DQF-COSY) (Rance et al. 1983), total correlation spectroscopy (TOCSY) (Bax and Davis 1985) and nuclear overhauser enhancement spectroscopy (NOESY) experiments were used for assigning spectra (Jeener et al. 1979) and data were processed on an Indy computer (Silicon Graphics) equipped with updated

Journal : Large 726 | Dispatch : 17-8-2011 | Pages : 12
Article No. : 1061 | LE | TYPESET
MS Code : AMAC-D-11-00212 | CP | DISK

TOPSPIN software (Bruker). Distance Geometry (DGII) software was used for providing a family of 50 structures. These structures were refined using a simulated annealing protocol (DISCOVER software). Structures having reasonable geometry and few distance and angle violations were selected.

Molecular modelling

The HLADRβ1*0401 human molecule (PDB code 1J8H) crystal structure was used as template for molecular modelling peptides **23426** and **22892** (6754 analogues) to ascertain their fit into this complex; in turn, this was used for analysing whether the three-dimensional structure of modified, immunogenic, protection-inducing peptide **23426** had been correctly obtained, compared with the fit of non-immunogenic, non-protection-inducing peptide **22892**. The amino acids have been written using one-letter code when they have been derived from the modified peptide and in three-letter code if they have been HLA-DRβ1* chain-derived. Replacements were made in this molecule's sequence based on the differences found in the protein-binding region (PBR), as reported in previous studies (Suarez et al. 2006; Patarroyo et al. 2010a). The amino acids replaced in the HLA-DRβ1*0403 molecule were Argβ71Lys, Gluβ74Ala and Valβ86Gly. Replacements made in haemagglutinin (HA) for modified peptide **23426** were Q4P, N5K, L6Y, T7V, G8K, D9Q, D10N, A12L, and D13K and Q4P, N5K, L6Y, S8K, D9Q, D10N, A12L, D13K and V16T for peptide **22892**.

A conjugate gradient algorithm was applied to minimise energy and build a more stable model showing atom position within the peptide-HLA-DRβ1*0403-like complex in terms of energy. Five to seven simulations using 10,000 iterations were carried out for both complexes (peptide **23426**-HLA-DRβ1*0403-like and peptide **22892**-HLA-DRβ1*0403-like) to obtain the most appropriate model using each sequence contained in the complete template. Insight II (2000) Biopolymer module software (Accelrys Software Inc., USA), run on an Indigo 2 Station (Silicon Graphics), was used for superimposing the calculated models onto the original template backbones (without further refinements).

Results and discussions

Peptide analysis

HPLC monomer analysis revealed one single peak after purification, which was pure enough for ^{1}H-NMR analysis; peptide masses were similar to theoretical masses (data not shown). The polymers used for immunisation had molecular masses ranging from 8 to 24 kDa, as assessed by size-exclusion chromatography (SEC).

Immunogenicity studies

Native conserved HABPs 6754 and 6733 were not immunogenic, given the antibody production against this protein was not induced after the third *Aotus* monkey immunisation with these polymer peptides, as assessed by IFA and Western blot. Likewise, protection against experimental challenge with the parasite was not induced (Table 1).

Immunogenicity was seen to have been induced when **13496** (peptide 6733 analogue) was modified by changing V5D, E6I, S10C, V16N and V17C, as assessed by the presence of high levels of IFA antibodies and Western blot reactivity, even though absolutely no protection was induced (Table 1). A similar thing occurred with **14536** (6733) with modifications P5D, N6I, S10C, H13L, I16N and V17C.

No antibodies were produced by modified peptide **22892** (6754 analogue) when replacing V7C, S8G, L14H, as assessed by IFA and Western blot reactivity, and no protection against experimental challenge was induced (Table 1). Similar results were obtained when other modifications were made, such as changing critical residues in other analogous peptides synthesised. On the contrary, immunogenicity and protection were induced in *Aotus* monkeys inoculated with modified HABP **23426** where changes were made to residues T7C, L14H and T16V (Table 1), categorically confirming that critical binding residues or their neighbours have to be changed for others having similar mass and volume but apposite polarity (Cifuentes et al. 2008; Patarroyo et al. 2008, 2011).

IFA and Western blot analysis

Immunofluorescence assay analysis (Fig. 1b) revealed that antibodies against SERA-derived modified HABPs displayed a diffuse intracytoplasmic fluorescence pattern in mature schizonts when the sera from *Aotus* monkeys immunised with previously reported modified HABPs **23422** (6725), **13496**(6733), **22834** (6737), **24216** (6746), **23426** (6754) and **24310** (6762) were used (Fig. 1b). Western blot analysis revealed strong reactivity between sera from protected monkeys immunised with HABP **23426** (6754) with a 111-kDa molecule, corresponding to the complete SERA protein precursor and its 74 kDa complex cleavage fragment (Fig. 1c). *Aotus* sera immunised with this HABP also recognised 53 and 27 kDa fragments corresponding to cleavage and processing products (being quite similar to this protein's 56 and 25 kDa fragments) (Fig. 1a,

Journal : Large 726 Dispatch : 17-8-2011 Pages : 12
Article No. : 1061 LE TYPESET
MS Code : AMAC-D-11-00212 CP DISK

Table 1 Humoral immune response and protective efficacy induced by native peptides 6733 and 6754 and their modified analogues and structural features of conserved HABP 6754 and its modified analogue **23426,** as determined by ^{1}H-NMR

A

Peptide No.	Sequence	PI	post I	post II	Prot.
	P1 P4 P6 P9				
*6733	Y A L G S **D** I P E K C D T **L** A **S** **N** **C** F L S	0	0	0	0/4
***13496**	A L G S **V** **E** P E K S D T L A S **V** **V** F L S	0	3(1280)	2(640)	0/6
14536	A L G S **P** **N** P E K S D T **H** A S **I** **V** F L S	0	5(640)	1(320)	0/4
13498	A L G S **V** **E** P E K S D T L A S **M** **S** F L S	0	0	0	0/4
13778	A L G S **V** **E** P E K S D T **H** A S **V** **V** F L S	0	0	0	0/4
13500	A L G S **P** **K** P E K S D T **L** A S **M** **S** F L S	0	0	0	0/4
12746	A L G S **P** **E** P E K S D T **H** A S **V** **S** F L S	0	0	0	0/4
14534	A L G S **P** **N** P E K S D T **H** A S N **V** F L S	0	0	0	0/4
10142	A L G S D I P E K S D T **H** A S **S** **S** F L S	0	0	0	0/4
10144	A L G S D I P E K **S** D T **A** A S **R** **S** F L S	0	0	0	0/4
10146	A L G S D **I** P E K S D T **R** A S A S F L S	0	0	0	0/4
*6754	Y K K **V** Q N L **C** **G** **D** D T A **D** H A **V** N I **V** G	0	0	0	0
***23426**	K K V Q N L **T** G D D T A D **L** A **T** N I V G	0	3(320)	ND	**1/9**
24220	K K V Q N L **T** G D D T A **I** **L** A **T** N I V G	0	3(320)	ND	0/7
***22892**	K K V Q N L **V** **S** D D T A D **L** A V N I V G	0	0	0	0/9
13848	K K **T** Q N L **S** **A** **P** D T A D H A **T** N I V G	0	0	0	0/5
22434	Q N L **S** G D D T A D **L** A V N I **T** G	0	0	0	0/6

B

						Haplotypes				
						DR1	DR52		DR53	
						% Binding HLA-DRβ1* alleles				
Peptide	Structure	NOEs Used	RMSD	Distance Å	#	0101	0301	1101	0401	0701
6754	Random	ND	ND	-	ND	0	15	5	8	5
23426	Type V β turn V3 to L6	212	0.39	24.31	23	0	16	13	**56**	19

Peptide amino acid sequences used for immunising *Aotus* monkeys are shown in one-letter code (numbered according to our Institute's serial system)

The number outside the bracket shows the total number of *Aotus* monkeys presenting these antibody titres

IFA reciprocal antibody titres (shown in brackets) determined from serum samples taken 20 days after the 1st and 2nd immunisations

Prot. total number of *Aotus* protected against experimental challenge from those presenting the antibody titres, *ND* Not determined

[a] Structures determined by NMR

[b] This peptide's percentage binding to different purified HLA-DRβ1* haplotype molecules (shown in bold, showing $\geq$50% binding affinity)

red arrows and corresponding cleavage sites' amino acids sequences and Western blot analysis shown in Fig. 1c).

Peptide binding to purified HLA-DRβ1* molecules

Native HABP 6754 did not bind to any of the molecules studied here (representative of the main HLA-DR1, DR52 and DR53 haplotypes); however, HABP **23426** (6754) did bind to HLA-DRβ1*0401 (Table 1). This suggested that the above modifications allowed this modified peptide's better fit into this HLA-DRβ1* molecule, thereby allowing more stable MHC II-Peptide–TCR complex formation and, therefore, a better immune response to be induced.

Binding motifs and reading registers

Binding profiles were not determined for modified HABPs **13496** and **14536** (6733) due to limitations in the availability of purified HLA-DR molecules for performing these

Journal : Large 726 Dispatch : 17-8-2011 Pages : 12
Article No. : 1061 LE TYPESET
MS Code : AMAC-D-11-00212 CP DISK

assays and because they did not induce protection. However, they did induce high antibody titres, similar to HABP **24220** (6754) which only induced high antibody titres with the first immunisation and which disappeared later on (Table 1). Such phenomena have been previously described by our group and named, respectively, non-protective, long-lasting antibody induction (Patarroyo et al. 2006) and short-lived antibody induction (Patarroyo et al. 2005) which we have thoroughly analysed at the 3D structural level, finding different structural features and residue orientation in such molecules which have induced these non-protective immune responses.

HABPs **13496** and **13498** (6733) also displayed a binding register characteristic of the HLA-DRβ1*0401 molecule (data not shown) according to Rammensse's classifications (Rammensee et al. 1995). No HLA-DRβ1 binding studies were performed with these and the other modified HABPs shown in Table 1 due to their low relevance in immunological activity.

HABP **23426** (6754) had 56% binding to purified HLA-DRβ1*0401 molecule, this being much more higher than its ability to bind to the other purified HLA-DRβ1* molecules. It also displayed characteristic HLA-DRβ1*0401 binding motifs, such as L6 in pocket 1, D9 in pocket 4, T11 in pocket 6 and L14 in pocket 9 (Table 1), just like HABP **22892** which displayed similar characteristic HLA-DRβ1*0401 binding motifs and reading registers in its sequence (data not shown). The same HLA-DRβ1*0401 binding motifs were observed when comparing HABPs **23426** and **22892** which had been modified in T7/V (pocket 2) G8/S (pocket 3) and T16/V, suggesting a different orientation for the contact of these residues' side chains with TCR residues. Modifications made to **23426** could thus be playing a critical role in the induction of protective immune responses, thereby altering polarity in T7C (pocket 2) and T16V to allow better contact with the TCR, besides allowing a perfect fit for L14H in HLA-DRβ1*0401 pocket 9.

CD determination of secondary structure for peptides 6733 and 6754 and their analogues

The secondary structures of monomer and polymer peptides 6754 and 6733 and their analogues, determined by circular dichroism (CD) in 30% TFE and 70% water, had similar spectrums and structural features. The native peptides had random conformation and modified peptides showed distorted structural features due to the displacement and change in spectrum shape and the minima present in the spectrum. The immunogenic modified peptides seemed to be more structured than the native peptides from which they had been derived according to spectrum distortion and minimum shifting patterns (close to 225 nm), as shown by deconvolution analysis using CONTINLL, SELCON and CDSSTR software (Fig. 2a).

3D structural analysis by ^{1}H-NMR

The peptides selected for ^{1}H-NMR 3D structure determination were representative of important immunological functions, such as immunogenicity and protection induction, as seen with **23426** (6754); those which had no specific immunological reactivity were used for comparing both structural conformations. ^{1}H-NMR analysis found the peptides' structural conformation and correlated them regarding immunogenicity and protection-induced response. Figure 2b shows all NOE connectivities observed.

Native peptides 6733 and 6754 only presented $d_{\alpha N}$ (i, $i+1$) and d_{NN}(i, $i+1$) sequential signals in NOESY spectra (Fig. 2b), indicating that these peptides did not present any conformational preferences and suggesting a random coil conformation throughout the whole peptide. These observations confirmed the previous CD data obtained in deconvolution analysis.

NMR analysis of **13496** (6733-derived peptide immunogenic but non-protective) displayed d_{NN} (i, $i+1$), $d_{\alpha\beta}$ (i, $i+3$) and $d_{\alpha N}$ (i, $i+4$) short- and medium-range interactions (Fig. 2b). NOE connectivities and low-temperature coefficients for amide proton chemical displacement revealed the presence of an α-helix conformation. A set of 50 structures was calculated for this HABP using 195 distance restraints and one hydrogen bond restraint. A family of 32 low-energy structures having 0.25 Å root-mean-square deviation (rmsd) allowed superimposing backbone atoms from residues E8 to L13 onto the structure having the lowest energy conformer; each structure did not have an angle-constraint violation larger than 1.10° or distance constraint violation larger than 0.23 Å. The NOE connectivity pattern, together with low-temperature coefficients, determined the presence of an α-helical structure between E8 and L13 (Fig. 3a).

Peptide **22892** (6754-derived, non-immunogenic and non-protective) had a distorted type III' β-turn between Q4 and V7; the ideal values for this type of structure are $\Phi i+1 = 60$, $\Psi i+1 = 30$, $\Phi i+2 = 60$, $\Psi i+2 = 30$, and the values observed for this peptide were 55.88, 56.50, 70.56 and 55.70, respectively (Table 1; Fig. 3b).

A set of 50 independently produced structures were obtained for **23426** (6754) satisfying experimental constraints when using 173 NOEs derived from distance restraints which had been previously classified according to signal strength (including 18 dihedral restraints). The structural calculations led to obtaining a family of 19 low-energy conformers having no distance violation larger than 0.35 Å. **23426** (immunogenic and fully protective for some monkeys) showed a type V β-turn structure between V3

Journal : Large 726 | Dispatch : 17-8-2011 | Pages : 12
Article No. : 1061 | LE | TYPESET
MS Code : AMAC-D-11-00212 | CP | DISK

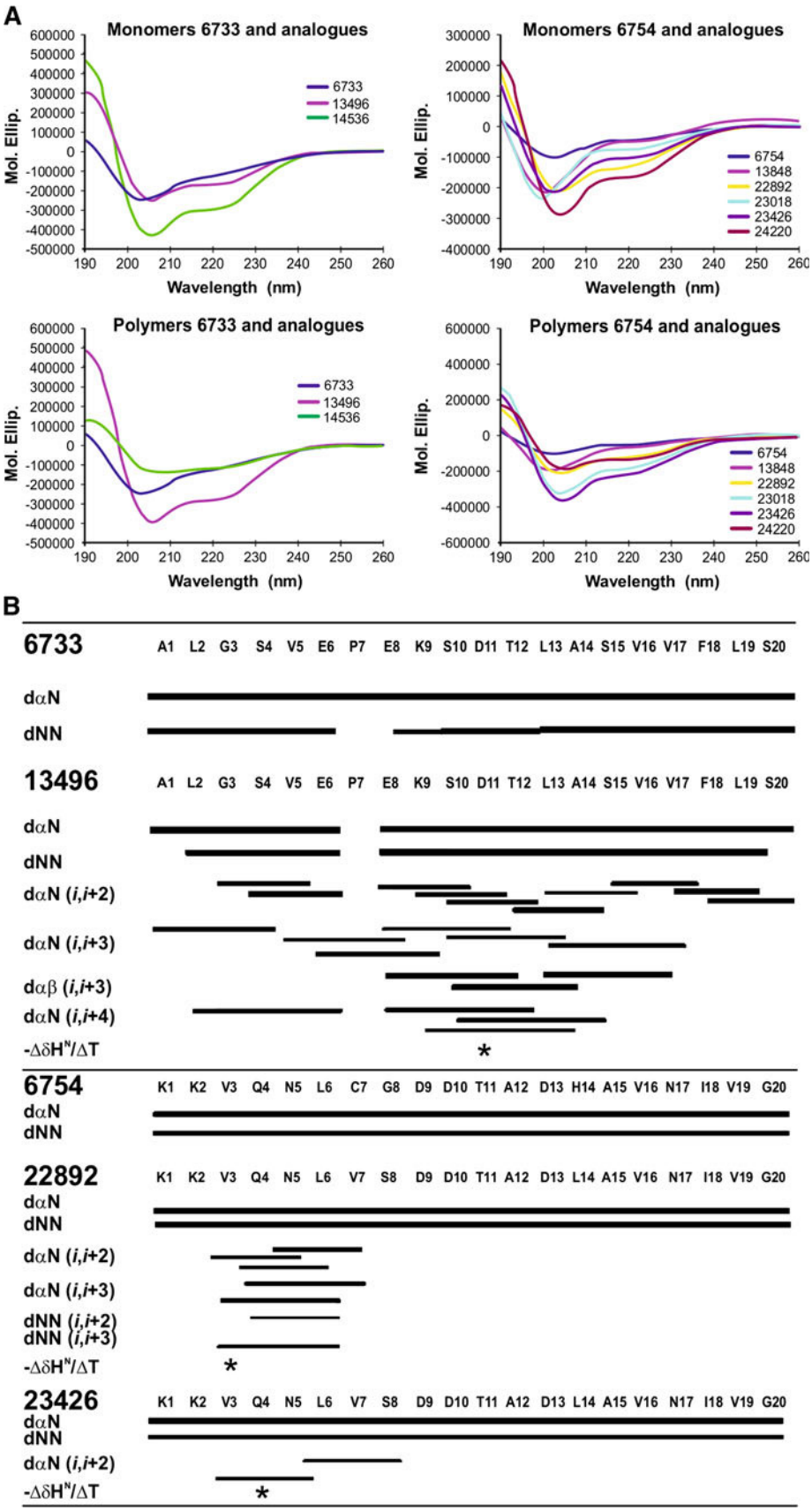

Fig. 2 **a** Circular dichroism for peptides 6733 and 6754 and their analogues in their monomer and polymer forms. **b** Summary of sequential medium-range NOE connectivity (NOE intensities are represented by *line thickness*); amide protons having low coefficients and used for structure calculations are marked with an *asterisk*

Journal : Large 726 Dispatch : 17-8-2011 Pages : 12
Article No. : 1061 LE TYPESET
MS Code : AMAC-D-11-00212 CP DISK

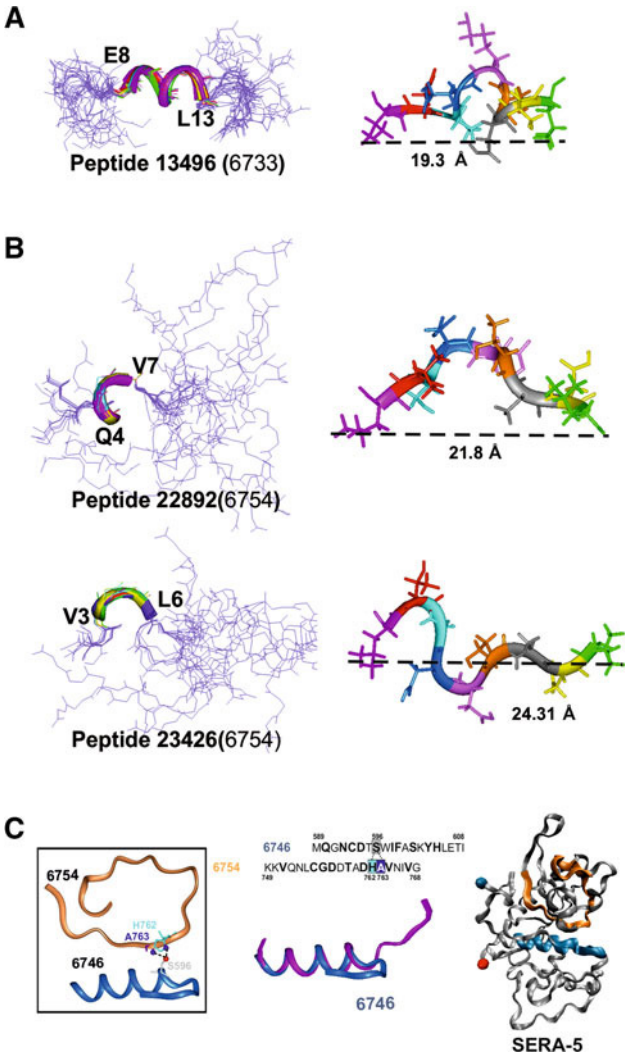

Fig. 3 Backbone and ribbon representation of SERA protein HABP solution structures. **a** and **b** *Left-hand* Front view of overlapping ^{1}H-NMR-derived structures of **13496** (6733), **22892** (6754) and **23426** (6754). *Right-hand* Front view of same structure based on the HLA-DRβ1*0401 allele binding reading register (Rammensee et al. 1995). The amino acid-colour code is based on HLA-DRβ1* binding activities, binding motifs and binding registers, as follows: pocket 1, *fuchsia*; P2, *red*; P3, *turquoise*; pocket 4, *dark blue*; P5, *rose*; pocket 6, *light brown*; P7, *grey*; P8, *yellow*; pocket 9, *green*. The distances between the farthest atoms of residues fitting inside pockets 1 and 9 were measured in Angstroms (Å). **c** *Right hand*, SERA-5 recombinant fragment 3D structure in *yellow* (PDB code 3CH2) and localisation of HABPs 6746 (*blue*) and 6754 (*orange*). In the middle, superimposition of HABP 6746 (*blue*) on the corresponding SERA-5 recombinant sequence. *Boxed*, two H-bonds from the catalytic triad present in this recombinant fragment and, in the middle, the amino acid sequences of 6746 and 6754 displaying the H-bonds established among them to form this protein's non-canonical catalytic triad

and L6. The ideal values for this turn are $\Phi i + 1 = -80$, $\Psi i + 1 = 80$, $\Phi i + 2 = 80$, $\Psi i + 2 = -80$; the values observed for **23426** were −92.23, 54.30, 68.86 and −73.03, respectively.

Three-dimensional structure results for all monomer peptides analysed by NMR in this article were consistent with those obtained in CD studies, thus complementing previous results and making them more robust.

Circular dichroism studies revealed that monomer and polymer structural characteristics remained unchanged, suggesting that the polymer form inoculated into *Aotus* monkeys simulated the same structure as that for the monomer form. Furthermore, unmodified native peptides did not present any type of special conformation whilst modified ones having some biological activity did so (even though having short structures, i.e. short α-helices and β-turns), thus clearly emphasising that suggest modifications must be made to conserved HABPs to render them immunogenic and protection-inducing.

Molecular modelling

Studies of **23426** and **22892** binding to HLA-DRβ1* purified molecules have shown strong **23426** binding to human HLA-DRβ1*0401 molecules (Table 1). Studies by Suarez et al. (2006) and Patarroyo et al. (2010b) have shown that the HLA-DRβ1*0403-like allele had higher frequency in the *Aotus* monkey population being studied, since immunisation and protection studies with these peptides were performed with a sequence from the *Aotus* HLA-DRβ1*0403 chain when using this non-human primate model (Suarez et al. 2006; Patarroyo et al. 2010a). It was thus decided to carry out molecular modelling analysis, making the corresponding β-chain replacements (residues highlighted in black in the turquoise ribbon shown in Fig. 4) and amino acid replacements for each peptide (designated initially in the methodology) in HLA-DRβ1*0401 3D structure. All these changes were carried out within the PDB code 1J8H template.

These studies have shown that the complex formed by the modified HLA-DRβ1*0403-like molecule and modified **23426** (6754) complex were stabilised by the spontaneous formation of 12 H-bonds (including the 11 canonical ones) (Dessen et al. 1997), compared with the six H-bonds found for peptide **22892** (data not shown), which includes five out six canonical H-bonds.

Figure 4a shows the spontaneously formed H-bonds (very small silver balls). Interatomic distances, determined in Angstroms, were measured between Hε22 from Glnα9 and O from D9 (2.40 Å); O Serα53 and HN from L6 (1.87 Å); Hδ22 from Asnα62 and O from D9 (2.14 Å); Oδ1 from Asnα69 and HN from L14 (1.98 Å); OH from Tyrβ30 and HN from A12 (2.20 Å); HH from Tyrβ30 and O from A12 (1.85 Å); HH from Tyrβ60 and O from D13 (1.92 Å); Hε1 from Trpβ61 and O from D13 (2.06 Å); HH11 from Argβ71 and O from D10 (2.34 Å); HH21 from Argβ71 and O from D10 (2.34 Å); Oδ1 from Asnβ82 and

Journal : Large 726 | Dispatch : 17-8-2011 | Pages : 12
Article No. : 1061 | LE | TYPESET
MS Code : AMAC-D-11-00212 | CP | DISK

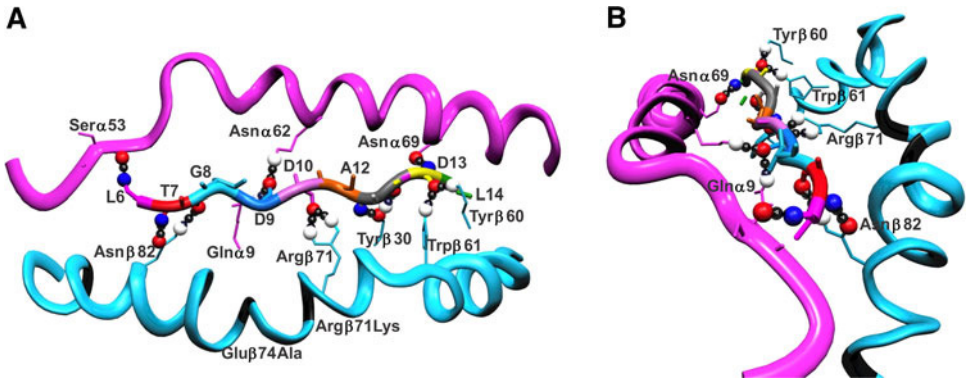

Fig. 4 **23426** interatomic interactions with HLA-DRβ1*0403. **a** Top view, **b** front view (in two directions). The orientation of some **23426** residues' lateral-chain atoms (represented as *sticks* and *balls*) is shown, as well as their positions inside MHCII molecules according to the previously established colour code in Fig. 3. The H-bonds (shown as small *silver balls*) established between **23426** backbone atoms (represented as *sticks*) and MHCII α- and β-chain residue side-chain atoms (depicted as *pink* and *blue ribbons*, respectively). Nitrogen, oxygen and hydrogen atoms have been shown as *blue*, *red* and *white balls*. *Black segments* in the β-chain show the residues that were modified according to HLA-DRβ1*0403 sequences

HN from T7 (2.04 Å); Hδ22 from Asnβ82 and O from T7 (2.47 Å). Except for Tyrβ30 and Tyrβ60, all H-bonds belonged to the canonical H-bonds forming bridges.

The **23426** lateral chain orientation (obtained from molecular modelling) agreed with the 3D structure obtained by ^{1}H-NMR, highlighting residue orientation of T7 corresponding to pocket 2 directed towards the TCR molecule (Fig. 4b), similar to that observed for A12 corresponding to pocket 7 as well as the downward orientation of L14 corresponding to the residue fitting into pocket 9. These findings confirmed the possible associations between such 3D structural features and these modified peptides in the immune response generated by this modified peptide in the *Aotus* monkeys in the study.

Atomic and immunological considerations

The best immunogenic and protection-inducing modified HABP was **23426** which bound to HLA-DRβ1*0401 and had a 24.31 Å distance between its furthest atoms, fitting into pockets 1–9 of this molecule and corresponding to residues L6 from pocket 1 and L14 from pocket 9. Non-immunogenic, non-protection-inducing modified HABP **22892** had a 21.8 Å distance between the furthest atoms (2.51 Å shorter), fitting into pockets 1–9; **22892** probably fits into HLA-DRβ1*0401 according to the register reading since no binding studies were performed with this peptide due to limitations regarding reagents. The differences in distances between these peptides showed the relevant role of polarity in the shifting of neighbouring residues, especially those spanning pocket 1–4 (T/V pocket 2, G/S pocket 3 and T/V pocket +2), regarding antibody induction and protection. This shorter distance could have led to a change in the conformation and orientation of the lateral chains pointing towards the TCR or MHC II molecules making this complex unstable for an appropriate immunological stimulation. Figure 3b shows that the lateral chains of residues fitting into pocket 2 and 7 (T7 and A12 respectively) became upwardly orientated in peptide **23426**, possibly providing better orientation for interacting with the TCR molecule in relation to modified HABP **22892** in which pocket 4, 6 and 8 fitting residue side chains were upwardly orientated toward the TCR. This was interesting, as D9 and T11 should have been downwardly orientated in **22892** to fit into MHCII molecules pockets 4 and 6, respectively; these residues' anomalous orientation could partially explain the reduced number of H-bonds (six in total established between this modified peptide **22892** and the HLA-DRβ1*0403 molecule) and the absence of immunogenicity and protective efficacy. This contrasted with **23426**, as the side chains in pockets 2 and 7 were directed upwards towards the TCR (these are critical TCR-contacting residues for this allele in the canonical system). There was also the appropriate downward orientation of D9 and T11 to fit into pockets 4 and 6 of HLA-DRβ1*0403 to allow the formation of 12 H-bonds with this MHCII molecule, thereby establishing a stable complex which could allow appropriate presentation to the TCR to induce protective immunity.

Another striking observation was that native HABPs 6737 and 6762 (Fig. 1a, red arrows) were located 20 ± 2 residues downstream of the SERA 111 kDa precursor molecule cleavage sites where SERA is processed by the *Pf*SUB1 enzyme to release the aforementioned 56/50 kDa fragment. This suggested that these conserved HABPs could be buried in the precursor molecule to be exposed later on by the *Pf*SUB1 enzyme and be relevant during invasive merozoite development and their release from erythrocytes.

Journal : Large 726 | Dispatch : 17-8-2011 | Pages : 12
Article No. : 1061 | LE | TYPESET
MS Code : AMAC-D-11-00212 | CP | DISK

On the other hand, it has been suggested for a long time that short peptides are unable to mimic native protein 3D structure, thereby casting some doubts on the minimal subunit-based, synthetic vaccine concept (Schueler-Furman et al. 2001). The 3D structures of our native conserved HABPs obtained by ^{1}H-NMR have been compared with their corresponding segments to prove whether conserved HABPs display the same structural conformation shown in the original recombinant protein sequence from which their amino acid sequences have been derived. Only a few malarial recombinant proteins have been analysed to date by X-ray crystallography (due to production and crystallisation problems); the 3D structure of a 284 amino acid-long recombinant fragment (residues V544–N828), included in the SERA-5 protein catalytic 50-kDa cleavage product, has been published very recently (Hodder et al. 2009). Our previously described HABP 6746 (Alba et al. 2003), which was located in this fragment, has displayed the same α-helical structure as its corresponding segment in the recombinant fragment; when superimposed onto residues M589–I608 it displayed a 0.95 rmsd (Fig. 3c in dark blue and fuchsia, respectively). This suggested a complete identity, despite the two different methodologies used for their 3D structure determination (i.e. X-ray crystallography for the recombinant molecule and ^{1}H-NMR for our 6746 HABP). Furthermore, HABP 6754 (residues K749–G768, included in this manuscript) has displayed a completely random structure in the recombinant protein, totally agreeing with the structure described by our CD and ^{1}H-NMR studies for this HABP (Fig. 3c in orange).

The SERA-5 recombinant fragment 3D structure has shown that our conserved HABP 6746 (residues M589–I608) established H-bonds between fundamental binding residue S596 and conserved HABP 6754 fundamental binding residues A763 and H762 (Fig. 3c, boxed), the latter being one of the close binding residues modified to render this conserved HABP highly immunogenic and protection inducing. Along with residue N787 (Hodder et al. 2009), the above have formed this molecule's non-canonical serine active catalytic triad which is deeply involved in the processing of merozoite proteins during parasite egress and invasion. Native peptide 6746 residue S596 was one of the fundamental binding residues which was modified to produce highly immunogenic and protection-inducing modified HABPs **24216**, **23230** and **24214** (Alba et al. 2003). This further confirmed our findings that residues establishing H-bonds amongst conserved HABPs in an invasion-relevant molecule are the fundamental residues which must be changed to induce a highly immunogenic and protective immune response against the *P. falciparum* parasite (Patarroyo et al. 2010b).

The pattern of these conformations has implied functionally relevant discontinuous structures bound by H-bonds (6746 and 6754 HABPs); thus, given that these HABPs mediate vital functions for parasite survival, their activities can be blocked by inducing an appropriate immune response against any one of these HABPs, thereby strongly supporting this strategy for a logical and rational approach to vaccine development.

Acknowledgments We would like to thank Jason Garry for helping in the translation of the manuscript, Sylvain Meguellatni for helping with technical support regarding Bruker equipment and Martha Forero and Yolanda Silva for their continued help with the immunochemical assays.

Conflict of interest The authors declare that they have no conflict of interest.

References

Alba MP, Salazar LM, Puentes A, Pinto M, Torres E, Patarroyo ME (2003) 6746 SERA peptide analogues immunogenicity and protective efficacy against malaria is associated with short alpha helix formation: malaria protection associated with peptides alpha helix shortening. Peptides 24:999–1006

Alba MP, Salazar LM, Purmova J, Vanegas M, Rodriguez R, Patarroyo ME (2004) Induction and displacement of an helix in the 6725 SERA peptide analogue confers protection against *P. falciparum* malaria. Vaccine 22:1281–1289

Bax A, Davis DG (1985) MLEV-17-based two-dimensional homonuclear magnetization transfer spectroscopy. J Magn Resonance 65:355–360

Bermudez A, Reyes C, Guzman F, Vanegas M, Rosas J, Amador R, Rodriguez R, Patarroyo MA, Patarroyo ME (2007) Synthetic vaccine update: applying lessons learned from recent SPf66 malarial vaccine physicochemical, structural and immunological characterization. Vaccine 25:4487–4501

Blake MS, Johnston KH, Russell-Jones GJ, Gotschlich EC (1984) A rapid, sensitive method for detection of alkaline phosphatase-conjugated anti-antibody on Western blots. Anal Biochem 136:175–179

Cifuentes G, Bermúdez A, Rodriguez R, Patarroyo MA, Patarroyo ME (2008) Shifting the polarity of some critical residues in malarial peptides' binding to host cells is a key factor in breaking conserved antigens' code of silence. Med Chem 4:278–292

Cubillos M, Alba MP, Bermudez A, Trujillo M, Patarroyo ME (2003) Plasmodium falciparum SERA protein peptide analogues having short helical regions induce protection against malaria. Biochimie 85:651–657

Dessen A, Lawrence CM, Cupo S, Zaller DM, Wiley DC (1997) X-ray crystal structure of HLA-DR4 (DRA*0101, DRB1*0401) complexed with a peptide from human collagen II. Immunity 7:473–481

Greenfield NJ (1996) Methods to estimate the conformation of proteins and polypeptides from circular dichroism data. Anal Biochem 235:1–10

Hodder AN, Malby RL, Clarke OB, Fairlie WD, Colman PM, Crabb BS, Smith BJ (2009) Structural insights into the protease-like antigen *Plasmodium falciparum* SERA5 and its noncanonical active-site serine. J Mol Biol 392:154–165

Jeener J, Meier B, Backman P, Ernst R (1979) Investigation of enhance processes by two dimensional NMR spectroscopy. J Chem Phys 71:4546

Journal : Large 726 | Dispatch : 17-8-2011 | Pages : 12
Article No. : 1061 | LE | TYPESET
MS Code : AMAC-D-11-00212 | CP | DISK

Merrifield RB (1963) Automated synthesis of peptides. Solid-phase peptide synthesis, a simple and rapid synthetic method, has now been automated. J am soc 85:2149

Patarroyo ME, Patarroyo MA (2008) Emerging rules for subunit-based, multiantigenic, multistage chemically synthesized vaccines. Acc Chem Res 41(3):377–386

Patarroyo ME, Alba MP, Vargas LE, Silva Y, Rosas J, Rodriguez R (2005) Peptides inducing short-lived antibody responses against *Plasmodium falciparum* malaria have shorter structures and are read in a different MHC II functional register. Biochemistry 44:6745–6754

Patarroyo ME, Bermudez A, Salazar LM, Espejo F (2006) High non-protective, long-lasting antibody levels in malaria are associated with haplotype shifting in MHC-peptide-TCR complex formation: a new mechanism for immune evasion. Biochimie 88(7): 775–784

Patarroyo MA, Bermudez A, Lopez C, Yepes G, Patarroyo ME (2010a) 3D analysis of the TCR/pMHCII complex formation in monkeys vaccinated with the first peptide inducing sterilizing immunity against human malaria. PLoS One 5:e9771

Patarroyo ME, Cifuentes G, Piraján C, Moreno-Vranich A, Vanegas M (2010b) Atomic evidence that modification of H-bonds established with amino acids critical for host-cell binding induces sterile immunity against malaria. Biochem Biophys Res Commun 394:529–535

Patarroyo ME, Bermudez A, Patarroyo MA (2011) Structural and immunological principles leading to chemically synthesized, multiantigenic, multistage, minimal subunit-based vaccine development. Chem Rev 111:3459–3507

Puentes A, Garcia J, Vera R, Lopez QR, Urquiza M, Vanegas M, Salazar LM, Patarroyo ME (2000) Serine repeat antigen peptides which bind specifically to red blood cells. Parasitol Int 49: 105–117

Rammensee HG, Friede T, Stevanoviic S (1995) MHC ligands and peptide motifs: first listing. Immunogenetics 41:178–228

Rance M, Sorensen OW, Bodenhausen G, Wagner G, Ernst RR, Wuthrich K (1983) Improved spectral resolution in cosy 1H NMR spectra of proteins via double quantum filtering. Biochem Biophys Res Commun 117:479–485

Rodriguez R, Moreno A, Guzman F, Calvo M, Patarroyo ME (1990) Studies in owl monkeys leading to the development of a synthetic vaccine against the asexual blood stages of *Plasmodium falciparum*. Am J Trop Med Hyg 43:339–354

Salazar LM, Bermudez A, Patarroyo ME (2008) HLA-DR allele reading register shifting is associated with immunity induced by SERA peptide analogues. Biochem Biophys Res Commun 372:114–120

Sato D, Li J, Mitamura T, Horii T (2005) *Plasmodium falciparum* serine-repeat antigen (SERA) forms a homodimer through disulfide bond. Parasitol Int 54:261–265

Schueler-Furman O, Altuvia Y, Margalit H (2001) Examination of possible structural constraints of MHC-binding peptides by assessment of their native structure within their source proteins. Proteins 45:47–54

Sinigaglia F, Romagnoli P, Guttinger M, Takacs B, Pink JR (1991) Selection of T cell epitopes and vaccine engineering. Methods Enzymol 203:370–386

Suarez CF, Patarroyo ME, Trujillo E, Estupinan M, Baquero JE, Parra C, Rodriguez R (2006) Owl monkey MHC-DRB exon 2 reveals high similarity with several HLA-DRB lineages. Immunogenetics 58:542–558

Vargas LE, Parra CA, Salazar LM, Guzman F, Pinto M, Patarroyo ME (2003) MHC allele-specific binding of a malaria peptide makes it become promiscuous on fitting a glycine residue into pocket 6. Biochem Biophys Res Commun 307:148–156

Journal : Large 726 | Dispatch : 17-8-2011 | Pages : 12
Article No. : 1061 | ☐ LE | ☐ TYPESET
MS Code : AMAC-D-11-00212 | ☑ CP | ☑ DISK

9. CAPÍTULO 5

Gauche+ side-chain orientation as a key factor in the search for an immunogenic peptide mixture leading to a complete fully protective vaccine.

En la búsqueda de nuevas herramientas para entender la respuesta inmune en malaria de acuerdo a estudios previos y conociendo que un solo epitope de una sola proteína probablemente no puede inducir una respuesta inmune completa, se realizaron mezclas de péptidos provenientes de proteínas del esporozoíto y del merozoíto. Estas mezclas fueron derivadas de péptidos relevantes individualmente en la respuesta inmune e incluyeron un péptido de la proteína STARP y un péptido de la proteína SERA 5. La respuesta inmune inducida por las mezclas de péptidos generó dos tipos de respuesta, algunas mezclas indujeron respuestas inmunes importantes, manteniendo sus propiedades inmunológicas individuales y en algunos casos incrementándolas, mientras que las características inmunogénicas individuales en otras mezclas fueron abolidas, posiblemente debido a actividades de competición o bloqueo de la respuesta inmune. En un análisis de los ángulos diedros ψ y φ de los péptidos involucrados en dichas mezclas existe la tendencia a la conformación $PPII_L$ y mediante un estudio comparativo del ángulo $\chi 1$ de las cadenas laterales de los aminoácidos en la posición 3 y 7 de los péptidos que individualmente han dado una respuesta inmune apreciable con péptidos generalmente antigénicos evaluados en moléculas MHC-II se destacan las propiedades estereoquímicas como la tendencia a las orientaciones $g+$ que probablemente garantizan una respuesta inmune apropiada.

Vaccine xxx (2014) xxx–xxx

Contents lists available at ScienceDirect

Vaccine

journal homepage: www.elsevier.com/locate/vaccine

Gauche$^+$ side-chain orientation as a key factor in the search for an immunogenic peptide mixture leading to a complete fully protective vaccine

Adriana Bermúdez[a,c], Dayana Calderon[a], Armando Moreno-Vranich[a], Hannia Almonacid[a], Manuel A. Patarroyo[a,c], Andrés Poloche[a], Manuel E. Patarroyo[a,b,*]

[a] *Fundación Instituto de Inmunología de Colombia (FIDIC), Carrera 50, # 26-20, Bogotá, Colombia*
[b] *Universidad Nacional de Colombia, Carrera 45, # 26-85, Bogotá, Colombia*
[c] *Universidad del Rosario, Calle 14, # 6-25, Bogotá, Colombia*

ARTICLE INFO

Article history:
Received 21 September 2013
Received in revised form 27 January 2014
Accepted 4 February 2014
Available online xxx

Keywords:
Gauche$^+$
χ^1 angle
Protective immunity
Peptide mixtures
Antimalarial vaccine

ABSTRACT

Topological and stereo-electron characteristics are essential in major histocompability class II–peptide–T–cell receptor (MHC–p–TCR) complex formation for inducing an appropriate immune response. Modified high activity binding peptides (mHABPs) were synthesised for complete full protection antimalarial vaccine development producing a large panel of individually fully protection-inducing protein structures (FPIPS) and very high long-lasting antibody-inducing (VHLLAI) mHABPs. Most of those which did not interfere, compete, inhibit or suppress their individual VHLLAI or FPIPS activity contained or displayed a polyproline II-like ($PPII_L$) structure when mixed. Here we show that amino acid side-chains located in peptide binding region (PBR) positions p3 and p7 displayed specific electron charges and side-chain *gauche*$^+$ orientation for interacting with the TCR. Based on the above, and previously described physicochemical principles, non-interfering, long-lasting, full protection-inducing, multi-epitope, multistage, minimal subunit-based chemically synthesised mHABP mixtures can be designed for developing vaccines against diseases scourging humankind, malaria being one of them.

1. Introduction

Many vaccine development strategies aimed at transmittable disease control (most of them biologically derived) have been followed for many decades now, but have had limited impact and disappointing results. Our institute has followed a chemical approach for achieving this purpose, selecting malaria as the prototype disease. A series of recently summarised physicochemical principles and rules have been described [1–3], but some still have to be defined to ensure a complete, fully protective, definitive, vaccine development methodology against diseases scouring humankind (i.e. malaria).

New physical-chemical principles for obtaining multiple chemically synthesised peptide mixtures for developing a complete, fully protective vaccine form this manuscript's *raizon d'être*; they have arisen from identifying *gauche*$^+$ side-chain orientation in mHABP regions binding to the MHC II PBR in positions 3 (p3) and 7 (p7) as a key factor in inducing fully protective immunity, very high long-lasting antibody titres and also differentiating only immunogenic from immunogenic and protection-inducing peptides.

It has now been generally accepted that a fully protective antimalarial vaccine must contain multiple, chemically synthesised minimal subunit-based peptides (multi-epitope) [1–3], derived from the parasite's different invasion stages (multi-stage) which are the potential lines of defence [2,3], as multiple proteins are involved in the tremendous complexity of the *Plasmodium falciparum* malaria parasite lifecycle and invasion stages. This parasite infects ~200 million people annually, leading directly to ~1.5 million deaths, mainly in children below 5 years of age and thus

Abbreviations: pMHC, peptide–major histocompability class; TCR, T-cell receptor; cHABP, conserved high activity binding peptide; mHABP, modified high activity binding peptide; FPIPS, full protection-inducing protein structure; VHLLAI, very high long-lasting antibody-inducing; HIPI, highly immunogenic protection-inducing.

* Corresponding author at: Fundación Instituto de Inmunología de Colombia (FIDIC), Bogotá, Colombia. Tel.: +57 1 4 81 52 19; fax: +57 1 4 81 52 69.
E-mail address: mepatarr@gmail.com (M.E. Patarroyo).

http://dx.doi.org/10.1016/j.vaccine.2014.02.003
0264-410X/

representing one of the main public health problems around the world [4].

It has been thoroughly demonstrated that peptides derived from conserved high activity binding peptides (cHABPs), present in the most relevant proteins involved in the invasion of host cells, become fully protection-inducing peptide structures (FPIPS) when their critical binding residues have been properly modified (mHABPs) or very high long-lasting antibody-inducing (VHLLAI) peptides, according to previously described steric-electron principles [2,3,5–8].

We have very recently shown that most FPIPS and VHLLAI mHABPs have predominantly $PPII_L$ structures [5,6]. Molecular modelling involving superimposing mHABP 3D structure onto the corresponding major histocompability complex class II (MHCII) (HLA-DRβ1* in humans) 3D structures to which they experimentally bind has shown that H-bonds or van der Waals interactions are established between their peptide bond N and O atoms and specific side-chain atoms of certain residues in the peptide binding region (PBR) of these MHCII molecules [5–8]. These bonds stabilise MHCII–peptide formation, confirming the elegantly shown results by other authors regarding crystallised antigenic p–MHCII complexes [9].

Although principles for antigenic MHC–p–TCR complex formation have been identified, principles for FPIPS and VHLLAI pMHCII interactions with the TCR still had to be defined.cHABPs and their corresponding mHABPs derived from *P. falciparum* circumsporozoite protein (CSP) [10,11], thrombospondin-related protein (TRAP) [12] and serine threonine asparagine-rich protein (STARP) [13] were thus chosen as the first line of defence [3] from amongst ~20 sporozoite (Spz)-derived molecules suggested as being directly involved in hepatocyte invasion (i.e. the sporozoite being the first stage of human infection by the malaria parasite). Merozoite surface proteins 1 and 2 (MSP-1 and MSP-2) [14–16], apical merozoite antigen 1 (AMA-1) [17], erythrocyte binding antigen 175 (EBA-175) [18–20], serine repeat antigen 5 (SERA-5) [21], ring-infected erythrocyte surface antigen (RESA-155) [22] and histidine-rich protein (HRP-II) [23] cHABPs were selected as components of the second line of defence from among the ~50 merozoite (Mrz) proteins suggested as being involved in RBC invasion [2]. Their cHABPs, their derived mHABPs and HLA-DRβ1* binding capacity, as well as their individual immunogenicity and protection-inducing ability, have been thoroughly demonstrated in many recently reviewed monkey trials [1–3,10–23].

Mrz-derived FPIPS or Spz-derived VHLAI mHABPs were mixed in more than 85 monkey trials when searching for the aforementioned fully protection-inducing vaccine to cover most MHCII genetic variants; such mixtures competed with [24], interfered with [25], inhibited or suppressed [26] their individual antibody-inducing ability and their protection-inducing capacity, a thoroughly described phenomenon in vaccine development. However, some specific mHABP mixtures did not (suggesting that complete protection might be induced).

In-depth stereo-electron analysis of these mHABP VHLLAI and FPIPS mixtures has led to reporting here, for the first time, that the residue located in position 3 (p3) of the PBR binding sequence in mHABP 3D structures (previously determined by ^{1}H NMR [2,3,5,6]) had side-chain *gauche*$^+$ orientation. Such orientation in FPIPS or VHLLAI mHABP mixtures was thus a key stereo-chemical factor in VHLLAI and FPIPS appropriate mHABP mixture formulation in a tailor-made anti-malarial vaccine, as opposed to mixtures involving mHABPs or other peptides inducing only very high antibody titres but no protection against experimental challenge displaying *gauche*$^-$ orientation in the same position. The latter conformation induced interference, suppression or inhibition when mixed.

2. Materials and methods

2.1. Synthetic peptide production and use

The procedure for producing and using synthetic peptides to date has been thoroughly described [12]. mHABPs are shown in bold from hereon and numbered according to our institutes' serial number (native cHABPs are not in bold and are not shown in parenthesis).

2.2. Monkeys and immunisation with individual or mHABP mixtures

Amazonian *Aotus* monkeys have been kept at our primate station in Leticia (Colombia), being maintained according to Colombian NIH guidelines and supervised by an expert veterinarian primatologist, all pertinent legal permits having been issued by the Colombian Ministry of the Environment (CORPOAMAZONIA) for more than 30 years. The relevant documentation is available on request (CORPOAMAZONIA, resolution 0042 (Jan/2011) being the most recent authorisation). The study was supervised weekly by CORPOAMAZONIA's veterinarians or biologists and all procedures were approved by an inter-institutional ethics committee.

6–10 randomly assigned *Aotus* monkeys per group were subcutaneously inoculated on day 0 with 125 μg polymerised individual or mixed mHABPs homogenised with Freund's Complete Adjuvant for the first dose and Freund's Incomplete Adjuvant for the second (day 20) and third (day 40) doses. Spz-derived humoral immune response determination involved blood samples (2 ml) being drawn for immunological studies on day 1 (P0) before the first immunisation and 20, 40, 60, 240, 320, 540 and 900 days thereafter in the first trial 1 (Fig. 1a), or also on day 365 and 600 in the second trial, on day 600 in the third one and day 540 in the fourth trial.

2.3. Challenge and parasitaemia assessment

Immunised and control *A. nancymae* monkeys were immunised on days 1, 20 and 40 for Mrz-derived mHABP protection-inducing immunity assessment and challenged by intravenous inoculation of 100,000 freshly obtained (from another infected *Aotus* monkey) *P. falciparum Aotus* adapted FVO-strain infected erythrocytes (Ei) 20 days after the second or third immunisation [27]. Blood was drawn on days 0 and 15 days after the 2nd (II_{15}) and 3rd (III_{15}) immunisation.

Full protection was defined as being the TOTAL absence of parasites in blood during the 15 days the experiments lasted and complete protection was taken as meaning protecting all monkeys, covering all MHCII genetic variants. Non-protected and control monkeys (immunised with just saline solution in Freund's adjuvant using the same regime) developed patent parasitaemia by day 5 or 6, >5% parasitaemia levels being reached between days 8 and 10.

Each monkey's parasitaemia was measured daily, starting on day 5 after challenge; immunofluorescence was used for reading parasites in terms of percentage parasitised RBC on a slide following Acridine Orange staining.

The monkeys were treated with paediatric doses of quinine after challenge, kept in quarantine for 40 more days and released back into the jungle close to their place of capture (>95% of the *Aotus* being returned in excellent conditions). CORPOAMAZONIA officials evaluated the monkeys' conditions every week and our Institute's ethical committee approved the overall process.

Please cite this article in press as: Bermúdez A, et al. *Gauche*$^+$ side-chain orientation as a key factor in the search for an immunogenic peptide mixture leading to a complete fully protective vaccine. Vaccine (2014), http://dx.doi.org/10.1016/j.vaccine.2014.02.003

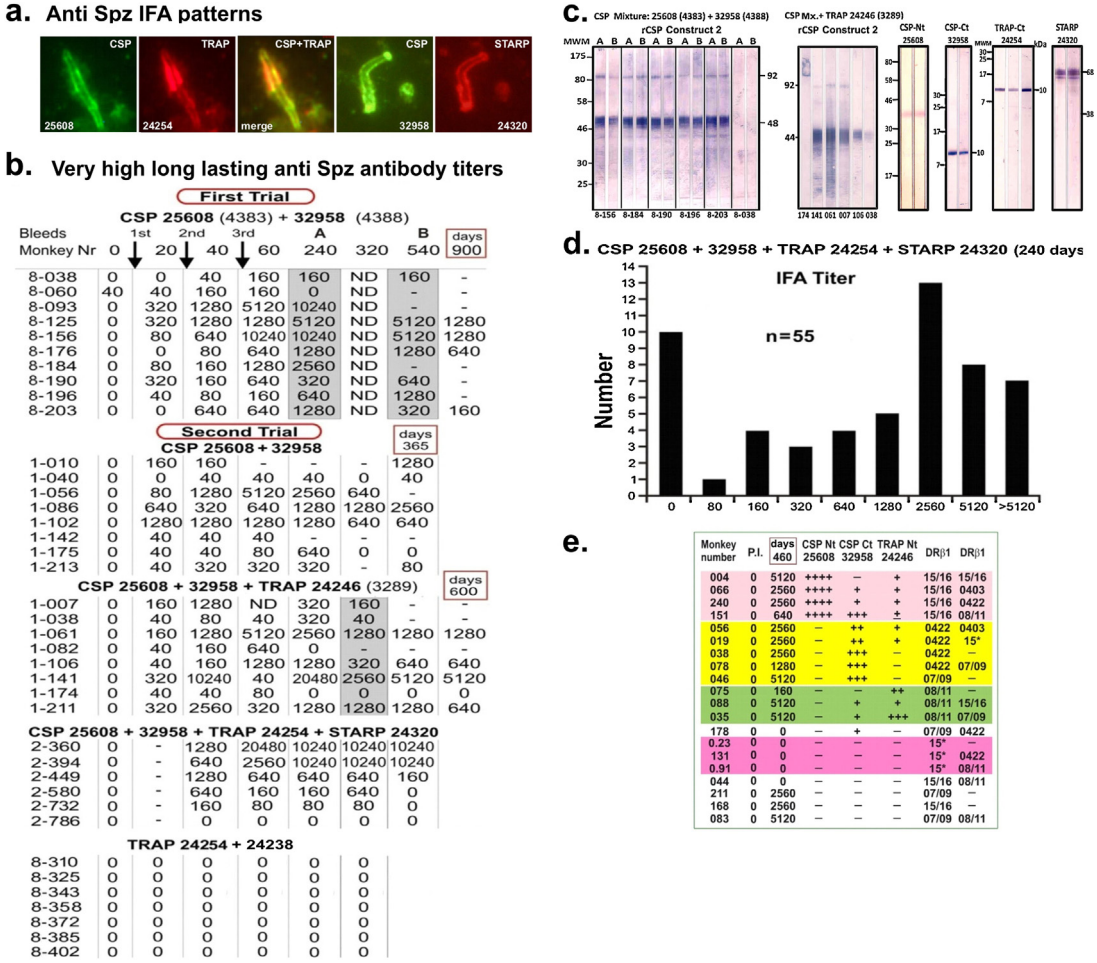

Fig. 1. Immunological studies with CSP, TRAP and STARP mHABP mixtures. (a) Anti-CSP **25608** and **32958** and anti-TRAP **24254** immunofluorescence patterns. (b) Anti-Spz antibody titres (IFA), induced by CSP **24258** + **32958** mixture in a first trial and repeated in a second trial and the days when these antibodies were determined after 1 st immunisation (up to 900 days); a third trial involved the CSP and TRAP mixture on day 365 (dashed on day 320). Arrows indicate immunisation day; shadowed lanes A or B are days when monkey sera was used for WB analysis. Mixture-induced (CSP **25608** + **32958** + TRAP **24246**) and (**25608** + **32958** + TRAP **24254** + STARP **24320**) anti-Spz antibody titres in further trials. The lower part of the figure shows a mixture of TRAP **24254** and **24238**, highlighting the complete suppression of their individual VHLLAI capacity when **24238** having *gauche*$^-$ orientation was added. (c) WB analysis showing the reactivity of *Aotus* sera (diluted 1:100) immunised with CSP-derived **25608**, **32958** and TRAP **24246** modified peptide mixture, analysed with rCSP construct 2, and WB analysis with rCSP-Nt, TRAP-Ct and rSTARP individual fragments and complete rSTARP, with their corresponding MWM. (d) IFA titre binomial distribution in 55 *Aotus* immunised with CSP **25608** and **32958** and TRAP **24246** mixtures. (e) Anti-Spz antibody titres induced by 25608, 32958 and 24246 associated with their HLA-DRβ1* and strength of reactivity ranked from 0 to ++++, HLA-DRβ1*15/16 (pale rose), HLA-DRβ1*0422 (yellow), HLA-DRβ1*08/11 (green), HLA-DRβ1*15* (fuchsia).

2.4. Immunological assays

Late-stage schizonts from a continuous *P. falciparum* culture (FCB-2 strain) were synchronised, washed and treated as described earlier [27]. Slides containing dry parasites were blocked for 10 min with 1% non-fat milk and incubated for 30 min with appropriate dilutions of monkey sera (starting at 1:40 dilution) for antibody analysis. Reactivity was observed by immunofluorescence microscopy [14–23].

The procedures for obtaining sporozoite IFA titres, subcellular location patterns and WB analysis have been described previously [3,11–13].

2.5. Aotus HLA-DRβ1*-like genotyping

The cDNA of each animal was synthesised from total RNA extracted from isolated peripheral blood mononuclear cells. Specific primers were used for amplifying MHC-DRB gene exon 2; the purified products were cloned into *Escherichia coli*. On average, 12 recombinant colonies per monkey were randomly selected and further sequenced bi-directionally by Sanger's method. The reported alleles had at least 2 identical clones [28].

2.6. Cloning, sequencing, expression and purification of CSP, TRAP and STARP recombinant forms

P. falciparum 3D7 strain TRAP- and CSP-encoding sequences (plasmoDB accession: PF13_0201 and PFC0210c, respectively) were selected for primer design. The TRAP-Nt amplified region (forward primer 5′-ATGGCTGATTCTGCATGGGA-3′ and reverse 5′-TATATTTTCGTTTGGTTTTT-3′) encoded aa 216–320 and TRAP-Ct amplified region (forward primer: 5′-ATGGCAGGATCAGATAATAAATA-3′ and reverse 5′-ATTCCACTCGTTTTCTTCAG-3′) encoded aa 504 to 574, including TRAP 3289 and cHABP 3347, parents of mHABPs **24246** and **24254**, respectively. The CSP-Nt amplified region (forward: 5′-ATGCAGGAATACCAGTGCTA-3′ and reverse 5′-ATCAGGATTACCATCCG-3′) encoded aa 21–103, including CSP

cHABP 4383 precursor of mHABP **25608** and the CSP-Ct amplified region (forward: 5′-ATGCACAATATGCCAAATGAC-3′ and reverse: 5′-ATTAAACACACTGGAACATT-3′) encoded aa 283–379, including CSP cHABP 4388, the mHABP **32958** parent. Products were cloned in pEXP-5-CT/TOPO vector (Invitrogen).

All recombinant proteins were expressed in *E. coli* BL21-Al (Invitrogen), following manufacturer's recommendations, purified by affinity chromatography and fractions were pooled and quantified using a Micro BCA protein assay kit (Thermo Scientific, Meridian, USA). The expected protein molecular weight bands were observed in Coomassie blue staining and Western blot (13 kDa rTRAP-Nt, not shown here, 10 kDa rCSP-Nt, and 10 kDa rCSPCt). The 46 and 92 kDa MW rCSP construct 2 (residues 6–408) was kindly provided by Dr. Mauricio Calvo-Calle (NYU); *P. falciparum* recombinant STARP was kindly provided by Professor Pierre Druilhe from the Pasteur Institute in Paris.

2.7. Structural analysis

VHLLAI and FPIPS mHABP 3D structures (obtained by ^{1}H NMR in solution) have been thoroughly described [2,3,10–23]. The lowest energy conformer was chosen from each family of conformers (corresponding number followed by dot), obtained according to mHABP connectivity (determined by ^{1}H NMR) and representing conformer family secondary structure, considering that the lowest energy conformers had the most stable conformation in solution. Such data was used for a comparative study of Φ, Ψ and χ^{1} angles using the Residue-Dihedral tool from Insight II software (ACCELRysInc, USA). An additional set of antigenic or experimentally used peptides eliciting different immune responses (their 3D structures having previously been determined by X-ray crystallography) were also analysed using the same methodology. X-ray crystallography coordinates for the 3D structure of peptides which were just antigenic were extracted from the following PDB codes: 1DLH [29], 1FYT [30], 1J8H [31], 1BX2 [32], 1ZGL [33], 2IAM [34], 3PDO [35], 1A6A [36], 1AQD [37], 1IEB [38] and 1KT2 [39]. Insight II software was also used for superimposing the structures, exported in .ps format for 3D representation in CorelDRAW Graphics Suite X5 software.

3. Results and discussion

3.1. VHLLAI anti-Spz mHABP mixtures for effective antimalarial vaccine development

The search for an appropriate anti-Spz and anti-Mrz mHABP mixture (including the most relevant malarial parasite developmental stages in humans) covering most human (or *Aotus*) immunogenetic variants has resulted from the tremendous complexity of the *P. falciparum* parasite life-cycle, the genetic constraints imposed by the immune system and the need to halt the parasite, at least at these two critical lines of defence. This endeavour led to more than 25 monkey trials, involving previously identified, individually highly immunogenic Spz-derived CSP [3,10,11], TRAP [12] and 60 Mrz-derived MSP-1 [14,15], MSP-2 [16], AMA-1 [17], EBA-175 [18–20], SERA [21], RESA [22], HRPPII [23] and some other mHABP mixtures, being performed to immunise 6 to 10 wild caught *Aotus* monkeys per trial (depending on their availability). Their individual highly specific antibody reactivity (determined by ELISA, IFA and WB) as well as their individual protective efficacy became completely abolished when mixed (lower part of Fig. 1b, Spz-derived mHABP mixture), suggesting competition [24], interference [25], blocking or suppression [26] activities, very common and well-known phenomena in vaccine development. However, some specific mHABP mixtures did not follow this pattern.

Remarkably, this endeavour revealed that an Spz-derived CSP mHABP **25608** (4383) and **32958** (4388) mixture induced very high, specific IFA antibody (VHLLAI) titres against Spz membrane when mixed (Fig. 1a), determined 240, 540 and 900 days (2½ years) after the 1st dose (shadowed A and B lanes, Fig. 1b). Such VHLLAI response was an outstanding result leading to a repetition with a new group of 8 *Aotus* (second trial, Fig. 1b); these results' complete reproducibility was shown up to 365 days after the first dose, when monkeys were released at CORPOAMAZONIA's request.

Western blot analysis of the first trial's *Aotus* sera, obtained 240 and 540 days (Fig. 1b shadowed) after the first dose, revealed reactivity against recombinant CSP construct 2 (including cHABP 4383 and 4388, parents of mHABPs **25608** and **32958**, respectively), confirming IFA data and supporting the results' specificity, having diffuse ~46 kDa and ~92 kDa bands, corresponding to CSP monomers and dimers, respectively (Fig. 1c).

Adding individually highly immunogenic liver stage antigen 1 or 3 (LSA 1, 3) sporozoite and liver stage antigen (SALSA) [40] or some TRAP mHABPs to this mixture completely abolished CSP **25608**- plus **32958**-induced antibody production [data not shown]. However, when TRAP mHABP **24246** (3289) [12] was added to this mixture, very high IFA-titres were maintained in another trial involving 8 monkeys (Fig. 1b) lasting >600 days, suggesting that **24246** did not interfere with, block, compete with or suppress this anti-Spz immune response in this mHABP mixture whilst this period of time elapsed.

Pooled data from a further trial repeated with 48 new *Aotus* monkeys immunised with a CSP **25608**, **32958** and TRAP **24246** mixture, including the 7 monkeys remaining in the previous one (totalling 55 *Aotus*), showed that ~73% of the sera displayed very high anti-Spz IFA titres 180 days after the first dose (≥1:320) in a binomial-like (Hardy–Weinberg-like) distribution pattern (Fig. 1d), lasting 600 days (>1½ years), suggesting this mixture's VHLLAI-inducing capacity and immune-dominant nature.

Another trial involving 20 DNA genotyped (Fig. 1e) *Aotus* monkeys immunised with the **25608** + **32958** + **24246** mixture behaved in the same way, showing very high antibody titres for at least 460 days after the first immunisation in ~75% of them.mHABP **24246** was not included in another trial involving 6 monkeys (Fig. 1b) due to low antibody reactivity (≤1:10) against recombinant TRAP-Nt as determined by WB (data not shown), contrasting with high antibody dilution recognition (>1:50) by WB with corresponding recombinant fragments induced by **25608** and **32958**. Thus **24246** was replaced by STARP mHABP **24320**, showing very high antibody titres for up to 365 days (1 year) specifically and strongly reacting with rCSP-Nt (10 kDa), rCSP-Ct (10 kDa) and rTRAP Nt (10 kDa) and rSTARP (68 kDa) corresponding fragments by WB (Fig. 1c) as well as by immunofluorescence (Fig. 1a).

Lower Fig. 1b gives an example of the most common phenomenon during mHABP mixture: the absolute blocking of **24254** VHLLAI capacity induced by TRAP mHABP **24238** [12].

3.2. Aotus HLA-DRβ1* genotyping

Aotus HLA-DRβ1*-like genotyping, according to Suarez *et al.* [28] (Fig. 1e), performed on 20 *Aotus* monkeys immunised with CSP-Nt **25608**, CSP-Ct **32958** and TRAP **24246** mixture, inducing VHLLAI titres and correlating with IFA titres (reciprocal dilution) and WB reactivity with their recombinant fragments (displayed as strength of reactivity for 0 to ++++), showed that most monkeys strongly reacting with rCSP-Nt were typed as HLA-DRβ1*15/16, most typed HLA-DRβ1*0422 reacted with CSP-Ct, those reacting with rTRAP-Nt were typed as HLA-DRβ1*08 while those not producing Spz IFA titres nor reacting with any recombinant fragment

were typed HLA-DRβ1*15*. A small group of monkeys producing very high IFA titres but not reacting with any one of the recombinant fragments displayed different HLA-DRβ1* genotypes (Fig. 1e), suggesting reactivity against conformational epitopes.

This data clearly showed strong, but not absolute, genetic control of the HLA-DRβ1* region-associated immune response and suggested that more mHABPs must be included to cover all HLA-DRβ1* variants to produce a fully effective anti-Spz malarial vaccine. This conclusion was based on only ~75% (15/20) of the monkeys producing very high antibody titres, 65% (13/20) of them strongly reacting with their corresponding recombinant fragments by WB; the number of HLA-DRβ1* genes identified was limited and few mHABPs were included in this mixture. However, this striking result led to defining principles for recognising VHLLAI and determining mixtures for complete vaccine development, as will be explained at the subatomic level later on.

3.3. Full protection induced by Mrz-derived FPIPS mixtures

Early on in our endeavour groups of two, three and up to 20 Mrz-derived FPIPS mHABPs [2] were mixed to immunise groups of 6–10 *Aotus* monkeys, leading to negative and very disappointing results (data not shown), highlighting a fully protective, complete antimalarial vaccine's complexity. No antibodies were induced and no protection was obtained with most of these mixtures (only two examples are given in Fig. 2b). Contrary to the high antibody titres and protection induced by individual mHABPs, some mixtures induced high (not like individual peptides) antibody titres and full protection in some monkeys (lower Fig. 2b).

The mixture of AMA-1-derived **10022** (4313) [17], binding with high capacity to HLA-DRβ1*0701, and MSP-1-derived **10014** (1585) [14], having high binding capacity to HLA-DRβ1*1101 [2], induced high IFA titres (1:160) 15 days after the second and third dose in 2/6 immunised monkeys. Immunofluorescence revealed that these antibodies reacted with Mrz proteins present on the schizont membrane (MSP-1) and showed small dots inside the schizont (probably AMA-1), as their corresponding individual antisera did too (Fig. 2a). Challenge involving an intravenous inoculation of 100,000 iE 20 days after the third dose with the highly virulent *Aotus* adapted *P. falciparum* FVO strain revealed full protection since both monkeys had no parasites in their blood during the 15 days the experiment lasted. The other 4 immunised monkeys which did not produce antibodies, as well as the 5 controls, were not protected (Fig. 2b, mixture C).

3.4. mHABP backbone Φ and Ψ angles leading to $PPII_L$ formation facilitated fitting into HLA-DRβ1* PBRs

Fig. 3a and b shows a frontal view of the previously described ^{1}H NMR-determined 3D structure of Spz CSP-derived **25608.37** and **32958.2**, TRAP-derived **24254.31** and STARP-derived **24320.18** as well as Mrz AMA-1 **10022.43**, MSP-2-derived **24112.39**, MSP-2-derived **10008.23**, MSP-1-derived **10014.35**, SERA-derived **23426.35**, EBA-175-derived **13790.46**, **24292.12** and **24166.48**, RESA-derived **13492.44** best fit conformers (number after dot). Table 1 displays their Φ and Ψ angles, as well as previously determined ^{1}H NMR TRAP-derived **24238.44** [12], HRPII-derived **24230.13** [23] and MSP1-derived **24148.7** [15] 3D structures in the region fitting into their corresponding experimentally determined HLA-DRβ1* PBRs [2,3].

Almost all VHLLAI and FPIPS mHABPs contained one or two polyproline II left-handed ($PPII_L$) regions (grey in Table 1), sometimes spaced by Gly to properly fit into their corresponding HLA-DRβ1* PBR, as previously described by molecular modelling [5,6]. However, a tantalising problem for us was that some VHLLAI and FPIPS mHABPs also displayed and/or contained short (3–5 mer long) α_R, α_L or β-turn regions (orange, lilac and light blue, respectively, Table 1). Porter and Rose's recently published elegant work [41] resolved this problem, based on deep subatomic analysis; they proposed a low-energy pathway converting $PPII_L$ into α-helices via γ-turn formation, without breaking H-bonds, which could occur via hyper-conjugation [42], thereby avoiding steric clashes (Lennard–Jones potential). This situation could have happened in **24254.31** containing a type III β-turn (light blue) region and **10008.23**, **24166.48**, **24230.13** and **24148.7** containing short α_R (orange) or **10014.35** containing short α_L (lilac) regions (Table 1).

a. Anti-Mrz IFA patterns

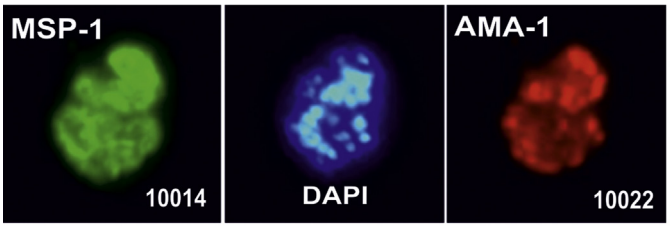

b. Invidual Mrz derived FPIPS mHABPs

Peptide	Sequence Merozoite	% Binding to HLA-DRβ1*	Ab Titers II15	Ab Titers III15	Prot	Ref
AMA-1 10022	DAEVAGTQYFHPSGKSPVFG	3	0	1(5120)	1/5	[17]
MSP-2 24112	SKYSNTFNINAYNMVIRRSM	4	2(5120)	ND	2/15	[48]
10008	KNESKYSNTFEVNAYNMSIR	X	2(5120)	1(5120)	1/3	[16]
MSP-1 10014	EVLYHVPLAGVYRSLKKQLE	1,11	2(640)	1(640)	2/4	[14]
SERA 23426	KKVQNLTGDDTADLATNIVG	4	3(320)	ND	1/9	[21]
EBA-175 13790	MAYGSDDNDDKNKSLDHKHN	4	1(320)	1(320)	2/4	[18]
EBA-175 24292	LTNQNINIDQEFNLMKHGFH	3,14	2(320)	ND	1/8	[19]
EBA-175 24166	FNNIPSRYNLYNLYDKKLDL	15	1(320)	2(640)	2/5	[20]
RESA-155 13492	MTDVIRYRYSNNYEASDHIS	4	2(5120)	0	1/6	[22]
HRPII 24230	SAFDDNLTAANAMGLILNKR	1,7	2(320)	ND	2/8	[23]
MSP-1 24148	MLNISMLQTVMMMTPQK	7	2(2560)	ND	2/8	[15]

Mrz-derived FPIPS mHABPs mixtures

A)	24112 SKYSNTFNINAYNMVIRRSM + 24148 MLNISMLQTVMMMTPQK	4 / 7	0/10	0/10	0/10
B)	24112 SKYSNTFNINAYNMVIRRSM + 24230 SAFDDNLTAANAMGLILNKR + 24148 MLNISMLQTVMMMTPQK	4 / 1 / 7	0/10	0/10	0/9
C)	10022 DAEVAGTQYFHPSGKSPVFG + 10014 EVLYHVPLAGVYRSLKKQLE	3 / 1,11	2(160)	2(160)	2/6

Fig. 2. (a) Immunofluorescence patterns. Anti-MSP-1 **10014** (green fluorescence, showing this protein's typical membranous pattern) and anti-AMA-1 **10022** (red dot immunofluorescence, suggestive of this protein's microneme location). DAPI blue immunofluorescence shows nuclei location. (b) Individual FPIPS mHABP amino-acid sequences used for *Aotus* monkey immunisations [14–23,49] and mixtures. These peptides were classified according to their experimentally determined binding capacity to isolated HLA-DRβ1* molecules, their corresponding binding motifs and binding registers, as previously described. Humoral immune response as assessed by IFA titres determined 15 days after the second (II15) and third (III15) immunisations, as well as protective efficacy induced by individual mHABPs and mixtures 20 days after the last immunisation. Prot.: total number of *Aotus* protected against challenge; the same experimental procedure which showed antibody titres. ND: not determined. Ref.: reference number.

Table 1

Φ, Ψ and χ^1 angles in VHLLAI and FPIPS mHABPs (column a) compared to antigenic or only immunogenic peptides right panel (column b). The colours of residues whose position is horizontally displayed on top follow the code in Fig. 3. The colours displayed in the Table correspond to structure regions: (grey: $PPII_L$), (orange: α_R), (lilac: α_L) and (pale blue: β-turn). All VHLLAI and FPIPS in the left column (a) p3 (violet) had χ^1 *gauche*$^+$ orientation (−24.7° to −174°) while red shows that those interfering with or poisoning immune reactivity had a *gauche*$^-$ orientation (+62° to +61.3°) while the right-hand column (b) shows that just antigenic or only immunogenic peptides had χ^1 *gauche*$^-$ orientation (+62° to +171.4°) in p3 (green). By the same token, all PIPS in p7 had *gauche*$^+$ orientation (−7.9° to −179°) while just immunogenic ones had arbitrary *gauche*$^+$, *gauche*$^-$ or trans orientation.

a.

mHABPs with *gauche+* conformation

Protein/ Allele	Pocket	P1	P2	P3	P4	P5	P6	P7	P8	P9
CSP 25608.37 - DRβ1*1501	AA	F	S	L	G	E	N	P	N	A
	ϕ	-77,7	-82,1	-80,6	-91,8	-77,9	-78,4	-46,5	-61,6	61
	ψ	129	114,9	122,5	85,1	125,5	128,1	149,4	119,8	44,9
	χ1	-174,5	-174,7	**-69,9**		-58,4	-174	**-7,4**	80	
CSP 32958.2 - DRβ1*0422	AA	M	N	N	P	P	N	F	N	V
	ϕ	-75,8	-157	-79,4	-56	-55,5	-159	-137,1	-166	-66,3
	ψ	-3	79,1	133	127,9	122,4	79,7	42,1	83,1	-32,1
	χ1	-75,1	-172	**-171,9**	8,9	8,1	-172	**-156,6**	-148	104,1
STARP 24320.18 - DRβ1*0101	AA	Y	Q	A	P	F	L	G	G	G
	ϕ	73,6	-109,8	-77,6	-72,7	-93,4	-87,8	-92,9	-180	-179
	ψ	79,7	34,5	-62,7	-12,1	133,2	103,7	100,4	-97,6	-96,2
	χ1	-166,6	-150,9		19,3	-170	-70,4			
TRAP 24254.31 - DRβ1*0403	AA	Y	S	G	E	P	S	P	F	D
	ϕ	-50	-8,1	-48,1	76,9	-67,6	-102	-51,5	-53,7	-44,9
	ψ	-73,1	87,9	-29	89	-144	93	-57	-28,7	-60,8
	χ1	-99,4	170,7		-36,7	24,1	174,3	**-25,9**	-151	-145
AMA-1 10022.43 - DRβ1*0302	AA	F	H	P	S	G	K	S	P	V
	ϕ	140,2	-129,1	-62,4	-90,8	-179	-83,7	-137,2	-62,7	-92,4
	ψ	131,1	108,3	95,5	115,6	-96,4	118	99	127	84,1
	χ1	-112,2	-170,8	**-24,7**	-173		61,5	**-69,8**	-24,8	-167
MSP-2 24112.39- DRβ1*0403	AA	Y	N	M	V	I	R	R	S	M
	ϕ	-66,2	-59,4	55,7	-93,8	-80,4	-83,5	-74,6	-86,1	-89,5
	ψ	-15	-42,5	166,7	87,5	-35,1	111,8	101,9	125,3	114,1
	χ1	-169,5	-85	**-57,1**	-73,9	61,3	-175	**-179,2**	-176	-173
MSP-2 10008.23 - DRβ1*X	AA	F	E	V	N	A	Y	N	M	S
	ϕ	49,9	-115,9	-95	-125	-146	-53	-67,8	-77,9	-114
	ψ	-67,4	86,9	74	78,8	-62,2	-50,6	-28,3	159,9	-76,5
	χ1	66,2	-175,4	**-169,3**	-172		-169	**-165,9**	-60,2	-63,5
MSP-1 10014.35 - DRβ1*0101	AA	Y	H	V	P	L	A	G	V	Y
	ϕ	-66,3	-149,7	-105,1	-88,7	-109	73,1	50,8	65,1	36,5
	ψ	-30,3	88,6	102,5	89,6	16,8	-0,7	48,6	31,2	34,2
	χ1	63,3	-173,6	**-174,3**	22,7	65,4			89,9	85,6
SERA 23426.35 - DRβ1*0403	AA	L	T	G	D	D	T	A	D	L
	ϕ	-117,7	-96,7	-178,9	62,4	63,2	-149	-163,3	-109	57
	ψ	55,6	28,4	-75	69,6	66,3	69,3	73,8	27	63,1
	χ1	-78,8	-169		-173	-176	-49,6		71,6	-64,4
EBA-175 13790.46 - DRβ1*0401	AA	Y	G	S	D	D	N	D	D	K
	ϕ	-144,8	-69	82,4	-85,5	-84	-101	-101,3	-92,8	-84,4
	ψ	-67,8	-86,9	135,8	64,6	111,6	112,9	97,7	119,2	-10,1
	χ1	28,5		**-43,2**	66	-62,5	-173	**-174,3**	-172	85,2
EBA-175 24292.12- DRβ1*14	AA	F	N	L	M	K	H	G	F	H
	ϕ	-78,1	-76,9	-127	-136	51	-78,2	91,2	-75	-80,8
	ψ	-75,1	127,1	88,4	86,3	97,7	-51	96,2	126,3	115,6
	χ1	-172,4	-171,4	**-162,6**	-69,7	72,1	-71,8		-166	-161
EBA-175 24166.48 - DRβ1*1502	AA	Y	N	L	Y	D	K	M	L	P9
	ϕ	-62,2	-97,4	50,6	-88	-51,9	-69,8	-73,5	68,7	-53,4
	ψ	-41,3	28,5	43,2	-72,6	-39,7	-38	-33	82,7	122,6
	χ1	-79,9	-158,6	**-64,4**	-165	60	-104	**-66,3**	-61,6	6,1
RESA-155 13492.44 - DRβ1*04	AA	Y	S	N	N	Y	E	A	S	D
	ϕ	-136,9	-150,1	76,4	74,8	-80,9	-77,4	-82,6	-81,8	-77,9
	ψ	99,5	117,4	-45,5	75,7	143,2	154,9	-179,5	104,4	-74
	χ1	-163,2	-67,9	**-60,2**	-60,5	-62	-171		-75,4	-67,3
HRPII 24230.13 - DRβ1*07	AA	L	T	A	A	N	A	M	G	L
	ϕ	-60,3	-66,2	-64,4	-61,9	-51,5	-71,2	-49,6	-65,3	-66,9
	ψ	-76,8	65,1	89,5	-8,2	-19,6	-37,6	-73,1	-20,5	-52,2
	χ1	**-70,1**	**18,5**			**108,9**		**-113,0**		**113,3**
mHABPs with *gauche-* conformation										
MSP-1 24148.7 - DRβ1*07 (MZT)	AA	L	N	I	S	M	L	Q	T	V
	ϕ	65,4	-71,9	51,0	-63,4	-83,8	-58,2	-54,4	-47,2	-100,9
	ψ	-48,3	106,3	18,2	-72,9	26,0	-59,4	-32,5	-52,9	175,0
	χ1	-57,1	61,0	**62,9**	63,0	75,8	167,2	**-94,3**	-60,5	68,3
TRAP 24238.44 - DRβ1*07 (SPZ)	AA	F	H	V	G	T	H	P	A	P
	ϕ	-92,8	-82,7	-68,2	-76,3	-54,7	-96,3	-70,4	-44,9	-71,2
	ψ	-28,9	-163,1	40,4	-54,7	98,2	154,9	-30,9	149,1	-68,9
	χ1	-147,2	-133,2	**61,3**		179,8	58,5	25,7		26,4

b.

Human Allele	Pocket	P1	P2	P3	P4	P5	P6	P7	P8	P9
DRβ1*0101 HA - 1DLH	AA	Y	V	K	Q	N	T	L	K	L
	ϕ	-81,4	-95,8	-87,4	-122,5	-81,6	-90,3	-77	-79,1	-67,1
	ψ	129,4	117,5	165,4	136,6	149	128,4	142,9	143,7	172,5
	χ1	-92,7	166,5	**87,7**	-175,9	-26,2	81,6	**-44,5**	-124,2	-72,2
DRβ1*0101 HA -1FYT	AA	Y	V	K	Q	N	T	L	K	L
	ϕ	-74,9	-117,3	-91,3	-111,8	-74,8	-80,9	-101	-75,8	-71,7
	ψ	147,7	131,8	168,3	133,9	139	150	143	142,3	158,8
	χ1	-87,8	164,3	**80,9**	-165,1	71,4	80,2	**-64,8**	-169,7	-96,8
DRβ1*0401 HA - 1J8H	AA	Y	V	K	Q	N	T	L	K	L
	ϕ	-71,1	-123,1	-86,4	-99,8	-74,5	-108	-75,3	-87,9	-61,2
	ψ	146,5	136,8	162,1	143,3	149,6	124,9	149	129,6	168,3
	χ1	-84,9	68,6	**73,7**	174,1	69,7	-67,1	**-64,4**	177,3	-86,3
DRβ1*1501MBP - 1BX2	AA	V	H	F	F	K	N	I	V	T
	ϕ	-89	-82,7	-111	-83,7	-73,9	-108	-148	-101,7	-119,9
	ψ	117,4	135,2	150,8	111,7	143	145,3	162,3	-176,4	-139,6
	χ1	169,6	-74,5	**73,3**	-154,7		-46,4	**-167**	-17,8	-67,7
DRβ5*0101 MBP - 1ZGL	AA	F	K	N	I	V	T	P	R	T
	ϕ	-73,4	-82,2	-143	-124,8	-134	52,2	-55,7	-95,1	-53,8
	ψ	137,9	171	156,9	161,6	-44,9	96,5	178,9	139,1	120,1
	χ1	-67	-142	**171,4**	-32,6	-153	179	**30,5**	154,2	-53,3
HLA-DR1 TPI - 2IAM	AA	I	G	I	L	N	A	A	K	V
	ϕ	-74,1	-97,8	-121	-127,5	-94,7	-37,6	-87,6	-81,8	-62,3
	ψ	137,4	156,6	174,5	145,6	131,1	131,2	136,6	132,1	160,3
	χ1	-64,7		**62**	-135,9	41,7			-57,4	-63,4
HLA-DR1 CLIP - 3PDO	AA	M	R	M	A	T	P	L	L	M
	ϕ	-75	-95,5	-108	-100,7	-111	-64	-94,8	-71,1	-74,2
	ψ	133,3	151,4	150,6	149,4	127,7	153	142,2	135,2	152,2
	χ1	-168,7	-69,4	**158,1**		-61,3	-8,8	**-84,5**	-100	-67,8
DRβ1*0301 CLIP - 1A6A	AA	M	R	M	A	T	P	L	L	M
	ϕ	-99,52	-88,36	-106	-88,89	-122	-71,4	-60,1	-84,23	-82,89
	ψ	124,6	137,4	143	161,97	133,4	126,2	146,3	137,1	156,9
	χ1	-76,9	-57,7	**68,2**		-63,9	29,6	**-97,4**	-170,1	-67,2
DRβ1*0101 A2 - 1AQD	AA	W	R	F	L	R	G	Y	H	Q
	ϕ	-88	-92,4	-144	-105,4	-124	-88,2	-84,6	-81,6	-60,1
	ψ	121,2	159,5	159,9	161,5	153,7	149,9	167,8	132,1	150
	χ1	-172,7	-68,5	**74,7**	-66,3	-174		**-56,3**	-71,4	-70,9
Experimental-used immunogenic peptides										
I-Ek-HSP 70 1IEB	AA	V	N	H	F	I	A	E	F	K
	ϕ	-64,1	-89,6	-139	-72,1	-75,9	-85,1	-130	-69,1	-85,6
	ψ	122,5	156,5	151,5	123,1	136,8	157,6	131,3	136	138,1
	χ1	-177,1	-89,5	**73,7**	-59	-60,5		**-51,6**	-59,2	-72,4
I-Ek-CYTO-C 1KT2	AA	I	A	Y	L	K	Q	A	T	K
	ϕ	-98,8	-86,3	-158	-83,4	-68,3	-77,4	-87,6	-84,4	-91,6
	ψ	131,5	174,7	162,1	120,8	131,4	134,3	147,8	134,4	155,9
	χ1	-73,9		**67,2**	-58,3	-73,1	-174		-71,5	-67,5
High antibody titers, non protection inducer										
AMA-1 13480.29 - DRβ1*1101	AA	F	L	P	S	G	K	S	P	V
	ϕ	-99	-152,4	-83,4	-153,6	146,7	-85,2	-117	-85,5	-98,8
	ψ	68,1	116,8	80,2	-83,1	106,9	118,3	103,7	68,8	95
	χ1	24,5	-173,8	**31,6**	-173,1		71,6	**-177**	32,8	60,7
EBA-175 1400.26- DRβ1*	AA	Y	G	S	D	D	N	N	D	K
	ϕ	-62,6	-81,1	66,4	-60,3	-136	-71,7	-138	-87,7	62,8
	ψ	158,9	81,5	135,4	-46,6	102,2	120,5	114,4	-80,6	-118,6
	χ1	-55,5		**63,9**	72,4	-69,6	71,3	**-69,9**	-168,9	-53,5

Please cite this article in press as: Bermúdez A, et al. *Gauche*$^+$ side-chain orientation as a key factor in the search for an immunogenic peptide mixture leading to a complete fully protective vaccine. Vaccine (2014), http://dx.doi.org/10.1016/j.vaccine.2014.02.003

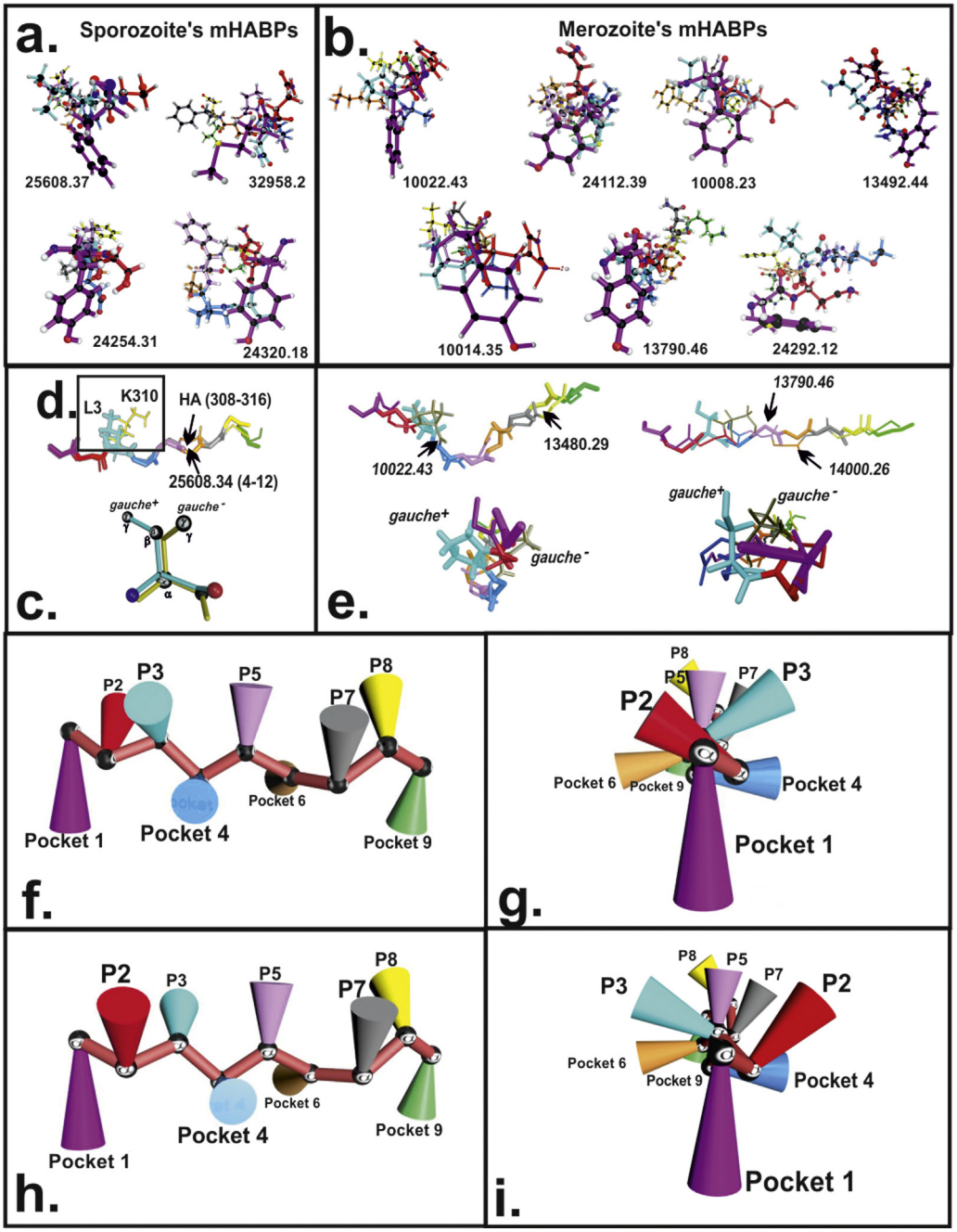

Fig. 3. Side-chain orientation in Spz and Mrz VHLLAI and FPIPS mHABPs (a and b). Frontal view of mHABP 3D structures determined by ^{1}H NMR from sporozoite and merozoite proteins (c and d). CSP protein **25608.34** VHLLAI mHABP (in thicker backbone stick) superimposed on the haemagglutinin influenza A (HA) peptide (strain specific only antigenic peptide). All other side-chains have been removed from this figure to show position 3 (p3) side-chain orientation as *gauche*$^{+}$ or *gauche*$^{-}$ in the lateral and front view, according to each immune response. (e) Side and front views of immunogenic, protection-inducing (thick backbone stick) AMA-1 protein **10022.43** mHABP superimposed on high antibody titre, non-protection-inducing (thin backbone sticks) **13480.29** and EBA-175 protein **13790.46** mHABP superimposed on **14000.26** (f and h). Diagram of side and (g and i) front view representation side-chain orientation for mHABPs which were just immunogenic and protection-inducing. Colour codes: pocket 1 (fuchsia), p2 (red), p3 (pale blue), pocket 4 (dark blue), p5 (rose), pocket 6 (orange), p7 (grey) p8 (yellow) and pocket 9 (green).

3.5. *Topological localisation and electron characteristics regarding upwardly orientated (or TCR contacting) mHABP residues*

It has been elegantly shown that the TCR adopts a canonical diagonal orientation to form a stable MHCII–p–TCR complex [43] for an appropriate immune response. Stereo-electron and topochemical characteristics of residues in VHLLAI and FPIPS mHABPs pointing away from the PBR (p2, p3, p5, p7 and p8) and theoretically contacting the TCR were thus analysed in detail.

Aotus genotyping by DNA sequencing (Fig. 1e) and experimentally determined HLA-DRβ1* binding capacity to purified HLA-DRβ1* molecules, binding motifs and binding register recognition [2,3] for VHLLAI and FPIPS mHABPs ^{1}H NMR-determined 3D structures (only 16 are shown in Table 1 and only 11 structures in Fig. 3a and b due to space limitations) have shown that when non-interfering, mHABP residues were orientated with p1 (fuchsia) pointing downwards, as the first HLA-DRβ1* residue fitting into pocket 1, all had p2 (red) pointing upwards and to the right-hand side, p3 (light blue) pointing upwards and towards the

Please cite this article in press as: Bermúdez A, et al. *Gauche*$^{+}$ side-chain orientation as a key factor in the search for an immunogenic peptide mixture leading to a complete fully protective vaccine. Vaccine (2014), http://dx.doi.org/10.1016/j.vaccine.2014.02.003

left-hand side, p4 (dark blue) downward and towards pocket 4 with right-hand side orientation, p5 (pink) upwards, p6 downwards and towards the left-hand side (pocket 6), p7 (grey) towards the right-hand side, p8 (yellow) upwards towards the left and p9 downwards (green) towards pocket 9 (Fig. 3h and i diagram summarising consensus structures). This was similar to the structures shown by other groups for antigenic (autoimmunity or tumour-associated epitopes) or thoroughly studied non-immune protection-inducing experimentally used highly immunogenic peptides like ovoalbumin (OVA), hen egg lysozyme (HEL), heat shock protein 70 (HSP-70) or cytochrome C (CytoC) [29,31–34,36,38,44,45] as determined by X ray crystallography.

It was also found that all non-interfering FPIPS and VHLLAI mHABPs had specific electron densities in their putative TCR-contacting residues. Strikingly, all mHABPs in p2 had charged residues with *p* orbitals (His or Glu) [7] or non-bonding electron pairs (Ser, Asn, Thr, Gln) while most residues in p3 were apolar or aliphatic like: Leu, Val, Met and Ala; Gly and Pro displaying different electrostatic characteristics with sigma (σ) orbitals.

Regarding the peptide–TCR interaction where p2 was in contact with the gem-line encoded CDR1α region and p3 contacted the somatic-encoded TCRV3 region, it can be suggested that CDRα1 and CDRα/β3 TCR contacting regions had different steric-electron preferences in p2 and p3 residues respectively, when determining protective immunity.

3.6. A gauche$^+$ orientation was critical in VHLLAI mHABP mixtures

It has been thoroughly demonstrated by X-ray crystallography of the 3D structures of the >40,000 proteins and peptides determined to date that the side-chain orientation of the χ^1 angle in proteins [46] and peptides has had a trimodal distribution, adopting *gauche*$^+$ (trans to the carbonyl group), *gauche*$^-$ (trans to the Hα) and trans (trans to the amino group) orientation. Therefore, rotamer populations for amino acid side-chains (except Gly, Ala, Pro) have been divided into −120° to 0° (*gauche*$^+$ conformer), 0° to +120° (*gauche*$^-$) and +120° to +240° bins (trans) [47].

It was originally found that all mixed non-deleterious VHLLAI mHABPs had *gauche*$^+$ orientation in PBR position 3 (p3) (Fig. 3a pale blue side-chain, towards the left) when their ^{1}H NMR structure-determined side-chain orientation was analysed, based on *Aotus* monkeys HLA-DRβ1* genotyping (Fig. 1e), mHABP binding motifs and binding registers. When retrospectively analysing this data, it was also found that some mHABPs had *gauche*$^-$ orientation in p3 in ALL monkey trials where interfering, blocking, competing or suppressing activities were observed (lower Fig. 1b), suggesting that if any mHABP having a different rotamer orientation was included in the mixture then deleterious or poisonous activity became induced.

This was further proved when retrospectively analysing the ~60 Mrz-derived FPIPS mHABP mixtures where ~20 monkey assays had been performed with FPIPS for which the 3D structure had been determined [2].

Fig. 2b (mixture A) shows that HIPI activity became completely abolished when high antibody titre and protection-inducing FPIPS mHABP **24112** (4044), having *gauche*$^+$ orientation in p3, was mixed with FPIPS mHABP **24148** (5501), having *gauche*$^-$ orientation in p3 (Table 1 bottom). Furthermore, when FPIPS mHABPs **24112** (4044) and **24230** (6800), both having *gauche*$^+$ orientation in p3, were mixed with **24148** (5501), having *gauche*$^-$ orientation in p3 (Table 1), the strong immunological activity induced by these first two FPIPS mHABPs became totally abolished by the third one (Fig. 2b, mixture B), this being the most commonly observed phenomenon.

Such poisonous activity induced by some peptides when mixed could not be attributed to binding competition for the PBR niche, since these FPIPS mHABPs had different purified HLA-DRβ1* molecule binding motifs, registers and capacity. Such negative activity could not be attributed to similar secondary structure conformation, as clearly seen in Table 1, the only difference being *gauche*$^+$ or *gauche*$^-$ orientation in p3 position of these peptides (highlighted in red in Table 1). This very potent negative feature must thus be taken very seriously into account when developing a complete fully protective vaccine, thereby stressing the importance of structural-functional analysis for appropriate vaccine component selection.

Conversely (Fig. 2b, mixture C) when highly immunogenic AMA-1-derived **10022** (4313) FPIPS mHABP (binding to HLA-DRβ1*03) was mixed with highly immunogenic MSP-1-derived **10014** (1585) FPIPS mHABP (binding to HLA-DRβ1*01 and 11), both having *gauche*$^+$ orientation, high antibody titres (1:160) were induced in 2/6 *Aotus* 15 days after the 2nd and 3rd immunisation and these 2 monkeys became fully protected against this lethal *P. falciparum* strain when challenged on day 20 after the last immunisation. Both FPIPS and mHABPs had *gauche*$^+$ rotamer orientation in p3 and p7. This data supported these two residues (p3 and p7) critical role in inducing protective immunity.

3.7. Further support regarding the relevant role of rotamer orientation in VHLLAI and FPIPS

The same *gauche*$^+$ orientation in p3 in all non-interfering FPIPS and VHLLAI mHABPs (Table 1, highlighted in violet) (−180°* to 0°, *= the range based on PDB MHCII–p–TCR coordinates) when amino acid χ^1 angles were determined represented a striking result associated with such rotamer disposition and a great impact on inducing long-lasting and/or fully protective immunity for providing/ensuring complete vaccine efficacy. Such orientation was completely opposite in the 12 only antigenic MHCII–p–TCR complexes reported (just 11 are shown here, to avoid repetition), where peptide p3 χ^1 angles had *gauche*$^-$ orientation (0° to +120°) (Table 1, highlighted in green). Such very diverse antigenic peptides (3D structure determined by X-ray crystallography) included hypervariable haemagglutinin A (HA binding residues 308–316 to DRβ1*0101 [29] and/or DRβ1*0401 [31]), self-reactivity myelin basic protein (MBP binding residues 89–97 to DRβ1*1501 [32], 92–100 to DRβ5*0101 [33], 85–99 to DRβ1*1501 [44]), mammary carcinoma mutant triose phosphate isomerase antigen (mTPI binding residues 26–34 to HLA-DR1) [34], CLIP (binding residues 107–115 to HLA-DR1; 91–99 to HLA-DRβ1*0301) [36], or HLA-A2-derived autologous antigen (A2 residues 5–15 binding to HLA-DRβ1*0101) and highly immunogenic experimentally used peptides heat-shock protein binding to I-Ek [38] and cytochrome C binding to I-Ek [39]. I-E is the mouse MHCII region equivalent to HLA-DRβ1* in humans and *Aotus* monkeys.

Striking differences were thus identified regarding VHLLAI and FPIPS mHABP p3 side-chain orientation compared to that of only antigenic or experimentally used highly immunogenic peptides, suggesting that the determinant factor involved in protective immunity induction is associated with two physicochemical principles: *gauche*$^+$ side-chain orientation and the apolar or aliphatic nature of p3.

By the same token, p7 χ^1 angles in all VHLLAI and FPIPS had *gauche*$^+$ orientation while the vast majority of only antigenic peptides p7 side-chains had arbitrary *gauche*$^+$, *gauche*$^-$ or *trans* orientation (Table 1).

It was also found that in all mHABPs in mixtures inducing blocking, interfering, competing or suppressing activity had residues in p3 and/or p7 having different rotamer orientation (data not shown), suggesting that all mHABPs must have appropriate *gauche* orientation in p3 and p7 residues in protection-inducing mHABP mixtures (i.e. *gauche*$^+$ orientation in p3). Should any one of them not be

Please cite this article in press as: Bermúdez A, et al. *Gauche*$^+$ side-chain orientation as a key factor in the search for an immunogenic peptide mixture leading to a complete fully protective vaccine. Vaccine (2014), http://dx.doi.org/10.1016/j.vaccine.2014.02.003

properly orientated, they might act as interface disrupting amino acids (Fig. 3f and g) poisoning or inducing deleterious activity suppressing their own and some other positive mHABPs' immune response.

Further support for these results came from different findings derived from different experimental data previously describing a large set of mHABPs inducing very high antibody titres (as assessed by ELISA, IFA and WB analysis) but having NO protection-inducing capacity against experimental challenge [48]. When their described 3D structures were analysed, these highly immunogenic non-protection-inducing mHABPs had *gauche*$^-$ orientation in p3 and had shifted their binding capacity to another HLA-DR haplotype. Only two structures are displayed here (Fig. 3e), showing that when highly immunogenic non-protection-inducing AMA-1 derived **13480.29** (4313) mHABP was superimposed onto **10022.43** (4313) highly immunogenic FPIPS analogue, with the only Lp2H difference in its PBR region (2.19 RMSD), mHABP **13480.29** Pp3 had *gauche*$^-$ orientation (Fig. 3e). These results were also confirmed by p3 *gauche*$^-$ orientation in another 4313-derived, highly immunogenic, non-protection-inducing analogue (mHABP **13766.43**, data not shown). By the same token, when highly immunogenic non-protection-inducing EBA-175-derived **14000.26** (1758) was superimposed onto highly immunogenic FPIPS analogue **13790.46** (1758), with Dp7N replacement (2.57 rmsd), Sp3 and Dp7 had shifted towards *gauche*$^-$ orientation in the former peptide (Fig. 3e). Additional confirmation of these findings came from side-chain shift in highly immunogenic non-protection-inducing analogue **14004** (data not shown).

More support for this seminal observation was obtained when VHLLAI mHABP **25608.37** was superimposed onto strain-specific HA peptide (3D structure determined by X-ray crystallography), having a 2.0 rmsd, the latter displaying a *gauche*$^-$ orientation in p3 (Fig. 3c and d).

4. Conclusions

The above data led to concluding that *gauche*$^+$ side-chain orientation in p3, as well as its polarity, are key topochemical and stereo-electron features associated with fully protective immunity induction, and long-lasting (or memory) antibody induction in minimal subunit-based, multi-epitope, multi-stage vaccine component mixtures and that such rotamer orientation is also very relevant in differentiating two closely related immunological phenomena, i.e. antigenicity and or just immunogenicity (without protective activity) from highly immunogenic protection-inducing immunity (summarised in Fig. 3f and g for antigenicity or only immunogenicity and Fig. 3h and i for highly immunogenic complete fully protection-inducing immunity). This subatomic analysis forms part of the set of rules or principles for a logical and rational methodology for very high, long-lasting, fully protective, minimal subunit-based, chemically synthesised peptide mixture for developing vaccines against diseases scouring humankind, malaria being one of them.

Contributors

AB, HA and AM-V were responsible for all 3D structure measurements and obtaining superimposed models of peptides and molecules involved in this study. DC and MAP were responsible for the immunological and immunogenetic studies and recombinant expression of the molecules used. AP was responsible for the *Aotus* monkey trials involving the peptide mixtures. MEP was responsible for the design and total development of this study.

Acknowledgements

We would like to thank Jason Garry for translating this manuscript and the chemical synthesis group at FIDIC for providing the appropriate peptides.

References

[1] Rodriguez LE, Curtidor H, Urquiza M, Cifuentes G, Reyes C, Patarroyo ME. Intimate molecular interactions of *P. falciparum* merozoite proteins involved in invasion of red blood cells and their implications for vaccine design. Chem Rev 2008;108(9):3656–705.
[2] Patarroyo ME, Bermudez A, Patarroyo MA. Structural and immunological principles leading to chemically synthesized, multiantigenic, multistage, minimal subunit-based vaccine development. Chem Rev 2011;111(5):3459–507.
[3] Curtidor H, Vanegas M, Alba MP, Patarroyo ME. Functional, immunological and three-dimensional analysis of chemically synthesised sporozoite peptides as components of a fully-effective antimalarial vaccine. Curr Med Chem 2011;18(29):4470–502.
[4] Murray CJ, Rosenfeld LC, Lim SS, Andrews KG, Foreman KJ, Haring D, et al. Global malaria mortality between 1980 and 2010: a systematic analysis. Lancet 2012;379(9814):413–31.
[5] Patarroyo ME, Moreno-Vranich A, Bermudez A. Phi (Φ) and psi (Ψ) angles involved in malarial peptide bonds determine sterile protective immunity. Biochem Biophys Res Commun 2012;429(1–2):75–80.
[6] Patarroyo ME, Bermudez A, Alba MP. The high immunogenicity induced by modified sporozoites' malarial peptides depends on their phi (Φ) and psi (Ψ) angles. Biochem Biophys Res Commun 2012;429(1–2):81–6.
[7] Moreno-Vranich A, Patarroyo ME. Steric-electronic effects in malarial peptides inducing sterile immunity. Biochem Biophys Res Commun 2012;423(4):857–62.
[8] Patarroyo ME, Cifuentes G, Pirajan C, Moreno-Vranich A, Vanegas M. Atomic evidence that modification of H-bonds established with amino acids critical for host-cell binding induces sterile immunity against malaria. Biochem Biophys Res Commun 2010;394(3):529–35.
[9] Jardetzky TS, Brown JH, Gorga JC, Stern LJ, Urban RG, Strominger JL, et al. Crystallographic analysis of endogenous peptides associated with HLA-DR1 suggests a common, polyproline II-like conformation for bound peptides. Proc Natl Acad Sci USA 1996;93(2):734–8.
[10] Suarez JE, Urquiza M, Puentes A, Garcia JE, Curtidor H, Ocampo M, et al. *Plasmodium falciparum* circumsporozoite (CS) protein peptides specifically bind to HepG2 cells. Vaccine 2001;19(31):4487–95.
[11] Bermudez A, Vanegas M, Patarroyo ME. Structural and immunological analysis of circumsporozoite protein peptides: a further step in the identification of potential components of a minimal subunit-based, chemically synthesised antimalarial vaccine. Vaccine 2008;26(52):6908–18.
[12] Patarroyo ME, Cifuentes G, Rodriguez R. Structural characterisation of sporozoite components for a multistage, multi-epitope, anti-malarial vaccine. Int J Biochem Cell Biol 2008;40(3):543–57.
[13] Bermudez A, Alba MP, Vanegas M, Patarroyo ME. 3D structure determination of STARP peptides implicated in *P. falciparum* invasion of hepatic cells. Vaccine 2010;28(31):4989–96.
[14] Espejo F, Cubillos M, Salazar LM, Guzman F, Urquiza M, Ocampo M, et al. Structure, immunogenicity, and protectivity relationship for the 1585 malarial peptide and its substitution analogues. Angew Chem Int Ed Engl 2001;40(24):4654–7.
[15] Torres MH, Salazar LM, Vanegas M, Guzman F, Rodriguez R, Silva Y, et al. Modified merozoite surface protein-1 peptides with short alpha helical regions are associated with inducing protection against malaria. Eur J Biochem/FEBS 2003;270(19):3946–52.
[16] Cifuentes G, Patarroyo ME, Urquiza M, Ramirez LE, Reyes C, Rodriguez R. Distorting malaria peptide backbone structure to enable fitting into MHC class II molecules renders modified peptides immunogenic and protective. J Med Chem 2003;46(11):2250–3.
[17] Purmova J, Salazar LM, Espejo F, Torres MH, Cubillos M, Torres E, et al. NMR structure of *Plasmodium falciparum* malaria peptide correlates with protective immunity. Biochim Biophys Acta 2002;1571(1):27–33.
[18] Guzman F, Jaramillo K, Salazar LM, Torres A, Rivera A, Patarroyo ME. ^{1}H-NMR structures of the *Plasmodium falciparum* 1758 erythrocyte binding peptide analogues and protection against malaria. Life Sci 2002;71(23):2773–85.
[19] Cifuentes G, Salazar LM, Vargas LE, Parra CA, Vanegas M, Cortes J, et al. Evidence supporting the hypothesis that specifically modifying a malaria peptide to fit into HLA-DRbeta1*03 molecules induces antibody production and protection. Vaccine 2005;23(13):1579–87.
[20] Cifuentes G, Espejo F, Vargas LE, Parra C, Vanegas M, Patarroyo ME. Orientating peptide residues and increasing the distance between pockets to enable fitting into MHC–TCR complex determine protection against malaria. Biochemistry 2004;43(21):6545–53.
[21] Bermudez A, Moreno-Vranich A, Patarroyo ME. Protective immunity provided by a new modified SERA protein peptide: its immunogenetic characteristics and correlation with 3D structure. Amino Acids 2012;43(1):183–94.

Please cite this article in press as: Bermúdez A, et al. *Gauche*$^+$ side-chain orientation as a key factor in the search for an immunogenic peptide mixture leading to a complete fully protective vaccine. Vaccine (2014), http://dx.doi.org/10.1016/j.vaccine.2014.02.003

[22] Alba MP, Salazar LM, Vargas LE, Trujillo M, Lopez Y, Patarroyo ME. Modifying RESA protein peptide 6671 to fit into HLA-DRbeta1* pockets induces protection against malaria. Biochem Biophys Res Commun 2004;315(4):1154–64.
[23] Cifuentes G, Patarroyo ME, Reyes C, Cortes J, Patarroyo MA. A pre-PEXEL histidine-rich protein II erythrocyte binding peptide as a new way for anti-malarial vaccine development. Biochem Biophys Res Commun 2007;360(1):149–55.
[24] Hunt JD, Jackson DC, Brown LE, Wood PR, Stewart DJ. Antigenic competition in a multivalent foot rot vaccine. Vaccine 1994;12(5):457–64.
[25] Sedegah M, Charoenvit Y, Minh L, Belmonte M, Majam VF, Abot S, et al. Reduced immunogenicity of DNA vaccine plasmids in mixtures. Gene Ther 2004;11(5):448–56.
[26] Fattom A, Cho YH, Chu C, Fuller S, Fries L, Naso R. Epitopic overload at the site of injection may result in suppression of the immune response to combined capsular polysaccharide conjugate vaccines. Vaccine 1999;17(2):126–33.
[27] Rodriguez R, Moreno A, Guzman F, Calvo M, Patarroyo ME. Studies in owl monkeys leading to the development of a synthetic vaccine against the asexual blood stages of *Plasmodium falciparum*. Am J Trop Med Hyg 1990;43(4):339–54.
[28] Suarez CF, Patarroyo ME, Trujillo E, Estupinan M, Baquero JE, Parra C, et al. Owl monkey MHC-DRB exon 2 reveals high similarity with several HLA-DRB lineages. Immunogenetics 2006;58(7):542–58.
[29] Stern LJ, Brown JH, Jardetzky TS, Gorga JC, Urban RG, Strominger JL, et al. Crystal structure of the human class II MHC protein HLA-DR1 complexed with an influenza virus peptide. Nature 1994;368(6468):215–21.
[30] Hennecke J, Carfi A, Wiley DC. Structure of a covalently stabilized complex of a human alphabeta T-cell receptor, influenza HA peptide and MHC class II molecule, HLA-DR1. EMBO J 2000;19(21):5611–24.
[31] Hennecke J, Wiley DC. Structure of a complex of the human alpha/beta T cell receptor (TCR) HA1.7, influenza hemagglutinin peptide, and major histocompatibility complex class II molecule, HLA-DR4 (DRA*0101 and DRB1*0401): insight into TCR cross-restriction and alloreactivity. J Exp Med 2002;195(5):571–81.
[32] Smith KJ, Pyrdol J, Gauthier L, Wiley DC, Wucherpfennig KW. Crystal structure of HLA-DR2 (DRA*0101, DRB1*1501) complexed with a peptide from human myelin basic protein. J Exp Med 1998;188(8):1511–20.
[33] Li Y, Huang Y, Lue J, Quandt JA, Martin R, Mariuzza RA. Structure of a human autoimmune TCR bound to a myelin basic protein self-peptide and a multiple sclerosis-associated MHC class II molecule. EMBO J 2005;24(17):2968–79.
[34] Deng L, Langley RJ, Brown PH, Xu G, Teng L, Wang Q, et al. Structural basis for the recognition of mutant self by a tumor-specific, MHC class II-restricted T cell receptor. Nat Immunol 2007;8(4):398–408.
[35] Gunther S, Schlundt A, Sticht J, Roske Y, Heinemann U, Wiesmuller KH, et al. Bidirectional binding of invariant chain peptides to an MHC class II molecule. Proc Natl Acad Sci USA 2010;107(51):22219–24.
[36] Ghosh P, Amaya M, Mellins E, Wiley DC. The structure of an intermediate in class II MHC maturation: CLIP bound to HLA-DR3. Nature 1995;378(6556):457–62.
[37] Murthy VL, Stern LJ. The class II MHC protein HLA-DR1 in complex with an endogenous peptide: implications for the structural basis of the specificity of peptide binding. Structure 1997;5(10):1385–96.
[38] Fremont DH, Hendrickson WA, Marrack P, Kappler J. Structures of an MHC class II molecule with covalently bound single peptides. Science 1996;272(5264):1001–4.
[39] Fremont DH, Dai S, Chiang H, Crawford F, Marrack P, Kappler J. Structural basis of cytochrome c presentation by IE (k). J Exp Med 2002;195(8):1043–52.
[40] Cifuentes G, Vanegas M, Martinez NL, Pirajan C, Patarroyo ME. Structural characteristics of immunogenic liver-stage antigens derived from *P. falciparum* malarial proteins. Biochem Biophys Res Commun 2009;384(4):455–60.
[41] Porter LL, Rose GD. Redrawing the Ramachandran plot after inclusion of hydrogen-bonding constraints. Proc Natl Acad Sci USA 2011;108(1):109–13.
[42] Hinderaker MP, Raines RT. An electronic effect on protein structure. Protein Sci 2003;12(6):1188–94.
[43] Rudolph MG, Stanfield RL, Wilson IA. How TCRs bind MHCs, peptides, and coreceptors. Annu Rev Immunol 2006;24:419–66.
[44] Hahn M, Nicholson MJ, Pyrdol J, Wucherpfennig KW. Unconventional topology of self peptide–major histocompatibility complex binding by a human autoimmune T cell receptor. Nat Immunol 2005;6(5):490–6.
[45] Zavala-Ruiz Z, Strug I, Anderson MW, Gorski J, Stern LJ. A polymorphic pocket at the P10 position contributes to peptide binding specificity in class II MHC proteins. Chem Biol 2004;11(10):1395–402.
[46] Janin J, Wodak S. Conformation of amino acid side-chains in proteins. J Mol Biol 1978;125(3):357–86.
[47] Dunbrack Jr RL, Karplus M. Backbone-dependent rotamer library for proteins. Application to side-chain prediction. J Mol Biol 1993;230(2):543–74.
[48] Patarroyo ME, Bermudez A, Salazar LM, Espejo F. High non-protective, long-lasting antibody levels in malaria are associated with haplotype shifting in MHC–peptide–TCR complex formation: a new mechanism for immune evasion. Biochimie 2006;88(7):775–84.
[49] Patarroyo ME, Salazar LM, Cifuentes G, Lozano JM, Delgado G, Rivera Z, et al. Protective cellular immunity against *P. falciparum* malaria merozoites is associated with a different P7 and P8 residue orientation in the MHC–peptide–TCR complex. Biochimie 2006;88(2):219–30.

Please cite this article in press as: Bermúdez A, et al. *Gauche*$^{+}$ side-chain orientation as a key factor in the search for an immunogenic peptide mixture leading to a complete fully protective vaccine. Vaccine (2014), http://dx.doi.org/10.1016/j.vaccine.2014.02.003

10. DISCUSIÓN GENERAL

La búsqueda de antígenos capaces de bloquear la invasión del esporozoíto/merozoíto a las célula humana blanco, primera y segunda línea de defensa contra la infección por *Plasmodium* (agente causal de la malaria), continua siendo de gran interés ya que existe evidencia que péptidos provenientes de algunas proteínas estudiadas de estas formas invasivas, al ser modificados en sus residuos críticos de unión, conllevan a un cambio conformacional evidente y a generar una respuesta inmune significativa en ensayos *in vivo* (9, 10). El fin de este trabajo fue principalmente seleccionar proteínas primordiales en el tránsito e invasión de las formas invasivas a células blanco e identificar de ellas nuevos candidatos relevantes para ser considerados en el diseño de vacuna contra malaria, además de encontrar una relación entre su estructura tridimensional y su actividad inmunológica así como determinar posibles principios generados de los resultados conformacionales para el entendimiento de dicha correlación.

De las proteínas del *P. falciparum* del estadio pre-eritrocítico que actualmente tienen una alta importancia, se destaca la proteína STARP proveniente del esporozoíto, ya que anticuerpos dirigidos contra esta proteína inhiben eficientemente la invasión de los esporozoítos a los hepatocitos (61, 63). Esta proteína es conocida también por poseer secuencias de aminoácidos repetidas en tándem (59), una característica compartida por muchos antígenos de *P. falciparum*, que son blanco para el reconocimiento celular ya que las regiones de repetición contienen a menudo un epitope de células B (139), como ocurre con la reconocida vacuna RTS y su fragmento repetido NANP, hoy en ensayo clínico fase III (48). Sin embargo, aún existe controversia sobre la importancia de dichas repeticiones en la respuesta inmune porque en contraposición a lo anterior se ha sugerido que los anticuerpos dirigidos contra las repeticiones son relativamente ineficaces, ya que éstas son altamente antigénicas e inmunogénicas pero no inducen protección (140). De acuerdo con lo anterior y con los estudios de unión de péptidos a células blanco realizados en un estudio previo (60), en el cual los péptidos 20546 (ubicado en el fragmento N-terminal, región conservada) y el 20570 (ubicado en el fragmento C-terminal, conservado), presentaron alta actividad de unión a células HepG2, los cuales no tienen fragmentos de secuencia repetitivos. La secuencia de los péptidos fueron modificadas (mHABP), y luego generados por síntesis química (ver capítulo 1, tabla 1), posteriormente grupos de monos *Aotus* fueron inmunizados con estos péptidos tanto nativos como modificados. Los péptidos nativos no indujeron anticuerpos, mientras la mayoría de los péptidos modificados fueron altamente

inmunogénicos, pero fueron los péptidos 24972, 24320 y 24322 los que mantuvieron la inducción de los títulos de anticuerpo altos durante casi todo el ensayo. El péptido 20546 y sus derivados modificados (24972, 24320, 24486), el péptido 20570 y su derivado (24322) fueron seleccionados para realizar el estudio conformacional mediante RMN ^{1}H en solución. El resumen de conectividades (capítulo 1, figura 2) que caracterizó a los péptidos así como sus estructuras (capítulo 1, Figura 3) presentan en común una conformación α helicoidal, pero con diferencias puntuales como son los desplazamientos y el acortamiento o alargamiento de los fragmentos α helicales, en este caso aunque los péptidos modificados tienen una mayor longitud de la hélice o la mantienen con respecto a su nativo, las modificaciones han hecho que su hélice se desplace hacia el fragmento N y/o C-terminal (capítulo 1, Tabla 2). Adicionalmente el péptido 20546 contiene el motivo PEXEL (RxLxE/Q/D) posiblemente transcendental en el transporte de esta proteína a los hepatocitos, uno de ellos fue modificado coincidiendo ser un residuo crítico de unión, sugiriendo que esta modificación es relevante para inducir de respuesta inmune y que además está involucrada en el cambio conformacional.

Los ensayos de unión de los péptidos a las moléculas HLA-DRβ1* evaluados en este trabajo (capítulo 1, tabla 2), se observa una tendencia en la mayoría de los péptidos a unirse al alelo HLA-DRβ1*0301 para la mayoría de los péptidos. Algunos péptidos modificados (24486 y el 24322) e incluso el péptido nativo 20546, presentaron una unión promiscua a dos o más moléculas HLA-DRβ1*. Se observó que el péptido 24972, que se caracteriza por generar altos títulos de anticuerpos después de cada inmunización y una unión a moléculas HLA-DRβ1*0301, presentó el registro apropiado de unión a este alelo correspondiendo a F7 (bolsillo 1), D10 (bolsillo 4), Q12 (bolsillo 6) y F15 (bolsillo 9) con modificaciones extras en las posiciones p7 (A13) y p8 (I14) (ver capítulo 1, tabla 1), donde el ácido aspártico en el bolsillo 4, es un residuo canónico para este tipo de alelo (101). A partir de las estructuras obtenidas por RMN de ^{1}H (Figura 3 del capítulo 1), para el péptido 24972 se observó diferencias en las orientaciones de las cadenas laterales (en la región de unión al péptido) no solo de los aminoácidos dirigidos hacia el PBR sino también aquellos dirigidos hacia el RCT, cuando se comparó con su respectivo péptido nativo 20546, dicho cambio probablemente resulta en una mejor presentación al receptor de células T, lo cual está asociado a las orientaciones obtenidas y las distancias entre los átomos más distantes de los aminoácidos que ajustan en los bolsillos 1 y 9. En este trabajo se sugiere que los péptidos modificados 24972, 24320 y 24322 derivados de los HABPs conservados de STARP 20546 y 20570 podrían ser algunos de los epitopes primordiales para inducir anticuerpos en monos *Aotus*, que se caracterizan por ser duraderos y cuya conformación estructural

cambia como efecto de las modificaciones realizadas convenientemente para una mejorada respuesta inmune comparados con los péptidos nativos.

Inicialmente el péptido 24320 de STARP no se tuvo en cuenta para el análisis estructural ya que el porcentaje de unión experimental a moléculas HLA-DRβ1*0301 no fue significativamente superior al obtenido con los otros péptidos, sin embargo los títulos de anticuerpos fueron altos y regulares después de todas las inmunizaciones realizadas en monos, así que fue pertinente realizar un estudio más profundo de su interacción con moléculas HLA-DRβ1*(ver capítulo 2). De acuerdo a reglas previamente establecidas en estudios realizados con proteínas del merozoíto (9) y a los registros y motivos de unión (141), se realizó el análisis para la secuencia de los péptidos de interés y el registro de unión al HLA-DRβ1*, en este caso el péptido 24320 presentó un registro de unión de Y11 (bolsillo 1) a G19 (bolsillo 9) concordante con el alelo HLA-DRβ1*0101. El péptido 24320 y su nativo fueron usados para inmunizar nuevos grupos de monos de monos *Aotus*, junto con dos péptidos de la proteína CSP importantes en la respuesta inmune previamente reportados (25608 y 32958) (40), se realizó un análisis estructural con la superposición de cada uno de los péptidos entre la molécula HLA-DRβ1*0101, 0422 y 0422 respectivamente (capítulo 2, Figura 2). De un grupo de 41 estructuras obtenidas del modelo estructural derivado de los datos de RMN de ^{1}H para el péptido 24320, se escogió el conformero # 18 por estar entre las estructuras de más baja energía para realizar la superposición en la molécula HLA-DRβ1*0101 teniendo en cuenta que el bolsillo 1 es el primordial en este tipo de alelo (Y11)(141) (Capítulo 2, Figura 2G).

El análisis de las estructuras que se llevó a cabo se basó en mediciones de los ángulos de torsión phi (φ) y psi (ψ) de los puentes de hidrógeno entre moléculas HLA-DRβ1* y el mHABP y de las orientaciones de la cadena lateral de los aminoácidos que ajustan en el PBR (Capítulo 2, Figura 2H). Los valores de ángulo obtenidos para los ángulos φ y ψ de cada aminoácido de las diferentes cadenas peptídicas muestran que existe regiones en los mHABPs cuyos valores de ángulos se aproximan a los que corresponden a una estructura parecida al tipo $PPII_L$ (142, 143), confirmándose también que las estructuras de las moléculas que se unen a moléculas del CMH clase II muestran características similares a las de $PPII_L$ como habría sido descrito preliminarmente (120). En este trabajo se encontró que los péptidos modificados inducen respuesta inmune humoral en ensayos de inmunización en un modelo animal (Capítulo 2, Figura 1). Asimismo, en las interacciones con las diferentes moléculas de HLA- DRβ1* y los mHABP todos presentaron formación de puentes de hidrogeno canónicos entre el esqueleto del mHABP y la cadena lateral de los aminoácidos de la molécula HLA-DRβ1* como

ha sido reportado por otros autores (108, 144), lo que parece explicar posiblemente la estabilización del complejo formado y así una respuesta inmune humoral (Capítulo 2, Tabla1).

Por otro lado, entre las proteínas relevantes de este trabajo y que también pertenecen al estadio pre-eritrocítico se encuentran CelTOSy TRSP. La primera, se reconoce como una proteína atractiva en estrategias de inhibición mediada por anticuerpos, debido a que permite al esporozoito atravesar células en los diferentes recorridos, desde la piel hasta el hepatocito final que será infectado (17). La proteína recombinante CelTOS también se ha destacado por ser una candidata en estudios preclínicos promisorios para inducir respuesta inmune, lo que la ha llevado a ser evaluada para determinar su seguridad y reactogenicidad en ensayos clínicos fase 1, por el grupo de investigación de la armada de los U.S.A. (67). La segunda proteína es primordial en la invasión a la célula hepática por tener un dominio de adhesión (69), se ha mostrado en ensayos *in vivo* e *in vitro* que la inactivación de este gen en esporozoítos impide la entrada de éstos al interior de las células diana y así se puede bloquear la infección inicial del hospedero. Dada su importancia anteriormente descrita las proteínas CelTOS y TRSP son blancos potenciales a ser estudiados.

Así, con el fin de identificar nuevos antígenos específicos que puedan participar en las interacciones patógeno-hospedero y poder evaluar su acción sobre la respuesta inmune en ensayos *in vivo*, gracias a modificaciones específicas en secuencia que generen un cambio estructural, estas dos proteínas fueron sintetizadas en este trabajo en fragmentos de 20 aminoácidos de largo mediante síntesis química en fase sólida y evaluadas en su interacción con células HeLa y HepG2 respectivamente (Capítulo 3). Los péptidos 34451, 34452 y 34458 para la proteína CelTOS y el 36075 para la proteína TRSP, fueron identificados como HABPs fundamentales en la unión a células blanco. De estos HABPs se diseñaron algunos péptidos modificados de acuerdo a las características previamente descritas (9). Estos mHABPs fueron utilizados en ensayos de inmunización en un grupo de monos *Aotus* en la estación de primates de Leticia-Amazonas (Capítulo 3, Figura 4). De este estudio de inmunización se destacaron los péptidos 38138 (del nativo 34451) y 38140 (del nativo 34458) por inducir una respuesta humoral considerable, sin embargo este último péptido posteriormente se descartó debido a que el HABP nativo de dónde provenía contiene 4 residuos no conservados entre las cepas evaluadas (Capítulo 3, Figura 2). Los ensayos de inmunofluorescencia mostraron que anticuerpos generados por inoculación de monos *Aotus* con los péptidos modificados 38138 y 38140 de CelTOS y 38148 de TRSP reconocieron las proteínas nativas, los primeros se observaron cómo pequeños puntos intracitoplasmáticos sugiriendo un patrón de micronemas y formas bilobuladas para

la segunda proteína. Además los sueros de los monos *Aotus* inmunizados con dichos mHABP reconocieron ambas proteínas de ~17 kDa y ~12kDa respectivamente, mediante western blot (WB) que corresponden a los pesos moleculares esperados.

De estas proteínas, algunos mHABPs como 38138 de CelTOS y 38142 y 38148 de TRSP, a los cuales se les hizo el estudio estructural mediante RMN de ^{1}H en solución, entraron a un segundo estudio de inmunización (Anexo 1) con resultados apreciables en la inducción de títulos de anticuerpos con algunos mHABP. En el anexo 2, parte a, se observan los espectros de DC (dicroísmo circular) para estos péptidos, presentando una tendencia α-helical para el nativo 34451 de CelTOS, mientras que sus modificados 38136 y 38138 presentan una tendencia menos estructurada casi al azar pero con un porcentaje menor de contribución α hélical luego de la deconvolución de los datos (145). Los espectros de DC de los mHABPs de TRSP son similares y tienen tendencias α helicales para todos los péptidos, concordante con lo obtenido por RMN.

Los estudios estructurales realizados por RMN de ^{1}H y calculo estructural, son presentados en los anexo 2 figura 1b y 3. Las interacciones NOE del espectro NOESY de los péptidos 38136, 38138, 36075, 38142, 38146 y 38148 mostraron conectividades de secuencia, así como NOEs de corto y mediano rango: $d_{NN}(i,i+1)$, $d_{\alpha\beta}(i,i+3)$, $d_{\alpha N}(i,i+3)$, $d_{\alpha N}(i,i+4)$ y bajos coeficientes de temperatura de protones amida $-\Delta\delta/\Delta T(*10^{3})$, que indican la presencia de estructuras α helicales en todos los péptidos. En cuanto a las conectividades NOE de los péptidos que pertenecen a la proteína CelTOS, el 38136 mostró una región helicoidal muy corta, entre los residuos I8 a S14, el péptido inmunogénico 38138 muestra también una α-hélice entre los residuos D8 a S14; mientras HABP nativo 34451 fue completamente insoluble en la concentración de péptido necesaria para los estudios de RMN de ^{1}H. Por otro lado, el péptido 38146 de la proteína TRSP, no inmunogénico, mostró una región α helical entre los residuos N11 a H18 mientras los péptidos 38142 y 38148 ambos inmunogénicos, presentaron también una región α helical, a partir de (K7 a I10; L14 a E17) y (S8 al H18), respectivamente (Anexo 3).

Según los resultados, los dos mHABPs modificados de la proteína CelTOS no generaron un cambio estructural apreciable pese a que 2 residuos de aminoácidos en su secuencia son distintos, sin embargo la respuesta inmune del 38138 fue evidente comparada con la del péptido 38136; la diferencia radica principalmente en la orientación de las cadenas laterales. El registro de unión (parte sombreada del anexo 1) de estos dos péptidos que ajustan en el alelo HLA-DRβ1*0301, presenta cambios en la

orientación en la posición 2 y 7, dejando la cadena lateral de la posición 3 hacia el RCT. Adicionalmente la diferencia de la distancia entre los átomos más lejanos del P1 al P9 entre los dos péptidos también es notoria siendo encontrada para este alelo en valores cercanos a los 20±1.5 Å (9) generando así un complejo de mayor estabilidad.

Mientras los mHABPS de la proteína TRSP fueron menos estructurados que su nativo 36075, ninguno presentó una conformación particular hacia la región N-terminal, más bien con tendencia de organización α helical hacia la región C-terminal. Los péptidos 38142 y 38148 presentaron una respuesta a anticuerpos significativa con las modificaciones realizadas, comparada con su péptido nativo, que no indujo títulos de anticuerpos. Se muestra una distancia mayor entre los átomos más lejanos desde el bolsillo 1 al bolsillo 9 con tendencia al registro de unión del alelo HLA-DRβ1*0301 para el péptido 38148 confiriéndole posiblemente una mejor estabilidad entre el complejo evidenciándose la importancia de estos mHABPs como posible candidato a ser incluidos en el diseño de vacunas multiepitópica y multiestadio.

Los hallazgos reportados en este trabajo, muestran que las proteínas STARP, CelTOS y TRSP, son blanco primordial en la primera línea de defensa contra malaria (estadio pre-eritrocítico) y son de gran importancia, por ser nuevos candidatos a vacuna, que se suman a los ya existentes provenientes del esporozoíto (40, 56, 146). Sin embargo es necesario tener cubierta también la segunda línea de defensa (estadío eritrocítico), de donde han surgido varias proteínas de interés (9) en las cuales la FIDIC centró sus estudios durante mucho tiempo, debido a que en esta etapa se presenta la mayoría de síntomas de la enfermedad, esto más el hecho de que existe una técnica para cultivar el parásito en este estadio, lo cual permite realizar ensayos de reto en monos *Aotus* inmunizados con mHABPs. Entre las proteínas pertenecientes al merozoíto, del estadio eritrocítico, está la proteína SERA 5 que ha sido implicada en la ruptura del esquizonte y salida de los merozoítos (147). Este proceso de salida es facilitado por un número de proteasas que intervienen en la degradación del parásito y de la membrana de los glóbulos rojos (148). En estudios previos (92-95) con 4 de los 6 péptidos identificados de alta unión a eritrocitos (84), que fueron modificados y evaluados a nivel de respuesta inmune, se hallaron varios mHABPs promisorios como candidatos a ser incluidos en el diseño de una vacuna multiestadio. Es por esta razón, que en esta parte del trabajo nos enfocamos en los otros dos péptidos faltantes para cubrir la totalidad de la proteína SERA 5, el péptido 6733 ubicado en el fragmento de 47 kDa y el péptido 6754 ubicado en el fragmento de 56 kDa. Estos péptidos fueron modificados en los residuos críticos de unión o sus vecinos (capítulo 4, Tabla 1) de acuerdo a reglas

preestablecidas (9, 14), se usaron para inmunizar monos *Aotus*, y los resultados fueron destacados a nivel de respuesta inmune generada. Los mHABPs 13496 y 14536 provenientes del cHABP 6733 produjeron altos títulos de anticuerpos pero no protegieron contra el reto experimental, mientras el nativo y otros modificados no generaron anticuerpos ni protección. Por otro lado los péptidos 23426 y 24220 (provenientes del cHABP 6754) indujeron títulos de anticuerpos altos y un mono *Aotus* se protegió de 9 que fueron inmunizados con el péptido 23426. Adicionalmente, se realizó un estudio conformacional mediante RMN de ^{1}H en solución y calculo molecular, de los péptidos nativo 6733 y modificado 13496 y nativo 6754 y sus derivados 23426 y 22892 (señalados con asterisco, tabla 1 del capítulo 4, correspondientes a las figuras 2 y 3) tratando de relacionar la estructura de los péptidos nativos y modificados con sus resultados a nivel de respuesta inmune. De este estudio se observó que los cHABP 6733 y 6754 solo presentaron interacciones a nivel de resonancia propias del aminoácido y conectividades secuenciales $d_{\alpha N}$ (*i,i+1*) y d_{NN} (*i,i+1*) de acuerdo al espectro NOESY (figura 2b del capítulo 4), mientras el mHABP 13496 proveniente del 6733 presentó conectividades propias de una hélice α de E8 a L13 y los mHABP 22892 y 23426 mostraron tendencia a tener un giro β: de Q4 a V7 tipo III' distorsionado y de V3 a L6 tipo V, respectivamente. El péptido 23426 que tuvo los resultados más promisorios en cuanto a generar una respuesta inmune significativa y presentar una unión fuerte a moléculas HLA-DRβ1*0401 (tabla 1, capítulo 4) fue elegido para el estudio de modelamiento molecular entre este tipo de molécula del sistema inmune (figura 4, capítulo 4). De acuerdo a un estudio previo (149) se reemplazaron aminoácidos de la cadena β del HLA (estructura tomada del PDB: 1J8H) (150) basados en diferencias encontradas en *Aotus* para el DRβ1*0403 con respecto a la secuencia de dicha cadena, adicionalmente se reemplazaron los aminoácidos de hemaglutinina (péptido unido a la molécula DRβ1*0401 original) de acuerdo a la secuencia del péptido 23426 en el registro y motivos de unión apropiados.

Posteriormente al péptido 23426 se le realizó el modelamiento molecular mediante procesos de minimización de energía, y se obtuvo un complejo estable, el cual mostró la presencia de 12 puentes de hidrógeno canónicos que comparados con los obtenidos para el péptido 22892 (6 puentes de hidrógeno) generó más estabilidad confiriéndole posiblemente la mejor respuesta inmune en los ensayos *in vivo*. Comparando las orientaciones de las cadenas laterales con lo obtenido por RMN se conservan dichas disposiciones, resaltando la orientación de los residuos en las posiciones p2 y p7 dirigidas hacia las moléculas del TCR. Así mismo, de las estructuras obtenidas por RMN se resalta la longitud que existe entre los átomos más distantes del Pocket 1 al 9 del péptido 23426 de 24.31Å que es mayor comparada con los otros mHABPs estudiados, concediendo posiblemente más

estabilidad al complejo. También es de destacar que los cHABPs 6754 y 6746 dentro del fragmento de 50 kDa cristalizado y analizado estructuralmente mediante cristalografía de rayos X (91), están situados lejanamente en la secuencia de aminoácidos de la proteína pero cercanos espacialmente y establecen puentes de hidrogeno entre los aminoácidos H762 (triada catalítica) y A763 con S596 (triada catalítica), y estos residuos fueron los fundamentales a ser modificados confirmando su relevancia para convertir un cHABP no inmunogénico en uno altamente inmunogénico y protectivo contra *P. falciparum*.

Para concluir, hemos tomado en conjunto los resultados hasta ahora discutidos acá, con los resultados de nuevos ensayos de inmunización de monos *Aotus*, abarcando mezclas de mHABPs significativos en la respuesta inmune individual, derivados de proteínas del esporozoito y del merozoito (capítulo 5, figura 1 y 2) e involucrando un estudio comparativo de los ángulos Φ, ψ y $\chi 1$ provenientes de dichos mHABP sintetizados químicamente y relevantes en la respuesta inmune con péptidos antigénicos o utilizados experimentalmente y obtenidos por cristalografía de rayos X en estudios de otros grupos de investigación (106-108, 144, 150-155). Se incluyeron los péptidos 24320 de la proteína STARP y 23426 de la proteína SERA 5 con el fin de encontrar nuevos principios y normas fisicoquímicas adicionales a las ya existentes (9, 14) que expliquen la correlación entre la estructura 3D y la actividad inmunológica y así aporten nuevos elementos en el diseño de una vacuna multiestadio contra malaria.

Los péptidos modificados, ahora en mezclas (capítulo 5), han generado dos escenarios: el primero donde la importancia individual de cada mHABP en cuanto respuesta inmune, ha sido eliminada ya que no inducen títulos de anticuerpos después de cada una de las inmunizaciones realizadas con estas mezclas (capítulo 5, figura 1b – 24254+24238 y figura 2b 24112+24148 y 24112+24230+24148) sugiriendo posiblemente efectos de competición o inhibición (156-158). El otro escenario, presenta mezclas de mHABP que han permitido la inducción de altos títulos de anticuerpos de larga duración en los ensayos de inmunización realizados (capítulo 5, figura 1 y 2, 25608+32958, 25608+32958+24246, 25608+32958+24254+24320 y 10022+10014), reconociendo y abriendo una serie de posibilidades para el análisis de la correlación entre la respuesta inmune y la estructura tridimensional de los mHABP.

De acuerdo con lo anterior, las estructuras de los péptidos de las proteínas CSP, STARP y TRAP del estadio hepático y AMA-1, MSP-1 y 2, SERA 5, EBA 175, RESA y HRP II del estadio sanguíneo, obtenidas por RMN de ^{1}H, fueron utilizadas para un análisis que involucra características

estereoquímicas (orientación de las cadenas laterales) de los aminoácidos. Para esto, la estructura que tuvo la conformación de energía más baja fue elegida de una familia de confórmeros obtenidos por RMN de ^{1}H, la cual fue nombrada con el número serial utilizado en la FIDIC, el número después del punto, indica el número de la molécula seleccionada (capítulo 5, tabla 1a). Para el estudio comparativo fueron seleccionados adicionalmente un conjunto de péptidos antigénicos previamente estudiados (106-108, 144, 150-155), que fueron acoplados a moléculas del tipo MHCII (Capítulo 5, tabla 1b). De esta comparación, se resalta la posición 2 (p2) para los mHABP, donde la mayoría de los residuos son polares, mientras la mayoría de los residuos en p3 son apolares (posiciones basada en la genotipificación de los monos *Aotus*, figura 1e). Lo anterior se corrobora con lo observado en la orientación de las cadenas laterales de dichos aminoácidos en las posiciones 2 y 3 para algunos mHABP, cuyas posiciones son dirigidas posiblemente hacia el RCT (capítulo 5, Figura 3 a y b). Por otro lado en los péptidos antigénicos y/o experimentales, los aminoácidos en p2 y p3 no tienen un rasgo particular en este contexto.

Asimismo fue observado que la mayoría de los mHABPs estudiados en esta parte (capítulo 5, tabla 1) presentan valores de ángulos diedros phi (φ) y psi (ψ) con tendencia a formar una estructura conocida como $PPII_L$ (143), como lo muestran también los péptidos antigénicos y experimentales y como previamente se había descrito con 3 mHABPs (capítulo 2).

Adicionalmente, se observó un rasgo característico presente en los mHABP con respecto al giro en torno al enlace que une el Cα con el Cβ de la cadena lateral el cual se mide con el ángulo chi 1 (χ1) y que tiene 3 conformaciones características: *gauche*$^{+}$ (*g*$^{+}$), *gauche* $^{-}$ (*g*$^{-}$) y trans (*t*) (159), en este caso particular la mayoría de los mHABP tienen una preferencia aproximada a la orientación *g*$^{+}$ en las posiciones 3 y 7 diferente a la presentada en los péptidos cristalizados con los diversos complejos (tabla 1b capítulo 5), presentando una orientación con tendencia *g*$^{-}$ para p3 y *g*$^{+}$, *g*$^{-}$ o *t* indiferentemente para p7.

Estas características estereoquímicas de los péptidos que son altamente inmunogénicos; explican en parte la respuesta inmune inducida por la mezcla de mHABPs lo que permite probablemente un apropiado ajuste dentro de las moléculas del complejo mayor de histocompatibilidad clase-II (CMH-II), lo que da lugar a la formación de una cantidad apreciable de puentes de hidrógeno e interacciones del tipo Van der Waals que estabilizarían el complejo y sugiriendo que sí existe algún mHABP en la mezcla que tenga un rotámero con rasgos diferentes a lo descrito anteriormente podría bloquear o

interferir en la acción de los otros mHABPs en la activación de la respuesta inmune. Así, para elegir una mezcla de péptidos adecuada en el contexto de vacunas multiestadio y multiepitopica se sugiere tener en cuenta inicialmente la relevancia individual en cuanto a respuesta inmune de cada uno de los péptidos, segundo tener en cuenta la polaridad específica de los aminoácidos puntualmente ubicados en la posición 2 y 3, tercero que contengan fragmentos en una conformación $PPII_L$, cuarto que conformacionalmente sea preferida una orientación *gauche*$^+$ para el ángulo χ1 en la posición 3 y 7 y quinto que la población HLA-DRβ1* sea involucrada tratando de abarcar la gran mayoría de éstas en la nueva generación de vacunas contra malaria. Los mHABPs de las proteínas evaluadas aquí, han generado la contribución de una serie de principios y normas fisicoquímicas arriba enumeradas que han aportado al diseño de una metodología para el desarrollo de una vacuna contra malaria, multi-epitópica, multi-estadio y sintetizada químicamente y así garantizar una protección completa y definitiva.

11. CONCLUSIONES GENERALES

- Al comparar las estructuras de los péptidos modificados estratégicamente, de las proteínas STARP, CelTOS y TRSP del estadio pre-eritrocítico y de la proteína SERA 5 del estadio eritrocítico, con las de sus correspondientes péptidos nativos, se observa que se ha generado un cambio conformacional que promueve en los primeros, aportes significativos a la respuesta inmune, cuando son inmunizados en grupos de monos *Aotus*. Sugiriendo que ciertos péptidos modificados podrían incluirse como posibles componentes en el diseño de una vacuna contra malaria.

- Dentro de las características estereoquímicas de los péptidos que son altamente inmunógenicos y que inducen protección contra el reto experimental, son significativos los ángulos diedros phi (φ) y psi (ψ) de los aminoácidos que forman la cadena peptídica, los cuales adquieren valores cercanos a la estructura secundaria conocida como $PPII_L$. Asimismo, los aminoácidos en las posiciones 2 y 3 de los péptidos modificados tienen un papel relevante debido a sus características polares y apolares respectivamente (posición de acuerdo con la genotipificación de monos *Aotus*).

- Los resultados obtenidos evidencian que el ángulo de torsión de la cadena lateral $\chi 1$ en las posiciones 3 y p7, con la conformación *gauche*$^+$, tiene un papel fundamental para que los péptidos modificados induzcan una respuesta inmune apropiada, permitiendo un aporte al diseño de vacunas contra malaria.

- Los resultados obtenidos de los modelamientos moleculares del complejo CMH II y los péptidos modificados, conllevan a la formación de un número considerable de puentes de hidrógeno, interacciones de Van der Waals y puentes salinos que hace inferir que son

esenciales para la estabilización del complejo péptido-CMH-II y por ende a una respuesta inmune eficaz.

- Péptidos conservados unidos por puentes de hidrogeno en estructuras ya establecidas de una proteína, permiten puntualmente elegir la modificación a realizar, con el fin de cambiar su conformación inicial y romper el silencio inmunológico.

12. PERSPECTIVAS

- Determinación de la estructura tridimensional mediante RMN de ^{1}H de nuevos péptidos modificados que en estudios recientes han mostrado la generación de una respuesta inmune significativa o importante, ya sea individualmente o en mezclas con el fin de complementar el estudio de las proteínas acá estudiadas.

- Estudio conformacional de las proteínas STARP, CelTOS, TRSP y SERA 5 fragmento de 42 kDa del parásito, por RMN multidimensional con el fin de determinar péptidos conservados cercanos estructuralmente y relevantes en función y así confirmar los principios establecidos en la búsqueda de candidatos a vacuna contra malaria.

- Con el fin de hallar péptidos con propiedades estructurales similares a $PPII_L$, pero de complejidad más reducida, se podrían estudiar moléculas cortas (15 amino ácidos) y realizar con ellas estudios de inmunización *in vivo*; la formación de este tipo de estructuras serían de gran importancia para el diseño de una serie de mHABPs cortos y poco estructurados, presuntamente capaces de inducir una respuesta inmune apreciable.

- Realizar un estudio estructural a nivel de RMN multidimensional entre la interacción de péptidos con tendencia $PPII_L$ y moléculas HLA-DRβ1* de humano purificadas con el fin de evaluar los sitios de unión probables en dicha interacción.

- Ensayos para la evaluación de la respuesta inmune celular T inducida tras la inmunización con los antígenos reportados de *P. falciparum* para cada uno de los *Aotus* inmunizados.

13. REFERENCIAS

1. Greenwood BM, Fidock DA, Kyle DE, Kappe SH, Alonso PL, Collins FH, et al. Malaria: progress, perils, and prospects for eradication. J Clin Invest. 2008;118(4):1266-76. Epub 2008/04/03.
2. Snow RW, Guerra CA, Noor AM, Myint HY, Hay SI. The global distribution of clinical episodes of Plasmodium falciparum malaria. Nature. 2005;434(7030):214-7. Epub 2005/03/11.
3. Greenwood BM, Bojang K, Whitty CJ, Targett GA. Malaria. Lancet. 2005;365(9469):1487-98. Epub 2005/04/27.
4. http://www.who.int/en/. World Malaria Report. 2014.
5. Aly AS, Vaughan AM, Kappe SH. Malaria parasite development in the mosquito and infection of the mammalian host. Annu Rev Microbiol. 2009;63:195-221. Epub 2009/07/07.
6. Gardner MJ, Hall N, Fung E, White O, Berriman M, Hyman RW, et al. Genome sequence of the human malaria parasite Plasmodium falciparum. Nature. 2002;419(6906):498-511. Epub 2002/10/09.
7. Bozdech Z, Llinas M, Pulliam BL, Wong ED, Zhu J, DeRisi JL. The transcriptome of the intraerythrocytic developmental cycle of Plasmodium falciparum. PLoS Biol. 2003;1(1):E5. Epub 2003/08/21.
8. Kappe SH, Buscaglia CA, Nussenzweig V. Plasmodium sporozoite molecular cell biology. Annu Rev Cell Dev Biol. 2004;20:29-59. Epub 2004/10/12.
9. Patarroyo ME, Bermudez A, Patarroyo MA. Structural and immunological principles leading to chemically synthesized, multiantigenic, multistage, minimal subunit-based vaccine development. Chem Rev. 2011;111(5):3459-507. Epub 2011/03/29.
10. Curtidor H, Vanegas M, Alba MP, Patarroyo ME. Functional, immunological and three-dimensional analysis of chemically synthesised sporozoite peptides as components of a fully-effective antimalarial vaccine. Curr Med Chem. 2011;18(29):4470-502. Epub 2011/10/28.
11. Hay SI, Guerra CA, Tatem AJ, Noor AM, Snow RW. The global distribution and population at risk of malaria: past, present, and future. Lancet Infect Dis. 2004;4(6):327-36. Epub 2004/06/03.
12. Murray CJ, Rosenfeld LC, Lim SS, Andrews KG, Foreman KJ, Haring D, et al. Global malaria mortality between 1980 and 2010: a systematic analysis. Lancet. 2012;379(9814):413-31. Epub 2012/02/07.
13. http://www.ins.gov.co/boletin-epidemiologico/Paginas/default.aspx. Boletin Epidemiologico SE50. 2014.
14. Patarroyo ME, Patarroyo MA. Emerging rules for subunit-based, multiantigenic, multistage chemically synthesized vaccines. Acc Chem Res. 2008;41(3):377-86. Epub 2008/02/13.
15. Coppi A, Tewari R, Bishop JR, Bennett BL, Lawrence R, Esko JD, et al. Heparan sulfate proteoglycans provide a signal to Plasmodium sporozoites to stop migrating and productively invade host cells. Cell Host Microbe. 2007;2(5):316-27. Epub 2007/11/17.
16. Mota MM, Pradel G, Vanderberg JP, Hafalla JC, Frevert U, Nussenzweig RS, et al. Migration of Plasmodium sporozoites through cells before infection. Science. 2001;291(5501):141-4. Epub 2001/01/06.
17. Kariu T, Ishino T, Yano K, Chinzei Y, Yuda M. CelTOS, a novel malarial protein that mediates transmission to mosquito and vertebrate hosts. Mol Microbiol. 2006;59(5):1369-79. Epub 2006/02/14.
18. Yuda M, Ishino T. Liver invasion by malarial parasites--how do malarial parasites break through the host barrier? Cell Microbiol. 2004;6(12):1119-25. Epub 2004/11/06.

19. Schwenk RJ, Richie TL. Protective immunity to pre-erythrocytic stage malaria. Trends Parasitol. 2011;27(7):306-14. Epub 2011/03/26.
20. Imwong M, Snounou G, Pukrittayakamee S, Tanomsing N, Kim JR, Nandy A, et al. Relapses of Plasmodium vivax infection usually result from activation of heterologous hypnozoites. J Infect Dis. 2007;195(7):927-33. Epub 2007/03/03.
21. Crompton PD, Moebius J, Portugal S, Waisberg M, Hart G, Garver LS, et al. Malaria immunity in man and mosquito: insights into unsolved mysteries of a deadly infectious disease. Annu Rev Immunol. 2014;32:157-87. Epub 2014/03/25.
22. Coombes JL, Robey EA. Dynamic imaging of host-pathogen interactions in vivo. Nat Rev Immunol. 2010;10(5):353-64. Epub 2010/04/17.
23. Patarroyo ME. El desarrollo de una vacuna antimalarica. Tribuna Medica. 1989;80(2):52-61.
24. Beeson JG, Brown GV. Pathogenesis of Plasmodium falciparum malaria: the roles of parasite adhesion and antigenic variation. Cell Mol Life Sci. 2002;59(2):258-71. Epub 2002/03/28.
25. Miller LH, Baruch DI, Marsh K, Doumbo OK. The pathogenic basis of malaria. Nature. 2002;415(6872):673-9. Epub 2002/02/08.
26. Miller LH, Ackerman HC, Su XZ, Wellems TE. Malaria biology and disease pathogenesis: insights for new treatments. Nat Med. 2013;19(2):156-67. Epub 2013/02/08.
27. Florens L, Washburn MP, Raine JD, Anthony RM, Grainger M, Haynes JD, et al. A proteomic view of the Plasmodium falciparum life cycle. Nature. 2002;419(6906):520-6. Epub 2002/10/09.
28. Kaiser K, Matuschewski K, Camargo N, Ross J, Kappe SH. Differential transcriptome profiling identifies Plasmodium genes encoding pre-erythrocytic stage-specific proteins. Mol Microbiol. 2004;51(5):1221-32. Epub 2004/02/26.
29. Vignali M, Speake C, Duffy PE. Malaria sporozoite proteome leaves a trail. Genome Biol. 2009;10(4):216. Epub 2009/05/14.
30. Kappe SH, Gardner MJ, Brown SM, Ross J, Matuschewski K, Ribeiro JM, et al. Exploring the transcriptome of the malaria sporozoite stage. Proc Natl Acad Sci U S A. 2001;98(17):9895-900. Epub 2001/08/09.
31. Menard R, Heussler V, Yuda M, Nussenzweig V. Plasmodium pre-erythrocytic stages: what's new? Trends Parasitol. 2008;24(12):564-9. Epub 2008/10/22.
32. Kumar KA, Sano G, Boscardin S, Nussenzweig RS, Nussenzweig MC, Zavala F, et al. The circumsporozoite protein is an immunodominant protective antigen in irradiated sporozoites. Nature. 2006;444(7121):937-40. Epub 2006/12/08.
33. Bongfen SE, Ntsama PM, Offner S, Smith T, Felger I, Tanner M, et al. The N-terminal domain of Plasmodium falciparum circumsporozoite protein represents a target of protective immunity. Vaccine. 2009;27(2):328-35. Epub 2008/11/06.
34. Dame JB, Williams JL, McCutchan TF, Weber JL, Wirtz RA, Hockmeyer WT, et al. Structure of the gene encoding the immunodominant surface antigen on the sporozoite of the human malaria parasite Plasmodium falciparum. Science. 1984;225(4662):593-9. Epub 1984/08/10.
35. Stewart MJ, Nawrot RJ, Schulman S, Vanderberg JP. Plasmodium berghei sporozoite invasion is blocked in vitro by sporozoite-immobilizing antibodies. Infect Immun. 1986;51(3):859-64. Epub 1986/03/01.
36. Pancake SJ, Holt GD, Mellouk S, Hoffman SL. Malaria sporozoites and circumsporozoite proteins bind specifically to sulfated glycoconjugates. J Cell Biol. 1992;117(6):1351-7. Epub 1992/06/01.

37. Tan K, Duquette M, Liu JH, Dong Y, Zhang R, Joachimiak A, et al. Crystal structure of the TSP-1 type 1 repeats: a novel layered fold and its biological implication. J Cell Biol. 2002;159(2):373-82. Epub 2002/10/23.
38. Peterson DS, Gao Y, Asokan K, Gaertig J. The circumsporozoite protein of Plasmodium falciparum is expressed and localized to the cell surface in the free-living ciliate Tetrahymena thermophila. Molecular and biochemical parasitology. 2002;122(2):119-26. Epub 2002/07/11.
39. Suarez JE, Urquiza M, Puentes A, Garcia JE, Curtidor H, Ocampo M, et al. Plasmodium falciparum circumsporozoite (CS) protein peptides specifically bind to HepG2 cells. Vaccine. 2001;19(31):4487-95. Epub 2001/08/03.
40. Bermudez A, Vanegas M, Patarroyo ME. Structural and immunological analysis of circumsporozoite protein peptides: a further step in the identification of potential components of a minimal subunit-based, chemically synthesised antimalarial vaccine. Vaccine. 2008;26(52):6908-18. Epub 2008/10/22.
41. Doud MB, Koksal AC, Mi LZ, Song G, Lu C, Springer TA. Unexpected fold in the circumsporozoite protein target of malaria vaccines. Proc Natl Acad Sci U S A. 2012;109(20):7817-22. Epub 2012/05/02.
42. Patarroyo ME, Romero P, Torres ML, Clavijo P, Moreno A, Martinez A, et al. Induction of protective immunity against experimental infection with malaria using synthetic peptides. Nature. 1987;328(6131):629-32. Epub 1987/08/13.
43. Valero MV, Amador LR, Galindo C, Figueroa J, Bello MS, Murillo LA, et al. Vaccination with SPf66, a chemically synthesised vaccine, against Plasmodium falciparum malaria in Colombia. Lancet. 1993;341(8847):705-10. Epub 1993/03/20.
44. Noya O, Gabaldon Berti Y, Alarcon de Noya B, Borges R, Zerpa N, Urbaez JD, et al. A population-based clinical trial with the SPf66 synthetic Plasmodium falciparum malaria vaccine in Venezuela. J Infect Dis. 1994;170(2):396-402. Epub 1994/08/01.
45. Sempertegui F, Estrella B, Moscoso J, Piedrahita L, Hernandez D, Gaybor J, et al. Safety, immunogenicity and protective effect of the SPf66 malaria synthetic vaccine against Plasmodium falciparum infection in a randomized double-blind placebo-controlled field trial in an endemic area of Ecuador. Vaccine. 1994;12(4):337-42. Epub 1994/03/01.
46. Alonso PL, Smith TA, Armstrong-Schellenberg JR, Kitua AY, Masanja H, Hayes R, et al. Duration of protection and age-dependence of the effects of the SPf66 malaria vaccine in African children exposed to intense transmission of Plasmodium falciparum. J Infect Dis. 1996;174(2):367-72. Epub 1996/08/01.
47. Agnandji ST, Lell B, Soulanoudjingar SS, Fernandes JF, Abossolo BP, Conzelmann C, et al. First results of phase 3 trial of RTS,S/AS01 malaria vaccine in African children. N Engl J Med. 2011;365(20):1863-75. Epub 2011/10/20.
48. Regules JA, Cummings JF, Ockenhouse CF. The RTS,S vaccine candidate for malaria. Expert Rev Vaccines. 2011;10(5):589-99. Epub 2011/05/25.
49. Cerami C, Frevert U, Sinnis P, Takacs B, Clavijo P, Santos MJ, et al. The basolateral domain of the hepatocyte plasma membrane bears receptors for the circumsporozoite protein of Plasmodium falciparum sporozoites. Cell. 1992;70(6):1021-33. Epub 1992/09/18.
50. Muller HM, Reckmann I, Hollingdale MR, Bujard H, Robson KJ, Crisanti A. Thrombospondin related anonymous protein (TRAP) of Plasmodium falciparum binds specifically to sulfated glycoconjugates and to HepG2 hepatoma cells suggesting a role for this molecule in sporozoite invasion of hepatocytes. EMBO J. 1993;12(7):2881-9. Epub 1993/07/01.

51. Kappe S, Bruderer T, Gantt S, Fujioka H, Nussenzweig V, Menard R. Conservation of a gliding motility and cell invasion machinery in Apicomplexan parasites. J Cell Biol. 1999;147(5):937-44. Epub 1999/12/01.
52. Adams JC, Tucker RP. The thrombospondin type 1 repeat (TSR) superfamily: diverse proteins with related roles in neuronal development. Dev Dyn. 2000;218(2):280-99. Epub 2000/06/08.
53. Tucker RP. The thrombospondin type 1 repeat superfamily. Int J Biochem Cell Biol. 2004;36(6):969-74. Epub 2004/04/20.
54. Whittaker CA, Hynes RO. Distribution and evolution of von Willebrand/integrin A domains: widely dispersed domains with roles in cell adhesion and elsewhere. Mol Biol Cell. 2002;13(10):3369-87. Epub 2002/10/22.
55. Lopez R, Curtidor H, Urquiza M, Garcia J, Puentes A, Suarez J, et al. Plasmodium falciparum: binding studies of peptide derived from the sporozoite surface protein 2 to Hep G2 cells. J Pept Res. 2001;58(4):285-92. Epub 2001/10/19.
56. Patarroyo ME, Cifuentes G, Rodriguez R. Structural characterisation of sporozoite components for a multistage, multi-epitope, anti-malarial vaccine. Int J Biochem Cell Biol. 2008;40(3):543-57. Epub 2007/11/13.
57. Tossavainen H, Pihlajamaa T, Huttunen TK, Raulo E, Rauvala H, Permi P, et al. The layered fold of the TSR domain of P. falciparum TRAP contains a heparin binding site. Protein Sci. 2006;15(7):1760-8. Epub 2006/07/04.
58. Gallivan JP, Dougherty DA. Cation-pi interactions in structural biology. Proc Natl Acad Sci U S A. 1999;96(17):9459-64. Epub 1999/08/18.
59. Fidock DA, Bottius E, Brahimi K, Moelans, II, Aikawa M, Konings RN, et al. Cloning and characterization of a novel Plasmodium falciparum sporozoite surface antigen, STARP. Molecular and biochemical parasitology. 1994;64(2):219-32. Epub 1994/04/01.
60. Lopez R, Garcia J, Puentes A, Curtidor H, Ocampo M, Vera R, et al. Identification of specific Hep G2 cell binding regions in Plasmodium falciparum sporozoite-threonine-asparagine-rich protein (STARP). Vaccine. 2003;21(19-20):2404-11. Epub 2003/05/15.
61. Pasquetto V, Fidock DA, Gras H, Badell E, Eling W, Ballou WR, et al. Plasmodium falciparum sporozoite invasion is inhibited by naturally acquired or experimentally induced polyclonal antibodies to the STARP antigen. Eur J Immunol. 1997;27(10):2502-13. Epub 1997/11/22.
62. Marti M, Good RT, Rug M, Knuepfer E, Cowman AF. Targeting malaria virulence and remodeling proteins to the host erythrocyte. Science. 2004;306(5703):1930-3. Epub 2004/12/14.
63. Suwancharoen C, Putaporntip C, Rungruang T, Jongwutiwes S. Naturally acquired IgG antibodies against the C-terminal part of Plasmodium falciparum sporozoite threonine-asparagine-rich protein in a low endemic area. Parasitol Res. 2011;109(2):315-20. Epub 2011/02/03.
64. Crompton PD, Kayala MA, Traore B, Kayentao K, Ongoiba A, Weiss GE, et al. A prospective analysis of the Ab response to Plasmodium falciparum before and after a malaria season by protein microarray. Proc Natl Acad Sci U S A.107(15):6958-63. Epub 2010/03/31.
65. Bergmann-Leitner ES, Mease RM, De La Vega P, Savranskaya T, Polhemus M, Ockenhouse C, et al. Immunization with pre-erythrocytic antigen CelTOS from Plasmodium falciparum elicits cross-species protection against heterologous challenge with Plasmodium berghei. PLoS One. 2010;5(8):e12294. Epub 2010/09/03.
66. Bergmann-Leitner ES, Legler PM, Savranskaya T, Ockenhouse CF, Angov E. Cellular and humoral immune effector mechanisms required for sterile protection against sporozoite challenge induced with the novel malaria vaccine candidate CelTOS. Vaccine. 2011;29(35):5940-9. Epub 2011/07/05.

67. https://clinicaltrials.gov/ct2/about-site/background.
68. Bergmann-Leitner ES, Chaudhury S, Steers NJ, Sabato M, Delvecchio V, Wallqvist AS, et al. Computational and experimental validation of B and T-cell epitopes of the in vivo immune response to a novel malarial antigen. PLoS One. 2013;8(8):e71610. Epub 2013/08/27.
69. Labaied M, Camargo N, Kappe SH. Depletion of the Plasmodium berghei thrombospondin-related sporozoite protein reveals a role in host cell entry by sporozoites. Molecular and biochemical parasitology. 2007;153(2):158-66. Epub 2007/04/10.
70. Holder AA, Blackman MJ, Burghaus PA, Chappel JA, Ling IT, McCallum-Deighton N, et al. A malaria merozoite surface protein (MSP1)-structure, processing and function. Mem Inst Oswaldo Cruz. 1992;87 Suppl 3:37-42. Epub 1992/01/01.
71. Blackman MJ, Whittle H, Holder AA. Processing of the Plasmodium falciparum major merozoite surface protein-1: identification of a 33-kilodalton secondary processing product which is shed prior to erythrocyte invasion. Molecular and biochemical parasitology. 1991;49(1):35-44. Epub 1991/11/01.
72. Angov E, Aufiero BM, Turgeon AM, Van Handenhove M, Ockenhouse CF, Kester KE, et al. Development and pre-clinical analysis of a Plasmodium falciparum Merozoite Surface Protein-1(42) malaria vaccine. Molecular and biochemical parasitology. 2003;128(2):195-204. Epub 2003/05/14.
73. Ockenhouse CF, Angov E, Kester KE, Diggs C, Soisson L, Cummings JF, et al. Phase I safety and immunogenicity trial of FMP1/AS02A, a Plasmodium falciparum MSP-1 asexual blood stage vaccine. Vaccine. 2006;24(15):3009-17. Epub 2005/12/17.
74. Stoute JA, Gombe J, Withers MR, Siangla J, McKinney D, Onyango M, et al. Phase 1 randomized double-blind safety and immunogenicity trial of Plasmodium falciparum malaria merozoite surface protein FMP1 vaccine, adjuvanted with AS02A, in adults in western Kenya. Vaccine. 2007;25(1):176-84. Epub 2006/01/04.
75. Otsyula N, Angov E, Bergmann-Leitner E, Koech M, Khan F, Bennett J, et al. Results from tandem Phase 1 studies evaluating the safety, reactogenicity and immunogenicity of the vaccine candidate antigen Plasmodium falciparum FVO merozoite surface protein-1 (MSP1(42)) administered intramuscularly with adjuvant system AS01. Malar J. 2013;12:29. Epub 2013/01/25.
76. Urquiza M, Rodriguez LE, Suarez JE, Guzman F, Ocampo M, Curtidor H, et al. Identification of Plasmodium falciparum MSP-1 peptides able to bind to human red blood cells. Parasite Immunol. 1996;18(10):515-26. Epub 1996/10/01.
77. Espejo F, Cubillos M, Salazar LM, Guzman F, Urquiza M, Ocampo M, et al. Structure, Immunogenicity, and Protectivity Relationship for the 1585 Malarial Peptide and Its Substitution Analogues. Angew Chem Int Ed Engl. 2001;40(24):4654-7. Epub 2002/10/31.
78. Espejo F, Bermudez A, Torres E, Urquiza M, Rodriguez R, Lopez Y, et al. Shortening and modifying the 1513 MSP-1 peptide's alpha-helical region induces protection against malaria. Biochem Biophys Res Commun. 2004;315(2):418-27. Epub 2004/02/10.
79. Cubillos M, Espejo F, Purmova J, Martinez JC, Patarroyo ME. Alpha helix shortening in 1522 MSP-1 conserved peptide analogs is associated with immunogenicity and protection against P. falciparum malaria. Proteins. 2003;50(3):400-9. Epub 2003/01/31.
80. Torres MH, Salazar LM, Vanegas M, Guzman F, Rodriguez R, Silva Y, et al. Modified merozoite surface protein-1 peptides with short alpha helical regions are associated with inducing protection against malaria. Eur J Biochem. 2003;270(19):3946-52. Epub 2003/09/27.
81. Miller SK, Good RT, Drew DR, Delorenzi M, Sanders PR, Hodder AN, et al. A subset of Plasmodium falciparum SERA genes are expressed and appear to play an important role in the erythrocytic cycle. J Biol Chem. 2002;277(49):47524-32. Epub 2002/09/14.

82. Yagi M, Bang G, Tougan T, Palacpac NM, Arisue N, Aoshi T, et al. Protective epitopes of the Plasmodium falciparum SERA5 malaria vaccine reside in intrinsically unstructured N-terminal repetitive sequences. PLoS One. 2014;9(6):e98460. Epub 2014/06/03.
83. Li J, Mitamura T, Fox BA, Bzik DJ, Horii T. Differential localization of processed fragments of Plasmodium falciparum serine repeat antigen and further processing of its N-terminal 47 kDa fragment. Parasitol Int. 2002;51(4):343-52. Epub 2002/11/08.
84. Puentes A, Garcia J, Vera R, Lopez QR, Urquiza M, Vanegas M, et al. Serine repeat antigen peptides which bind specifically to red blood cells. Parasitol Int. 2000;49(2):105-17. Epub 2000/07/07.
85. Fox BA, Xing-Li P, Suzue K, Horii T, Bzik DJ. Plasmodium falciparum: an epitope within a highly conserved region of the 47-kDa amino-terminal domain of the serine repeat antigen is a target of parasite-inhibitory antibodies. Exp Parasitol. 1997;85(2):121-34. Epub 1997/02/01.
86. Pang XL, Horii T. Complement-mediated killing of Plasmodium falciparum erythrocytic schizont with antibodies to the recombinant serine repeat antigen (SERA). Vaccine. 1998;16(13):1299-305. Epub 1998/07/31.
87. Pang XL, Mitamura T, Horii T. Antibodies reactive with the N-terminal domain of Plasmodium falciparum serine repeat antigen inhibit cell proliferation by agglutinating merozoites and schizonts. Infect Immun. 1999;67(4):1821-7. Epub 1999/03/20.
88. Horii T, Shirai H, Jie L, Ishii KJ, Palacpac NQ, Tougan T, et al. Evidences of protection against blood-stage infection of Plasmodium falciparum by the novel protein vaccine SE36. Parasitol Int. 2010;59(3):380-6. Epub 2010/05/25.
89. Palacpac NM, Ntege E, Yeka A, Balikagala B, Suzuki N, Shirai H, et al. Phase 1b randomized trial and follow-up study in Uganda of the blood-stage malaria vaccine candidate BK-SE36. PLoS One. 2013;8(5):e64073. Epub 2013/06/01.
90. Kanodia S, Kumar G, Rizzi L, Pedretti A, Hodder AN, Romeo S, et al. Synthetic peptides derived from the C-terminal 6kDa region of Plasmodium falciparum SERA5 inhibit the enzyme activity and malaria parasite development. Biochim Biophys Acta. 2014;1840(9):2765-75. Epub 2014/04/29.
91. Hodder AN, Malby RL, Clarke OB, Fairlie WD, Colman PM, Crabb BS, et al. Structural insights into the protease-like antigen Plasmodium falciparum SERA5 and its noncanonical active-site serine. J Mol Biol. 2009;392(1):154-65. Epub 2009/07/14.
92. Alba MP, Salazar LM, Puentes A, Pinto M, Torres E, Patarroyo ME. 6746 SERA peptide analogues immunogenicity and protective efficacy against malaria is associated with short alpha helix formation: malaria protection associated with peptides alpha helix shortening. Peptides. 2003;24(7):999-1006. Epub 2003/09/23.
93. Alba MP, Salazar LM, Purmova J, Vanegas M, Rodriguez R, Patarroyo ME. Induction and displacement of an helix in the 6725 SERA peptide analogue confers protection against P. falciparum malaria. Vaccine. 2004;22(9-10):1281-9. Epub 2004/03/09.
94. Cubillos M, Alba MP, Bermudez A, Trujillo M, Patarroyo ME. Plasmodium falciparum SERA protein peptide analogues having short helical regions induce protection against malaria. Biochimie. 2003;85(7):651-7. Epub 2003/09/25.
95. Salazar LM, Bermudez A, Patarroyo ME. HLA-DR allele reading register shifting is associated with immunity induced by SERA peptide analogues. Biochem Biophys Res Commun. 2008;372(1):114-20. Epub 2008/05/17.
96. Abul K. Abbas AHL, Shiv Pillai. Inmunología Celular y Molecular. 6a Edicion.Elsevier.

97. Cohen S, Mc GI, Carrington S. Gamma-globulin and acquired immunity to human malaria. Nature. 1961;192:733-7. Epub 1961/11/25.
98.http://www.currentprotocols.com/WileyCDA/http://www.currentprotocols.com/WileyCDA/.
99. Weissensteiner T, Lanchbury JS. TNFB polymorphisms characterize three lineages of TNF region microsatellite haplotypes. Immunogenetics. 1997;47(1):6-16. Epub 1997/01/01.
100. Stern LJ, Calvo-Calle JM. HLA-DR: molecular insights and vaccine design. Curr Pharm Des. 2009;15(28):3249-61. Epub 2009/10/29.
101. Marsh SGEP, P.; Barber, L. D. . The HLA factsbook. Academic Press: San Diego. 2000.
102. Andersson G, Andersson L, Larhammar D, Rask L, Sigurdardottir S. Simplifying genetic locus assignment of HLA-DRB genes. Immunol Today. 1994;15(2):58-62. Epub 1994/02/01.
103. Suarez CF, Patarroyo ME, Trujillo E, Estupinan M, Baquero JE, Parra C, et al. Owl monkey MHC-DRB exon 2 reveals high similarity with several HLA-DRB lineages. Immunogenetics. 2006;58(7):542-58. Epub 2006/06/23.
104. Li Y, Li H, Martin R, Mariuzza RA. Structural basis for the binding of an immunodominant peptide from myelin basic protein in different registers by two HLA-DR2 proteins. J Mol Biol. 2000;304(2):177-88. Epub 2000/11/18.
105. Dessen A, Lawrence CM, Cupo S, Zaller DM, Wiley DC. X-ray crystal structure of HLA-DR4 (DRA*0101, DRB1*0401) complexed with a peptide from human collagen II. Immunity. 1997;7(4):473-81. Epub 1997/11/14.
106. Fremont DH, Hendrickson WA, Marrack P, Kappler J. Structures of an MHC class II molecule with covalently bound single peptides. Science. 1996;272(5264):1001-4. Epub 1996/05/17.
107. Ghosh P, Amaya M, Mellins E, Wiley DC. The structure of an intermediate in class II MHC maturation: CLIP bound to HLA-DR3. Nature. 1995;378(6556):457-62. Epub 1995/11/30.
108. Stern LJ, Brown JH, Jardetzky TS, Gorga JC, Urban RG, Strominger JL, et al. Crystal structure of the human class II MHC protein HLA-DR1 complexed with an influenza virus peptide. Nature. 1994;368(6468):215-21. Epub 1994/03/17.
109. Wider G. Structure determination of biological macromolecules in solution using nuclear magnetic resonance spectroscopy. Biotechniques. 2000;29(6):1278-82. Epub 2000/12/29.
110. Berg J.M. TJLaSL. Biochemistry. Editorial Reverté, SA. 2008;Fifth Edicion.
111. Whitford D. Proteins: Structure and Function. New York: Wiley-VCH, Inc. 2005.
112. Albert B, Johnson A, Lewis J, Raff M, Robert K, Walter P. Molecular Biology of the cell. 4th ed Garland. 2002.
113. Barlow DJ, Thornton JM. Helix geometry in proteins. J Mol Biol. 1988;201(3):601-19. Epub 1988/06/05.
114. Karpen ME, de Haseth PL, Neet KE. Differences in the amino acid distributions of 3(10)-helices and alpha-helices. Protein Sci. 1992;1(10):1333-42. Epub 1992/10/01.
115. Cifuentes G, Espejo F, Vargas LE, Parra C, Vanegas M, Patarroyo ME. Orientating peptide residues and increasing the distance between pockets to enable fitting into MHC-TCR complex determine protection against malaria. Biochemistry. 2004;43(21):6545-53. Epub 2004/05/26.
116. Rose GD. Prediction of chain turns in globular proteins on a hydrophobic basis. Nature. 1978;272(5654):586-90. Epub 1978/04/13.
117. Ball JB, Andrews PR, Alewood PF, Hughes RA. A one-variable topographical descriptor for the beta-turns of peptides and proteins. FEBS Lett. 1990;273(1-2):15-8. Epub 1990/10/29.
118. Mansiaux Y, Joseph AP, Gelly JC, de Brevern AG. Assignment of PolyProline II conformation and analysis of sequence--structure relationship. PLoS One. 2011;6(3):e18401. Epub 2011/04/13.

119. Adzhubei AA, Sternberg MJ, Makarov AA. Polyproline-II helix in proteins: structure and function. J Mol Biol. 2013;425(12):2100-32. Epub 2013/03/20.
120. Jardetzky TS, Brown JH, Gorga JC, Stern LJ, Urban RG, Strominger JL, et al. Crystallographic analysis of endogenous peptides associated with HLA-DR1 suggests a common, polyproline II-like conformation for bound peptides. Proc Natl Acad Sci U S A. 1996;93(2):734-8. Epub 1996/01/23.
121. Pellecchia M, Sem DS, Wuthrich K. NMR in drug discovery. Nat Rev Drug Discov. 2002;1(3):211-9. Epub 2002/07/18.
122. Wüthrich K. NMR of proteins and Nucleic Acids. (New York, USA: John Wiley and Sons). 1986(2nd Edition):p.p. 207 - 15.
123. Banci L, Bertini I, Luchinat C, Mori M. NMR in structural proteomics and beyond. Prog Nucl Magn Reson Spectrosc. 2010;56(3):247-66. Epub 2010/07/17.
124. Kitmitto A. Applications of electron cryo-microscopy to cardiovascular research. Methods Mol Med. 2006;129:315-27. Epub 2006/11/07.
125. Bieri M, Kwan AH, Mobli M, King GF, Mackay JP, Gooley PR. Macromolecular NMR spectroscopy for the non-spectroscopist: beyond macromolecular solution structure determination. FEBS J. 2011;278(5):704-15. Epub 2011/01/11.
126. Kwan AH, Mobli M, Gooley PR, King GF, Mackay JP. Macromolecular NMR spectroscopy for the non-spectroscopist. FEBS J. 2011;278(5):687-703. Epub 2011/01/11.
127. http://www.pdb.org/pdb/home/home.do.
128. Harris RK. Nuclear Magnetic resonance Spectroscopy. A Physicochemical View. England, Longman Scientific & Technical

1986.
129. Satterthwait AC, Arrhenius T, Hagopian RA, Zavala F, Nussenzweig V, Lerner RA. Conformational restriction of peptidyl immunogens with covalent replacements for the hydrogen bond. Vaccine. 1988;6(2):99-103. Epub 1988/04/01.
130. Bundi A, Wüthrich K. 1H-nmr parameters of the common amino acid residues measured in aqueous solutions of the linear tetrapeptides H-Gly-Gly-X-L-Ala-OH. Biopolymers. 1979;18(2):285-97.
131. Andreu D, Rivas L. Péptidos en Biologia y Biomedicina. CSIC. 1997.
132. Wagner G, Neuhaus D, Worgotter E, Vasak M, Kagi JH, Wuthrich K. Nuclear magnetic resonance identification of "half-turn" and 3(10)-helix secondary structure in rabbit liver metallothionein-2. J Mol Biol. 1986;187(1):131-5. Epub 1986/01/05.
133. Crippen GM, and Havel TF. Distance Geometry and Molecular Conformation. Research Studies Press. 1988;Taunton, England.
134. Discover 2.9.7/95.0/3.0.0 Forcefield Simulations. San Diego: Biosym/Molecular Simulations. 1995.
135. Guntert P. Automated NMR structure calculation with CYANA. Methods Mol Biol. 2004;278:353-78. Epub 2004/08/20.
136. Schwieters CD, Kuszewski JJ, Tjandra N, Clore GM. The Xplor-NIH NMR molecular structure determination package. J Magn Reson. 2003;160(1):65-73. Epub 2003/02/05.
137. Fidock DA, Sallenave-Sales S, Sherwood JA, Gachihi GS, Ferreira-da-Cruz MF, Thomas AW, et al. Conservation of the Plasmodium falciparum sporozoite surface protein gene, STARP, in field isolates and distinct species of Plasmodium. Molecular and biochemical parasitology. 1994;67(2):255-67. Epub 1994/10/01.

138. Delplace P, Fortier B, Tronchin G, Dubremetz JF, Vernes A. Localization, biosynthesis, processing and isolation of a major 126 kDa antigen of the parasitophorous vacuole of Plasmodium falciparum. Molecular and biochemical parasitology. 1987;23(3):193-201. Epub 1987/04/01.
139. Anders RF, Coppel RL, Brown GV, Kemp DJ. Antigens with repeated amino acid sequences from the asexual blood stages of Plasmodium falciparum. Prog Allergy. 1988;41:148-72. Epub 1988/01/01.
140. Hisaeda H, Yasutomo K, Himeno K. Malaria: immune evasion by parasites. Int J Biochem Cell Biol. 2005;37(4):700-6. Epub 2005/02/08.
141. Rammensee HG, Friede T, Stevanoviic S. MHC ligands and peptide motifs: first listing. Immunogenetics. 1995;41(4):178-228. Epub 1995/01/01.
142. Stapley BJ, Creamer TP. A survey of left-handed polyproline II helices. Protein Sci. 1999;8(3):587-95. Epub 1999/03/26.
143. Shi Z, Chen K, Liu Z, Kallenbach NR. Conformation of the backbone in unfolded proteins. Chem Rev. 2006;106(5):1877-97. Epub 2006/05/11.
144. Hennecke J, Carfi A, Wiley DC. Structure of a covalently stabilized complex of a human alphabeta T-cell receptor, influenza HA peptide and MHC class II molecule, HLA-DR1. EMBO J. 2000;19(21):5611-24. Epub 2000/11/04.
145. Kelly SM, Jess TJ, Price NC. How to study proteins by circular dichroism. Biochim Biophys Acta. 2005;1751(2):119-39. Epub 2005/07/20.
146. Cifuentes G, Vanegas M, Martinez NL, Pirajan C, Patarroyo ME. Structural characteristics of immunogenic liver-stage antigens derived from P. falciparum malarial proteins. Biochem Biophys Res Commun. 2009;384(4):455-60. Epub 2009/05/09.
147. Delplace P, Bhatia A, Cagnard M, Camus D, Colombet G, Debrabant A, et al. Protein p126: a parasitophorous vacuole antigen associated with the release of Plasmodium falciparum merozoites. Biol Cell. 1988;64(2):215-21. Epub 1988/01/01.
148. Blackman MJ. Malarial proteases and host cell egress: an 'emerging' cascade. Cell Microbiol. 2008;10(10):1925-34. Epub 2008/05/28.
149. Patarroyo MA, Bermudez A, Lopez C, Yepes G, Patarroyo ME. 3D analysis of the TCR/pMHCII complex formation in monkeys vaccinated with the first peptide inducing sterilizing immunity against human malaria. PLoS One. 2010;5(3):e9771. Epub 2010/03/25.
150. Hennecke J, Wiley DC. Structure of a complex of the human alpha/beta T cell receptor (TCR) HA1.7, influenza hemagglutinin peptide, and major histocompatibility complex class II molecule, HLA-DR4 (DRA*0101 and DRB1*0401): insight into TCR cross-restriction and alloreactivity. J Exp Med. 2002;195(5):571-81. Epub 2002/03/06.
151. Smith KJ, Pyrdol J, Gauthier L, Wiley DC, Wucherpfennig KW. Crystal structure of HLA-DR2 (DRA*0101, DRB1*1501) complexed with a peptide from human myelin basic protein. J Exp Med. 1998;188(8):1511-20. Epub 1998/10/23.
152. Li Y, Huang Y, Lue J, Quandt JA, Martin R, Mariuzza RA. Structure of a human autoimmune TCR bound to a myelin basic protein self-peptide and a multiple sclerosis-associated MHC class II molecule. EMBO J. 2005;24(17):2968-79. Epub 2005/08/05.
153. Deng L, Langley RJ, Brown PH, Xu G, Teng L, Wang Q, et al. Structural basis for the recognition of mutant self by a tumor-specific, MHC class II-restricted T cell receptor. Nat Immunol. 2007;8(4):398-408. Epub 2007/03/06.
154. Gunther S, Schlundt A, Sticht J, Roske Y, Heinemann U, Wiesmuller KH, et al. Bidirectional binding of invariant chain peptides to an MHC class II molecule. Proc Natl Acad Sci U S A. 2010;107(51):22219-24. Epub 2010/12/01.

155. Murthy VL, Stern LJ. The class II MHC protein HLA-DR1 in complex with an endogenous peptide: implications for the structural basis of the specificity of peptide binding. Structure. 1997;5(10):1385-96. Epub 1997/11/14.
156. Hunt JD, Jackson DC, Brown LE, Wood PR, Stewart DJ. Antigenic competition in a multivalent foot rot vaccine. Vaccine. 1994;12(5):457-64. Epub 1994/04/01.
157. Fattom A, Cho YH, Chu C, Fuller S, Fries L, Naso R. Epitopic overload at the site of injection may result in suppression of the immune response to combined capsular polysaccharide conjugate vaccines. Vaccine. 1999;17(2):126-33. Epub 1999/02/13.
158. Sedegah M, Charoenvit Y, Minh L, Belmonte M, Majam VF, Abot S, et al. Reduced immunogenicity of DNA vaccine plasmids in mixtures. Gene Ther. 2004;11(5):448-56. Epub 2004/02/20.
159. Dunbrack RL, Jr., Karplus M. Backbone-dependent rotamer library for proteins. Application to side-chain prediction. J Mol Biol. 1993;230(2):543-74. Epub 1993/03/20.

14. ANEXOS

Anexo 1. Respuesta inmune de los péptidos 38136 y 38138 de la proteína CelTOS y 36075, 38142, 38146 y 38148 de la proteína TRSP. Resumen del cálculo de estructura de dichos péptidos. # = número de estructuras superpuestas, Máx viol. de dis. Å= Maxima violación de distancia en Å, RMSD = root-mean-square deviation, Máx viol. de AD ω (º) = Máxima violación de ángulo diedro ω en (º).

	Péptido	Secuencia (P1 P4 P6 P9)	PI	I_{20}	II_{20}	III_{20}	#	Estructura α-Helical	NOEs used	Máx. viol. de dis. (Å)	RMSD (Å)	Máx. viol. de AD ω (º)
CelTOS	34451	NV **L** TFRG**N**NGHN**S**SSSLYNG	0	0	0	0	I	ND	ND	ND	ND	ND
	38136	NV **H**TFRG**I**NGHN**S**SSSL	0	0	0	0	32	8-14	166	0.18	0.24	2.0
	38138	NV **H**TFRG**D**N**V**HN**S**SSSL	0	0	1(320)	1(320)	18	8-14	193	0.15	0.53	2.8
		Secuencia (P1 P4 P6 P9)										
TRSP	36075	SD **V**RYNK**S**FINN**R**L**L**NEHAH	0	0	0	0	24	11-20	221	0.25	0.24	1.5
	38142	SD **T**RYNK**D**FINN**K**LLNEHAH	0	0	1(160)	1(80)	11 12	7-10 14-17	205	0.18	0.15	2.6
	38146	SD **T**RYNK**D**FINN**KH**LNEHAH	0	0	0	0	24	11-18	215	0.30	0.15	2.5
	38148	SD **T**RYNKSFINN**KH**LNEHAH	0	0	1(160)	1(80)	16 23	8-12 13-18	212	0.22	0.63 0.39	1.8

Anexo 2. Rasgos estructurales de péptidos de las proteínas CelTOS y TRSP.

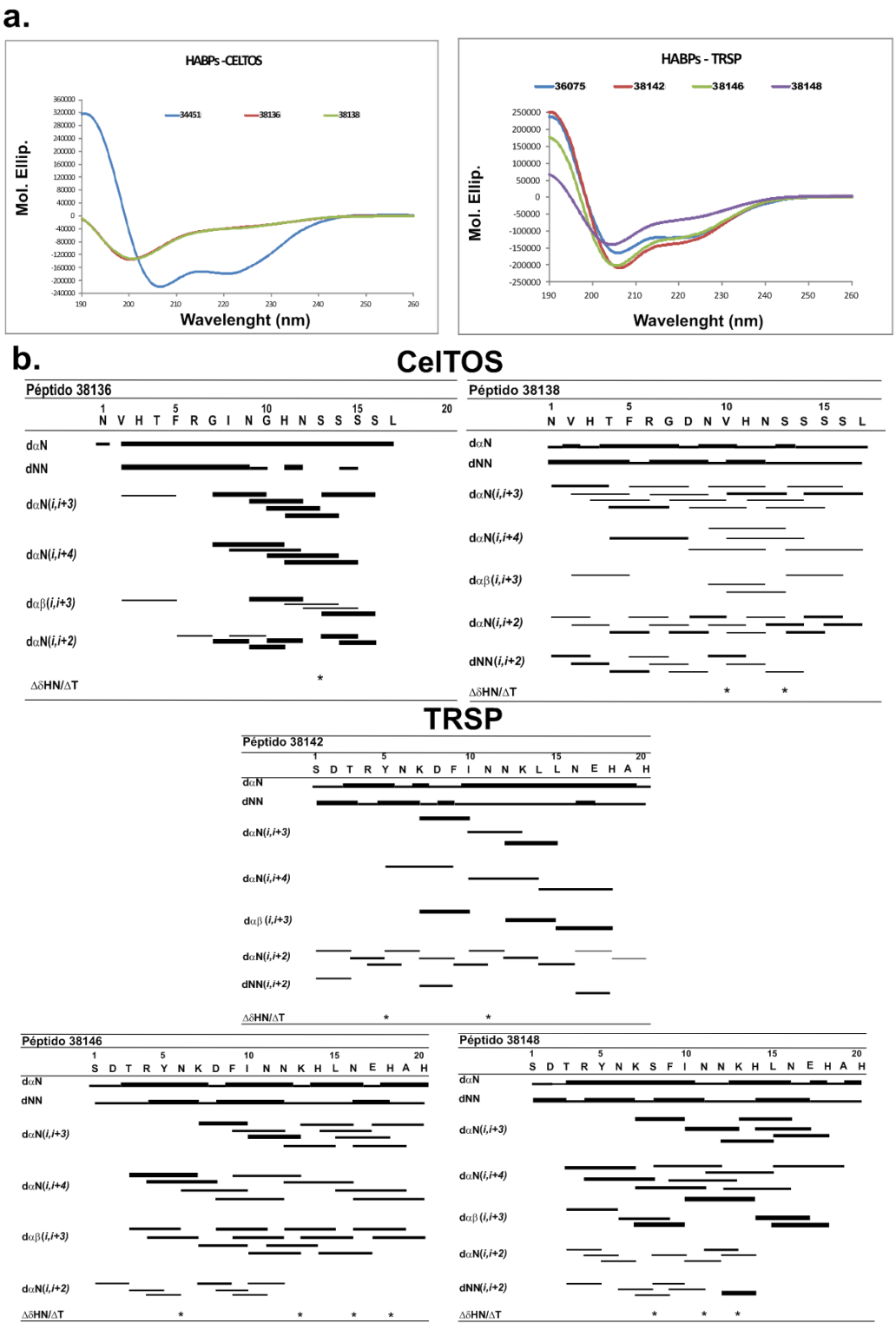

Anexo 3. Superposición de las estructuras de péptidos de las proteínas CelTOS y TRSP.